TECHNICAL REPORT TR 1.1

INTERMEDIATE REPORT

ON

DVB-NGH CONCEPT STUDIES

17TH SEPTEMBER 2011

Editor: Catherine Douillard

Telecom Bretagne, France

EXECUTIVE SUMMARY

Task Force TF1 "System concept refinements for DVB-NGH" aims at solving fundamental issues for reaching required capacity and performance for DVB-NGH. MIMO issues are not dealt with in this Task Force, they are covered by Task Force TF3.

TF1 mainly deals with the following topics:

- Study and proposal of a DVB-NGH system architecture;
- Study and optimization of BICM (Bit-Interleaved Coded Modulation) functions for DVB-NGH;
- Study of advanced modulations techniques for DVB-NGH;
- Study of interference mitigation techniques, PAPR reduction for DVB-NGH;
- Study of TFS feasibility analysis for DVB-NGH.

This report aims at synthesizing the main achievements and results obtained within task force TF1 during the first 18 months of the ENGINES project. This report comes as a mid-term technical report for TF1 and takes part in the overall technical work of work package WP2 "System Architecture".

The first part of this report describes the different system architectures and frame structures that have been studied and proposed for DVB-NGH. The second part is dedicated to advanced component techniques that have been devised or refined in order to solve fundamental issues for reaching required capacity and performance for DVB-NGH.

Most of the early contributions in the project have been submitted to the DVB-NGH Call for Technologies in late February 2010 and to the *ad-hoc* working group subsequently.

TABLE OF CONTENTS

1 LIST OF CONTRIBUTORS

The following ENGINES members, listed in alphabetical order, have contributed to this report:

- BBC
- CNES
- DiBcom
- INSA-IETR
- MERCE
- Nokia
- Orange Labs/France Telecom
- Teamcast
- Telecom Bretagne (editor)
- Teracom
- Thomson Broadcast
- Universidad Politécnica de Valencia/ iTEAM

2 SYSTEM ARCHITECTURE PROPOSALS FOR DVB-NGH

Most of the early work performed towards the definition of the new DVB-NGH system was dedicated to the definition of an overall architecture for the system. All the devised architectures assume that DVB-NGH services should be deployable on an existing DVB-T2 network infrastructure.

The T2-4-NGH proposal, described in Section 2.1 is mainly a subset of DVB-T2, suited for mobile reception with an optional satellite component, inspired from the DVB-S2 or DVB-SH standards. This proposal was partly use for the definition of the so-called "T2-Lite" profile of DVB-T2, intended primarily for reception of broadcast services in mobile environments (see Section 2.2).

The "Flexible Time Division Multiplex based on DVB-T2" system concept described in Section 2.3 takes advantage of the Future Frame Extension (FEF) concept embedded in DVB-T2 to alternate transmissions of several type of waveforms, each optimised for a specific population of receivers. A set of frames is designed to serve efficiently several network structures (broadcast, wireless broadband, mobile telecommunications networks).

Based on the DVB-T2 structure, two particular NGH frame structures have been studied. Section 2.4 deals with embedding a 3GPP E-MBMS frame in a DVB-T2 FEF, which could be seen as the cornerstone of the convergence of the E-MBMS and NGH mobile broadcasting standards. Section 2.5 presents a super frame structure, compliant with both terrestrial and satellite requirements, and based on a flexible position of NGH frames to address terrestrial mixed T2/NGH transmission and NGH-only transmission.

2.1 T2-4-NGH proposal

This NGH system architecture proposal was elaborated and proposed to the NGH Call for Technology by a group of DVB members, including three ENGINES members, **BBC**, **Nokia**, and **Teracom**.

2.1.1 General overview

The NGH system proposed here affects the physical and the upper layers. The physical layer part consists of a terrestrial branch and an optional satellite branch. The terrestrial one is widely identical with DVB-T2, but suggests the following restrictions:

The number of constellations has been limited to those useful for mobile reception. The set of code rates was adjusted to those applicable for mobile reception, i.e. a few rates were added, whereas some of the original T2 ones were not adopted. Also the number of FFT sizes was limited following the same approach.

For the optional satellite branch DVB-S2 and DVB-SH were chosen as the reference points.

The upper layer part of this proposal puts emphasis on the IP route with OMA-BCAST applications on the application layer. But also the TS branch is considered and illustrated.

2.1.2 System architectural model

As a reference for NGH, Figure 1 gives the architectural model defined for DVB-T2 systems. The chain is composed of 5 sub-systems (SS1, SS2, SS3, SS4, SS5), and 4 interfaces (A, B, C, D): SS1, SS2, and SS3 subsystems with interfaces A, B, and C are at the network side, whereas SS4 and SS5 with interface D are located on the receiver side. In the following, we briefly describe the network subsystems and interfaces.

SS1 deals with the encoding and multiplexing of all input program signals plus associated PSI/SI information and other L2 signalling. It performs the main following functions:

1. Encoding of the input signals using A/V codecs.
2. Multiplexing of encoded streams into CBR MPEG-2 TS streams and/or GSE streams.
3. Re-multiplexing of CBR TS and/or GSE streams to form the TS partial streams (TSPS), where each TSPS maps to one data PLP. This also includes the insertion of common data for some groups of TS streams and mapping it into common PLPs.

SS2 (T2-Gateway) receives the TSPS streams from SS1 via the interface A, and generates T2-MI packets that are passed then via the interface B (T2-MI) to SS3 (T2 Modulator). The SS2 T2-Gateway performs pre-analysis of the first stages of the DVB-T2 modulation process, which enables it to create BB frames, signaling and SFN synchronization information, all encapsulated into the sequence of T2-MI packets. The interface B "T2-MI" enables distribution of the packets over legacy DVB-T (TS) or IP distribution networks.

SS3 (T2-Modulator) receives the T2-MI packets via interface B and generates corresponding DVB-T2 frames, which are then sent over the RF channel as DVB-T2 signal through the interface C.

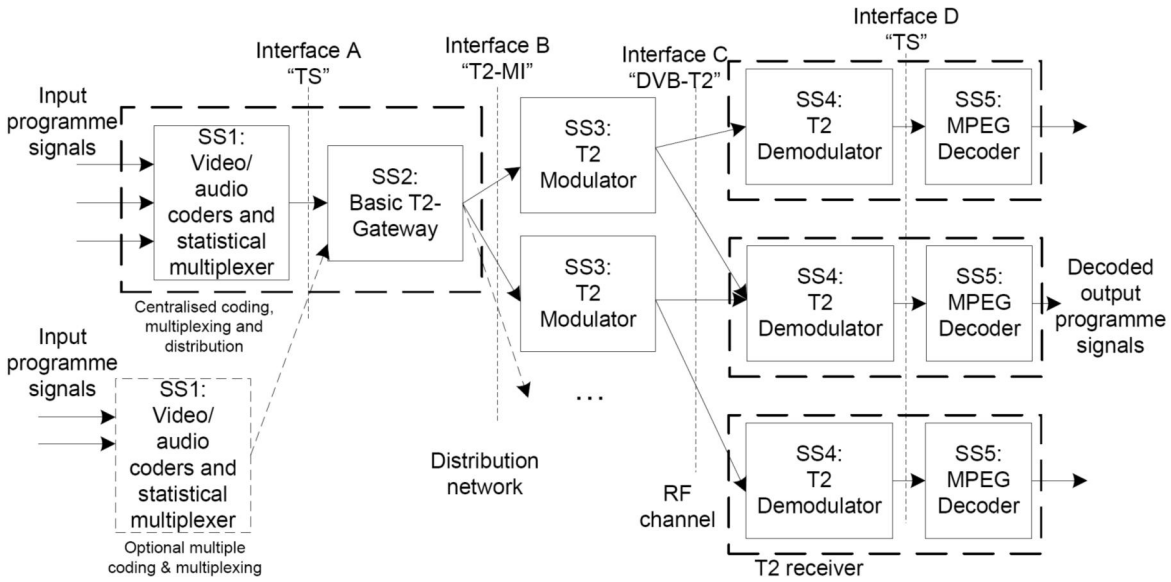

Figure 1: Block diagram of DVB-T2 chain

Figure 2 depicts our NGH system proposal aiming for the maximum reuse of T2 functionalities and infrastructure up to the interface B (i.e. distribution network).

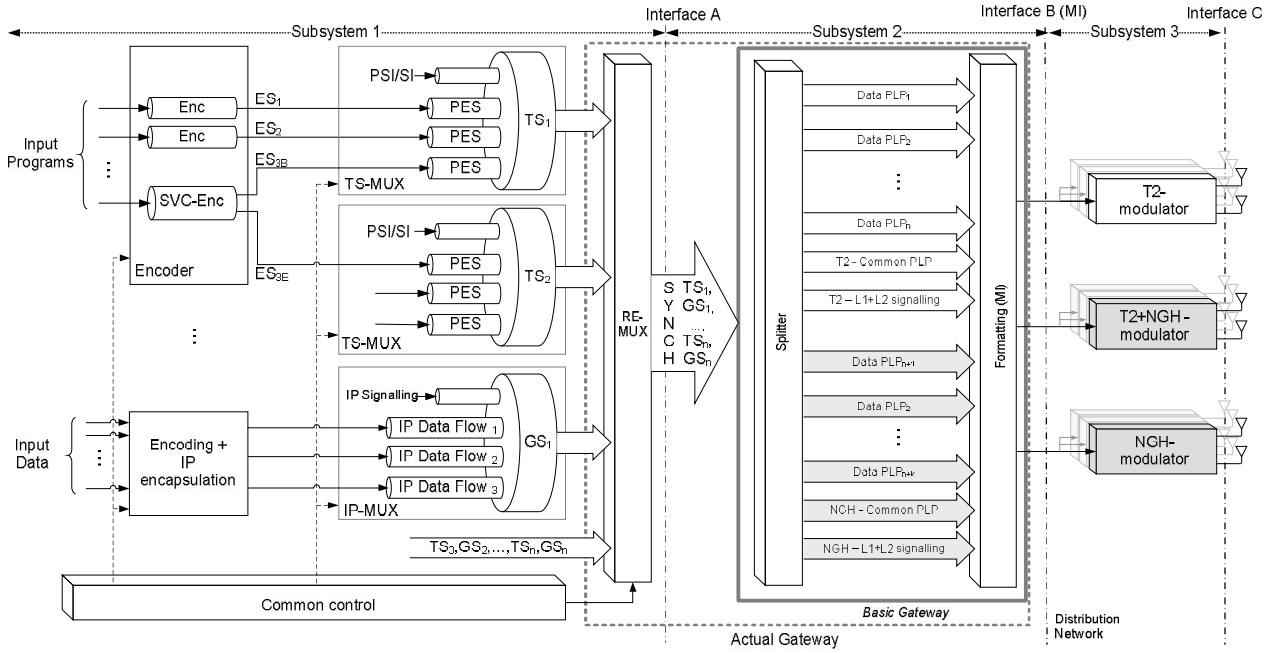

Figure 2: Architectural model for DVB-NGH network.

As observed in Figure 2, current NGH proposal is flexible to transmit both Transport Streams (TS) and Generic Streams (GS). The mapping between TS/GS(s) and PLP(s) is arbitrary. This is explicitly reflected in the previous figure by the Splitter block which separates the T2 and NGH services. Both NGH and T2 mapped PLPs may be combined later to comply with the format expected at the input of the interface B (a.k.a. Modulator Interface – MI). The PLP mapping and MI encapsulation are performed by the Basic Gateway, although actual gateways also perform the service re-multiplexing (as in T2).

Following current proposal, NGH and T2 would share the same interfaces A and B leading to minor modifications to SS1 and SS2. Farther to interface B, the NGH and T2 modulators have the possibility to be the same or different, whilst still using the same RF transmitter (i.e. T2 and NGH operate simultaneously in the same interface C).

Nevertheless, note that only the network side is depicted in Figure 2, since the receiver side follows the same structure as in Figure 1 substituting the SS4 T2 demodulator by an NGH demodulator.

Note that receivers need to decode several PLPs in parallel, e.g. a video-, and an audio-carrying PLP plus the common PLP. If SVC is used, the number of PLPs to be decoded in parallel gets even higher.

From the above architecture, the integration of NGH with T2 appears to be the most natural scenario. The integration refers to when the NGH and T2 services co-exist both on the same network. The FEF integration approach is shown in Figure 3 below:

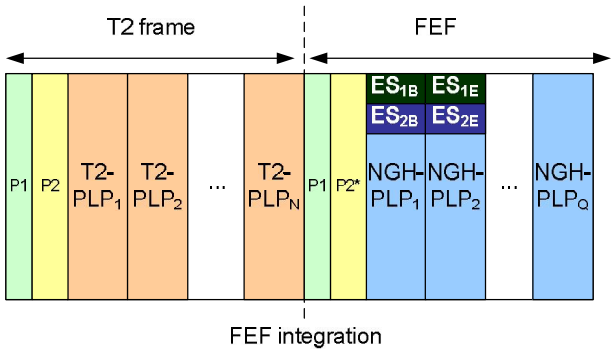

Figure 3: NGH and T2 signal in the same RF channel

FEF integration:

The NGH services are carried within the FEF part of the T2 signal, thus, will map to NGH PLPs. This gives more flexibility for NGH enhancements through specific design and configuration of the data PLP and signalling. The NGH signalling PLP is used in the FEF integration and hence this approach is mutually very close and at the same time fully backwards compatible with DVB-T2.

If SVC is permitted for NGH receivers, the Base (ESB) and Enhanced (ESE) layers of the elementary stream will map to different PLPs. In the context of SVC, it might be possible to achieve an even higher degree of integration between NGH and T2, in which the ESB maps to NGH PLPs, whereas the ESE maps to T2 PLPs. This tighter integration would reduce the amount of bandwidth required when the same service is provided for both, NGH and T2 systems, at different quality levels. However, provided the implications this would have on current T2 receivers, this solution is unlikely to be considered for the current NGH system specification.

Finally, the particular context, where the NGH system is standalone on an independent RF network, is illustrated in Figure 4 below, where the NGH frame structure is equivalent to the T2 frame structure with P1 and P2 symbols.

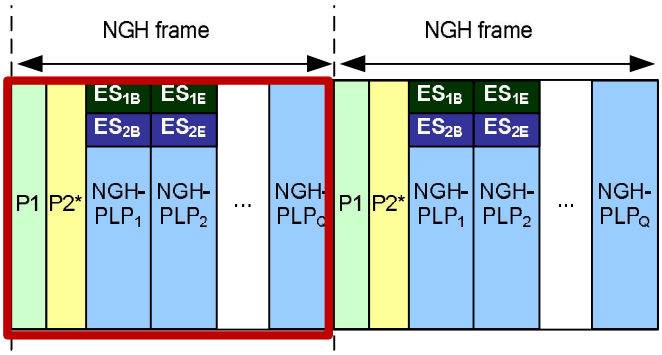

Figure 4: NGH signal occupying its own RF channel (standalone case)

In such context, the degrees of freedom for the design of the NGH signal remain similar and the degree of freedom for the selection of parameters is even higher than in the combined T2/NGH case, though a T2-like design is likely to be the most viable approach.

2.1.3 Overview of the NGH protocol stack

The NGH protocol stack is split into two core parts, i.e., the Upper layer and the DVB-NGH bearer, where the IP layer behaves as an interface. The Figure 5 illustrates the generic protocol stack of the end-to-end

NGH system where OMA-BCAST is carried over IP on the top of NGH bearer. The NGH bearer consists of the encapsulation&multiplexing layer, signaling within the L1 and L2 layers and of the physical layer. The header compression layer is located below the IP layer and it affects RTP/RTSP, UDP, IP and L2 encapsulation protocols.

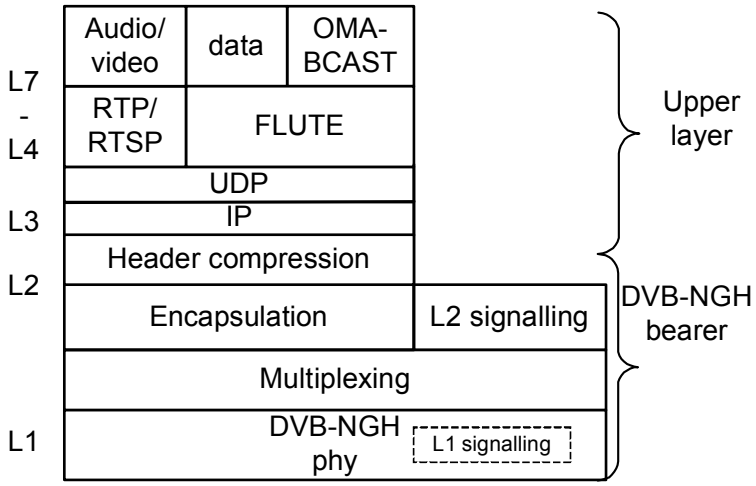

Figure 5: The IP protocol stack of the entire NGH system.

2.1.3.1 OMA-BCAST

OMA-BCAST is the application layer on top of the IP layers and it is transparent to the NGH bearer for other than some enhanced functionality, such as device management objects similar to those defined in the DVB-H context. OMA-BCAST used for NGH is the same as is used e.g. for DVB-H, FLO and ATSC M/H.

2.1.3.2 Encapsulation and multiplexing

The encapsulation is needed for IP datagrams and the multiplexing is needed for the encapsulated IP datagrams and L2 signalling which are carried over the NGH bearer.

2.1.3.3 Signalling

The signalling is split into the L2 and L1 part. The OMA-BCAST-specific signalling, including legacy and NGH specific amendments is not fully in the scope of this document.

2.1.3.3.1 L2 signalling

The purpose of the L2 signalling is to associate the IP streams with the physical layer pipes and with the network information. Also the bootstrap functionality of the ESG is enabled by the L2 signalling.

2.1.3.3.2 L1 signalling

The L1 signalling structure in its widest extent is adopted from DVB-T2. However, new signalling elements were defined to meet the NGH-specific needs e.g. related to mobility and handover. This new L1 signalling is carried within the dedicated NGH signaling PLP. The new L1 signalling provides information e.g. about the neighbouring frequencies, i.e. handover candidates, for each cell.

2.1.3.4 DVB-NGH physical layer

The DVB-NGH physical layer is based on the DVB-T2 physical layer, except for the removal of code rates, FFT sizes and other OFDM parameters which are not applicable to NGH.

2.1.4 Network elements and interfaces

In T2, a T2-GW carries out scheduling and allocation of BB frames to the T2 frame. T2-MI is the interface that carries this information from the T2-GW to a T2 modulator or set of T2 modulators which can be used to form a synchronised SFN. The T2-MI carries complete BB frames and therefore has no knowledge of their contents. It would therefore most likely be suitable for carrying NGH BB frames containing L2-encapsulated IP packets.

T2-MI is packet based and a number of different packet types are defined for T2. For the use with NGH, the existing packet type for BB frames could be re-used. If a change is made to the L1 signalling, a new packet type could be defined specifically for NGH L1. A new timestamp packet could also be defined to support bandwidths and fundamental time periods different from those defined for T2.

The T2-MI packets are always carried over conventional TS to ensure compatibility with existing DVB-T distribution networks. The overhead associated with this is small (typically 2%). Optionally RTP can be used to in turn carry this conventional TS over an IP network according to the DVB specification for TS transport over IP. For NGH, if the link based on the TS should be replaced, a direct T2-MI to UDP/RTP mapping could be defined.

2.2 Definition of "T2-Lite"

The ad-hoc group TM-H chaired by Frank Herrmann (Panasonic) has been working on the standardisation of the DVB-NGH and it has been decided that it should consist of a 'T2-Lite' profile. ENGINES members, such as **BBC** and **Teracom**, actively participated to its definition. This profile is also added to the DVB-T2 specification [1] in Annex I and the relationship between T2, T2-Lite and NGH is shown in Figure 6 below:

- DVB-T2 forms the basis for both the DVB-NGH and the DVB-T2-Lite
- DVB-T2-Lite is a subset of DVB-T2 with a few additions and it is the entire subset of DVB-NGH

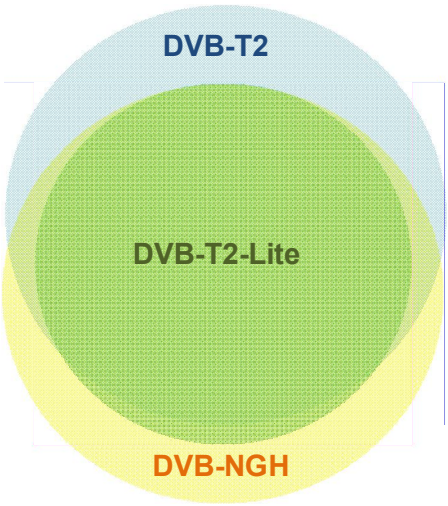

Figure 6: Relationship between DVB-T2, DVB-NGH and DVB-T2-Lite.

T2-Lite was previously known as T2-mobile and the new name has been adopted since 13th July 2011. All the work and documents leading to that have been using T2-mobile as the working name.

The T2-Lite profile is intended primarily for reception of broadcast services in mobile environments, although conventional stationary receivers may also receive these services. To aid the implementation of mobile receivers, the T2-Lite is based on a limited subset of the modes in the original T2 (now referred to as 'T2-base') profile and the key changes are:

i) The FFT sizes are restricted to 2k, 4k, 8k and 16k, meaning 1k and 32k FFT sizes removed
ii) Scattered pilot patterns allowed are PP1 to PP7, meaning PP8 removed
iii) Three combinations of FFT size, guard interval and scattered pilot pattern removed. Refer to Table I.5 and Table I.6 in Annex I for the allowed combinations
iv) Long FEC blocks removed
v) Time-interleaving memory halved - this is acceptable due to low data rates
vi) In-band signalling type B made mandatory to help receiver acquisition
vii) Code rates & rotated constellation changes
- Code rates 1/3 and 2/5 taken from DVB-S2 are added to improve mobile performance
- Code rates 5/4 and 5/6 removed
- Code rates 2/3 and 3/4 not used with 256-QAM (refer to Table I.4 in Annex I)
- Rotated constellations not used with 256-QAM (refer to Table I.4 in Annex I)

viii) Maximum data rate reduced to 4 Mbits/s
ix) Assuming processing rate for FEC decoder to be reduced by limiting rate at which cells are processed in Receiver Buffer Model
x) FEF length of up to 1 second allowed – this is to allow for low ratio of T2-Lite to T2-base frames

The complete description of this profile can be found in the Annex I of the DVB-T2 specification [1].

Due to the addition of the T2-Lite profile in DVB-T2, the specification needs to be revised to V1.3.1 and the proposed changes were presented to the Technical Module (TM) of the DVB Project. During the 88th TM meeting on the 8th and 9th of June 2011 in Geneva, the proposed revision to the draft DVB-T2 standard was approved.

This specification was later presented to the DVB Steering Board (SB) on the 7th July 2011 for their 68th meeting and it was approved with the request of changing the original 'T2-mobile' name to 'T2-Lite' before proceeding through ETSI.

The new name avoids the misconception that DVB-T2 was not designed to work in the mobile environment. In fact the original DVB-T2 (specification V1.2.1) can be configured to work in fixed, portable or mobile reception. A DVB-T2 network targeting stationary receivers with rooftop reception can be configured to maximise the data rate but the penalty is poor mobile reception. Hence the T2-Lite profile allows a more robust OFDM mode to be transmitted alongside with a high data rate service within the same channel of T2.

2.3 Flexible Time Division Multiplex based on DVB-T2

The "Flexible Time Division Multiplex based on DVB-T2" system concept for DVB-NGH, has been elaborated by a group of 7 ENGINES partners: **CNES**, **DiBcom**, **Teamcast**, **INSA-IETR**, **MERCE**, **Orange Labs/France telecom** and **Telecom Bretagne** with the aim to fulfil the Commercial Requirements elaborated by the DVB forum for the DVB "Next Generation to Handheld terminals" system.

Three main ideas have driven the works:

- DVB-NGH services shall be deployable on an existing DVB-T2 network infrastructure,
- DVB-NGH systems might be tailored to address various populations of nomadic/mobile receivers over a whole country and/or over cities and/or inside buildings,
- DVB-NGH shall anticipate the future landscape of "Mobile Multi Media" services resulting from the "Digital Dividend" (790-862 MHz), the forthcoming 4G-LTE deployment and the technical evolutions of the handheld devices.

2.3.1 Rationale of the system concept

Even if the DVB-NGH Commercial requirements constituted our reference framework, some additional considerations emerged from our works:

- Mobile TV services still look for an adequate "Business Model": the translation of the classical broadcast business models (i.e. "Free-to-air" and "PayTV") do not exhibit nowadays a noticeable commercial success story,
- Successful deployment of Mobile TV services seems to be linked to the capability of the broadcast infrastructure to provide several services simultaneously.

Accordingly, it seems mandatory to design the DVB-NGH system in order to allow – as an initial step – the deployment of DVB-NGH services over an existing broadcast platform (similarly to the "One-Seg" scheme introduced on the Japanese Digital TV broadcast system ISDB-T).

But, following the introduction phase, which essentially aims to build up a park of receiving terminals, the DVB-NGH system should be able to be extended in order to offer more services to more users, in other words to extend its capacity and coverage to address more receiving situations (thus to avoid the impasse noticed by some broadcast systems in some countries).

On another hand, interestingly, "broadcast modes" are announced in the new generation of bidirectional wireless networks (i.e. WiMax, B3G-LTE and 4G-LTE-A) showing the strong asset of the "broadcast topology" to provide wireless terminals with high-bitrates Multi-Media contents.

This also lets anticipate that future handhelds terminals will be equipped with "broadcast mode" demodulators and that it should be adequate to ease the apparition of silicon performing universal broadcast demodulation, instead of using a "multi-modems" approach which characterises, nowadays, the "Smart-Phones".

As far as receiving terminals are concerned, it should be also noticed that the recent technological evolutions make "handheld TV" not only restricted to access uniquely a broadcast network, but embed means to become "connected devices" to either a wireless broadband network or a mobile telecom networks.

This suggested that the Hybrid Broadcast Broadband TV (HbbTV) services organisation, which uses the connected capability of stationary set top boxes, should constitute a suitable basis for the definition of Mobile DVB-NGH services.

The broadcast market trends observed at the terminal level seems to show a clear path to the harmonisation of the "broadcast mode" used in wireless access networks: the work engaged by DVB-NGH should be an excellent opportunity to provide to the forthcoming intelligent terminals a way to insure the continuity of Mobile TV services and to make DVB-NGH service network agnostic!

Based on these considerations, came our conclusions:

- DVB-T2 shall be the starting point of the DVB-NGH system design,
- DVB-NGH system shall offer capability of evolution to a range of network architectures (i.e. broadcast, cellular, hybrid),
- DVB-NGH shall offer paths for convergence with other categories of networks.

2.3.2 NGH as a flexible "Time Division Multiplex"

By construction, DVB-T2 offers three ways to transmit broadcast services having different physical layer characteristics: multi-PLP, auxiliary streams and Future Extended Frame.

The two first features require that all services share the same waveform (one FFT size, one guard interval, one time interleaver…). With this definition, it should be difficult to serve efficiently & simultaneously

various topologies of network contributing to serve nomadic/mobile handheld devices.

On the contrary, the Future Frame Extension (FEF) concept embedded in DVB-T2, allows to alternate transmission of several type of waveforms, each optimised for a specific population of receivers (i.e. Fixed / Portable / Mobile), each population accessing to a given service (i.e. HDTV / SDTV / LDTV).

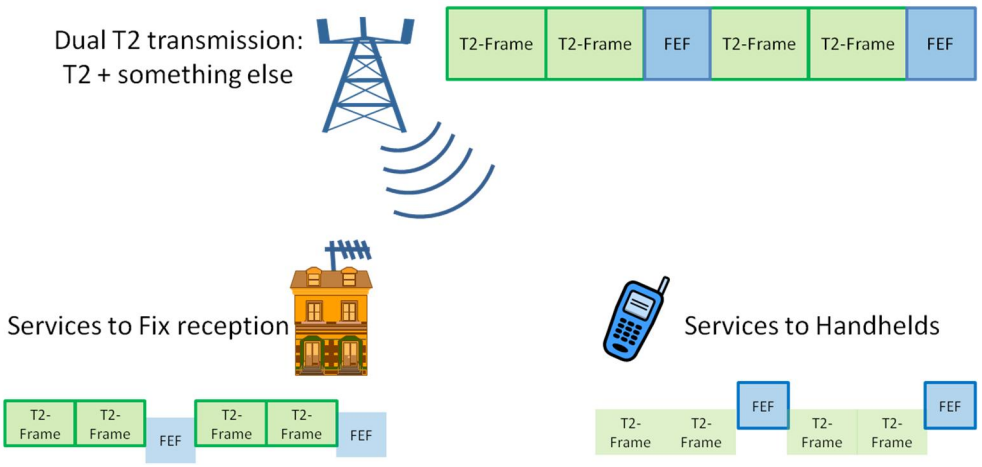

Figure 7: Dual transmissions "T2 & something else"

In its current definition, DVB-T2 allows two sets of services, as illustrated in Figure 7:

1. The CORE T2 service carried in one category of DVB-T2 frame,
2. "*Something else*" carried in the "Future Extension Frame" (FEF).

With this definition, it is somehow difficult to address simultaneously various kinds of requests, especially if it is needed to tune the transmission parameters – and not only the BICM ones - to optimally deliver a service over a unique network of transmitters...

For instance, some broadcasters should wish to use a pure DVB-T2 waveform but to use alternatively three sets of DVB-T2 parameters to specifically target three dedicated population of receivers:

a. Those using a roof top antenna ➔ HDTV over Fixed receivers,
b. Those using a set top antenna ➔ SDTV over Portable receivers,
c. Those using a built-in antenna ➔ LDTV over Mobile receivers.

The difficulty with the current DVB-T2 definition is to signal three independent DVB-T2 multiplexes (of PLPs) broadcasted in a single RF channel, but carried by a dedicated waveform having specific physical properties (i.e. FFT/GI/MIMO/Pilot Pattern).

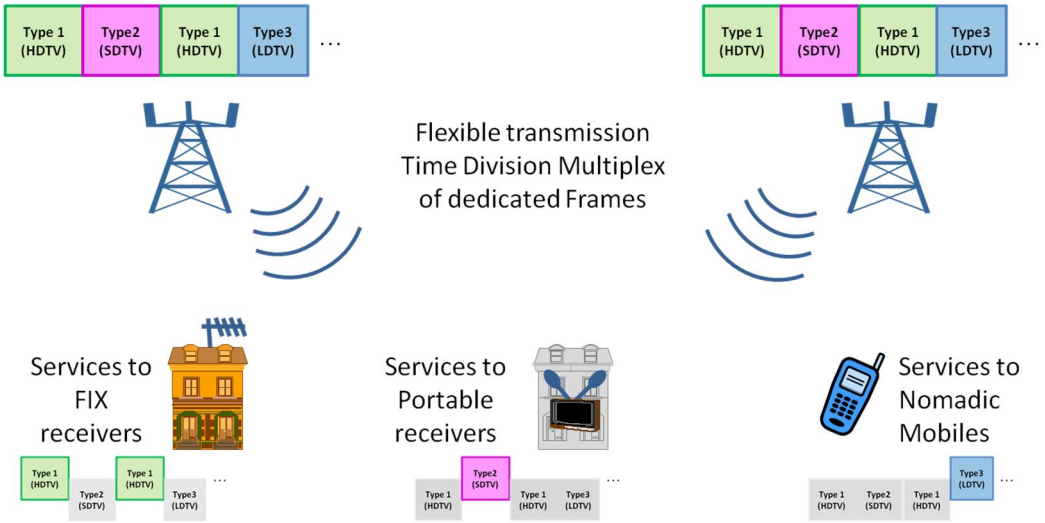

Figure 8: DVB-NGH as a flexible TDM of "frames starting with P1"

The conclusion of our analysis is that the definitions of the DVB-T2-FEF and the related P1 signalling messages must be "relaxed" in order to allow a free organisation of the sequential transmission of any type of "frames starting with the P1 preamble", as illustrated in Figure 8.

The purpose of making DVB-NGH a free multiplex of frames, based on the underlining structure specified in DVB-T2, is clearly to offer to the DVB-NGH network operator a full flexibility in the transmission resources allocation. This "flexibility in Broadcast Services" should furthermore be managed either statically (i.e. fixed organisation of the TDM) or dynamically (i.e. variable organisation of the TDM along day/week/month to face special demands/events).

2.3.3 Is a unique "DVB-NGH frame" able to satisfy every CR needs?

If the "in-band Mobile TV" scenario is foreseen to ease the introduction of Mobile TV services over an existing DVB-T2 transmission infrastructure, it is also foreseen that the initial network coverage will have to be improved and to be extended.

In this progressive scenario, it should be noted that everything performed to improve coverage will benefit to all services. Also, if the broadcast service to Handheld is commercially successful, it should be anticipated that new networks/new transmission capacities will be required using not only the broadcast UHF spectrum, but also other bands made available for Mobile Multimedia services.

Globally, it seems that the number of scenarios should be of extreme variety and accordingly the topology of the DVB-NGH broadcast network should be able to evolve in various directions.

Ultimately, high performance DVB-NGH networks could include three categories of transmission cells, each having a specific purpose and accordingly implementing a specific waveform.

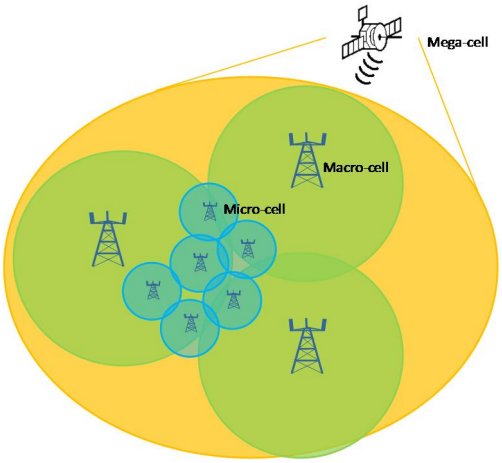

Figure 9: DVB-NGH network topology involving 3 categories of transmission cells

As tentatively pictured in Figure 9, three types of broadcast components are co-operating to contribute to a universal availability of DVB-NGH services over a wide area:

1) **Macro cells**: are served by traditional Digital TV broadcast sites, characterised by high power (x KW) / high elevation (x00 m). These sites would insure essentially the **urban outdoor coverage,**
2) **Mini cells:** which use "cellular" sites, characterised by low power (xW) / low elevation (x0 m). These would be used mainly to deliver the DVB-NGH services for **urban indoor receivers,**
3) **Mega cells**: will be served by geostationary satellite (or possibly by constellation of satellites with inclined orbits offering permanently a high elevation angle), which will produce a broadcast signal characterised by high power (xKW) / very high elevation (x000 km) which turns out to offer low power density at the ground level perfectly adapted to serve **rural/countryside outdoor receivers.**

Due to the richness of foreseen network topologies, notably in terms of cell sizes and channel characteristics (indoor/outdoor/satellite), it seems difficult to determine a unique frame structure which possesses adequate characteristics to cover efficiently every transmission cell case.

Our system concept proposes then to define a set of frames designed to serve efficiently all network structures. A set of NGH-frames can be freely combined to constitute the NGH-TDM and even, each NGH-Frame being introduced by the regular DVB-T2-P1 preamble, they could be embedded in a regular DVB-T2 transmission, as shown in Figure 10, without disturbing classical DVB-T2 receivers.

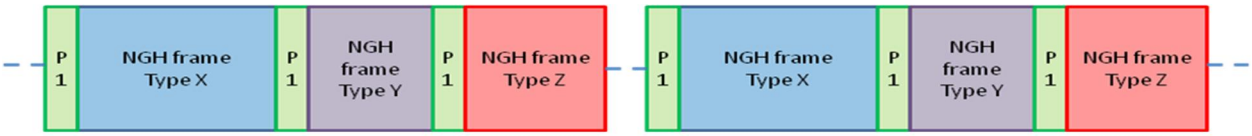

Figure 10: DVB-NGH transmission based on a flexible time multiplex

The conclusion of our analysis is that a unique type of NGH-frame cannot satisfy the wide diversity of network topologies which will be needed to address the wide variety of demands/constraints the future DVB-NGH-system will be faced on the markets. We proposed a DVB-NGH system offering a wide variety of "NGH-Frames" to cover optimally several deployment scenarios.

2.3.4 A set of NGH-Frame to optimise NGH-Services

In order to provide optimal "Flexibility of Services" and "Flexibility of Network Topologies" we have identified seven frame types which could be assembled to constitute a Time Division Multiplex articulated in compliance with the architecture previously described:

- NGH01 – Full DVB-T2: Targeting fixed reception through roof-top antenna,
- NGH02 – Modified DVB-T2: same target but proposing enhanced P2 format,
- NGH03 – Enhanced DVB-T2: introducing enhanced BICM and MIMO component,
- NGH04 – NGH Hybrid: reusing DVB-SH elements,
- NGH05 – SC-OFDM: optimised satellite component for hybrid network,
- NGH06 – OFDM/OQAM: optimising cellular coverage,
- NGH07 – LTE Broadcast (E-MBMS): optimising convergence of networks.

The main technical features of these frames are summarised in Table 1.

	Chanel Coding			SSS			Modulation	
	FEC	Constellation	Time Interleaving	Sync.	Signalling	Sounding	MISO MIMO	Waveform
NGH01 Full T2	T2	T2	T2	T2	T2	T2	T2	T2
NGH02 T2 with P2'	T2	T2	T2	T2	**Compressed & Scrambled L1 messages**	T2	T2	T2
NGH03 Enhanced T2	**LDPC w All DVB-S2 code rate**	T2	T2	T2	**Compressed & Scrambled L1 messages**	**Subset of T2**	**STBC 3D- MIMO**	**CP-OFDM 1K 2K 4K 8K**
NGH04 NGH Hybrid	**TC-3GPP2 (or LDPC)**	**QPSK 16QAM (64QAM) Rotated)**	**Long Convolut. TI**	T1	**T1**	T1 **Joint PAPR/CS I**	**STBC 3D- MIMO**	**CP-OFDM 1K 2K 4K 8K**
NGH05 NGH Satellite	**TC or LDPC**	**QPSK 16QAM (64QAM)**	**Possibly Longer than T2**	T2	**Compressed & Scrambled L1 messages**	See MERCE doc	**STBC / SFBC or SDMA or Both**	**SC-OFDM 1K 2K 4K 8K**
NGH06 NGH Cellular	**TC or LDPC**	**QPSK 16QAM 64QAM**	T2	T2	T2	T2	**Spatial Multiplexing Like**	**OFDM-OQAM 1K 2K 4K 8K (16K)**
NGH07 NGH LTE	**Turbo Codes**	**QPSK 16QAM 64QAM**	**E-MBMS**	**E-MBMS**	**E-MBMS**	**E-MBMS**	**LTE (i.e. none)**	**CP-OFDM 128 256 512 1K 2K**

Table 1: Proposed DVB-NGH Frame Set

2.3.5 Conclusion

This system concept proposal was intended to provide a "Flexible Time Division Multiplex based on DVB-T2" with the following suggestions:

- **relax the definition of the Future Extension Frame (T2-FEF)** of DVB-T2 in order to allow transmission of any combination of frames "*starting with preamble P1*";

- **define a set of specific "NGHxx" frames** each specifically optimised for a component of the DVB-NGH transmission network or population of receivers.

We were convinced that DVB-NGH should offer extended flexibility to address efficiently a forthcoming market (i.e. Mobile Multi Media) which will involve a wide variety of actors / business models themselves involving various topology & cooperation of networks... and it seems the commercial success of DVB-NGH is strongly linked to its ability to satisfy a wide variety of demands.

2.4 Proposal of a DVB-T2 Future Extension Frame based on 3GPP LTE broadcast mode (E-MBMS) for DVB-NGH

This NGH frame structure was studied and proposed by **Orange Labs/ France Telecom**. It is based on the following rationale: both DVB and 3GPP standardization bodies aim to define new standards for mobile TV broadcast. On DVB side, the DVB-NGH standardization phase is open and ETSI standard is expected to be published in 2011 in order to reach the market in 2013. On 3GPP side, LTE will be launched in the next couple of years, including the so-called E-MBMS, LTE embedded broadcast mode. Both standard organizations target the same timing for devices availability and market launch. Both organizations work tightly with ETSI to deliver successful standards.

So, in order to avoid market fragmentation while enlarging the ecosystem on mobile broadcasting, it is studied here in which extent DVB and 3GPP mobile broadcasting standards could be merged.

2.4.1 Use cases

Two use cases must be clearly separated here: on the one side the networks and operators use cases, for which networks rolling out and related costs, spectral efficiency and robustness, covered areas and density of users are parameters to take into account while dealing with specific national regulation rules; on the other side the end-user use cases, which is mainly service-driven.

Mobile broadcasting is **a "point to area unidirectional wireless access"** for massively pushed mobile services (continuously or not), with a controlled QoS over a given area, regardless of the number of active end-users. **Broadcast dedicated frequencies** in the UHF-VHF spectrum insure good indoor reception and good coverage performance (i.e. over large or medium-sized cells). An overlay broadcasting mode may allow the optimization of the networks instant loading (e.g. at peak time) and could offer "catch-up" access, by downloading popular contents into the **terminal cache memory** (somehow a hidden network), prior to the user's real-time demand. Mobile operators could complement the broadcast capacities of their own mobile networks, by using a **native optimized broadcast access,** mainly in highly populated areas.

A mix of linear and non-linear services could benefit from this optimized system: live TV or live radio could always be delivered even if this is not a sufficient service to roll out a new network; pre-download of contents (stock market updates, weather/traffic information, music games, e-books ...) before the users would wish to see it could also be a valuable service.

An optimized system, embedding both broadcasters' and mobile operators' requirements, and based on 3GPP existing standard for ease of integration in smart phones, could also lead to cooperation in terms of coverage.

2.4.2 E-MBMS overview

E-MBMS stands for Evolved Multimedia Broadcast and Multicast System and is the broadcast mode of 3GPP LTE.

2.4.2.1 Spectrum allocations

E-MBMS system is defined for the following bandwidths: 1.4 MHz, 3 MHz, 5MHz, 10MHz, 15MHz and 20MHz, which covers 15 & 20MHZ cases as required by DVB-NGH commercial requirements.

2.4.2.2 Duplex modes

Both FDD (Frequency Division Duplex) and TDD (Time Division Duplex) are defined in 3GPP standards; TDD could be preferred in order not to reserve unused UL (uplink) spectrum. As TDD does not define a 100% DL (downlink) mode, this study will focus on FDD physical layer.

2.4.2.3 Frame structure

In LTE, unicast and broadcast signals can be multiplexed in time in the same frame (shared carrier between both transmission types). It is also possible to use a dedicated carrier for broadcast (even if not defined for all ISO layers in the standard). This case will be presented here as it is more comparable with conventional DVB standards.

Basic time unit in LTE is Ts = 1/(15000*2048) seconds (inverse of maximum sampling frequency Fs = 30.72MHz). A radio frame has a duration Tf = 307200.Ts = 10ms. A radio frame contains 20 slots of length Tslot = 15360.Ts = 0.5ms, numbered from 0 to 19.

Two consecutive slots are parts of a sub-frame: sub-frame i is composed of slot 2i and slot 2i+1.

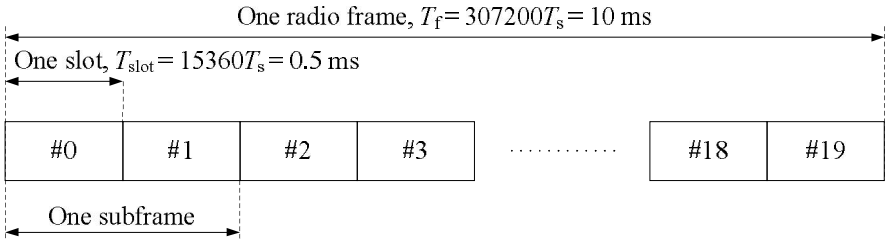

Figure 11: Frame structure.

Sub-carrier spacing is fixed and equal to 15kHz, whatever the bandwidth (value used either in unicast or when multiplexing unicast and broadcast in time); a 7.5kHz spacing is available only for dedicated MBSFN (Multimedia Broadcast Single frequency Network) carriers.

2.4.2.4 Downlink parameters, resource definition and allocation

Downlink transmission is based on OFDMA (Orthogonal Frequency Division Multiple Access), leading to high flexibility in resource allocation in frequency domain and scalability in bandwidths management.

Several sub-carriers are grouped together to form resource blocks in frequency. The minimum resource size in frequency is equal to 180 KHz (either 12*15kHz or 24*7.5kHz according to sub-carriers spacing).

Several different lengths of the cyclic prefix have been defined in order to compensate the delay spread of the multi-path channel for different environments and cell sizes. The long cyclic prefix (16.67µs) is especially needed for multi-cell transmission in a synchronised network. For large cells and especially for multi-cell transmission (for MBMS service for instance), an alternative parameter set was added allowing for a guard interval up to 33.3µs. Here, the sub-carrier spacing has been reduced to 7.5 kHz in order to keep the overhead to a reasonable level. Note that a longer cyclic prefix increases the overhead and reduces the number of data symbols transmitted within a sub-frame and thus the throughput, if the sub-carrier spacing is kept constant.

Spectrum allocation	1.4MHz	3MHz	5MHz	10MHz	15MHz	20MHz
Sub-frame duration	1ms (= 2 sub-frame of 0.5ms)					
Subcarrier spacing	15kHz (7.5kHz can be used for dedicated MBSFN carriers)					
Sampling Frequency	1.92MHz	3.84MHz	7.68MHz	15.36MHz	23.04MHz	30.72MHz
FFT size	128	256	512	1024	1536	2048
Number of occupied subcarriers	76	181	301	601	901	1201
Number of OFDM symbols per slot versus CP length for normal CP	7 symbols / 4.69us for symbols 1 to 6 and 5.21us for symbol 0					
Number of OFDM symbols per slot versus CP length for extended CP	6 symbols / 16.67us (3 symbols / 33.3us extended CP for 7.5kHz spacing)					
Physical Resource Block	180kHz = 12 subcarriers (24 subcarriers for 7.5kHz spacing)					
Typical VRB size (depending on amount of control signals)	14 OFDM symbols x 12 sub-carriers = 168 symbols Typical overhead: 3x12 symbols of control + 12 add. reference symbols Total number of payload symbols for normal CP: 120					
Number of available physical resource blocks for transmission	6	15	25	50	75	100

The transmitted signal in each slot is described by a resource grid of sub-carriers and OFDM symbols. A subcarrier and an OFDM symbol constitute a Resource Element. So for frame structure type 1 (FDD), a physical resource block is constituted of 12x7 resource elements The resource grid is illustrated in Figure 12 in the FDD case.

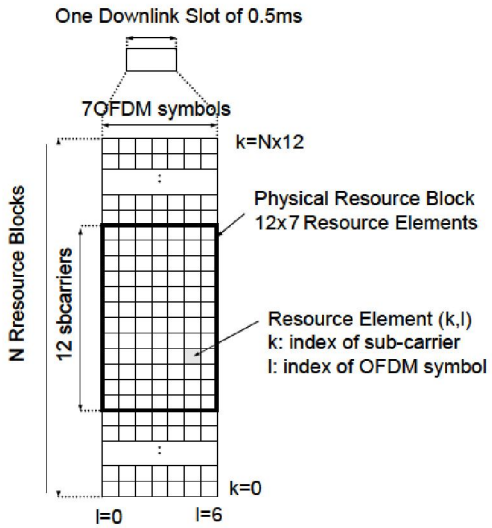

Figure 12: DL resource grid FDD frame structure and normal CP.

2.4.2.5 Channel coding

UMTS Rel6 Turbo Codes are used for channel coding with a mother code rate of 1/3. A new contention-free internal interleaver (quadratic permutation polynomial or QPP) was specified in order to allow parallel processing and higher throughputs. Typical code rates may range from 1/3 to 8/9 and are obtained using rate

matching; for very low rates, repetition coding can also be applied. Trellis termination is used for the turbo coding. Before the turbo coding, transport blocks are segmented into byte aligned segments with a maximum information block size of 6144 bits. Error detection is supported by the use of 24 bit CRC (Cyclic redundancy Check).

2.4.2.6 Constellations

Data can be modulated using QPSK, 16QAM or 64QAM constellations.

2.4.2.7 Synchronisation, sounding and signalling

Mapping of reference signals (used for channel estimation for instance) are depicted in the two following figures.

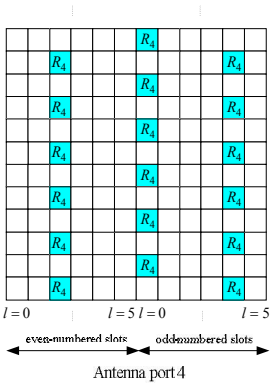

Figure 13: Mapping of MBSFN reference signals (extended cyclic prefix $\Delta f = 15\,\text{kHz}$).

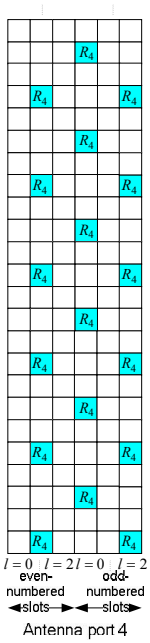

Figure 14: Mapping of MBSFN reference signals (extended cyclic prefix $\Delta f = 7.5\,\text{kHz}$).

Synchronisation process in a LTE network is called cell search. This consists of a series of synchronization stages by which the receiver determines time and frequency parameters that are necessary to demodulate the downlink and to transmit uplink signals with the correct timing. The receiver also acquires some critical system parameters. Cell search is based on DL cell specific signals: the Primary and Secondary Synchronization CHannels (P-SCH and S-SCH), and the Downlink Reference Signals (see previous subsection). The P-SCH and the S-SCH used in any cell are two sequences that belong to a set of sequences known by both the transmitter and the receiver. The receiver detects the pair of P-SCH and S-SCH sequences in use in the cell by trying several hypotheses among all the possibilities and by performing correlation products between the received signal and candidate sequences: i.e. the receiver performs a search of the actual sequences in use among all the possibilities. The P-SCH and the S-SCH use a fixed transmission bandwidth corresponding to 72 sub-carriers independent of the system bandwidth, which may not be known during the cell search procedure, and are sent every 5ms, on the last and second last OFDM symbols of the slot, as shown in Figure 15 below. The P-SCH is utilized for timing detection, frequency offset estimation and channel estimation for coherent detection of the S-SCH index.

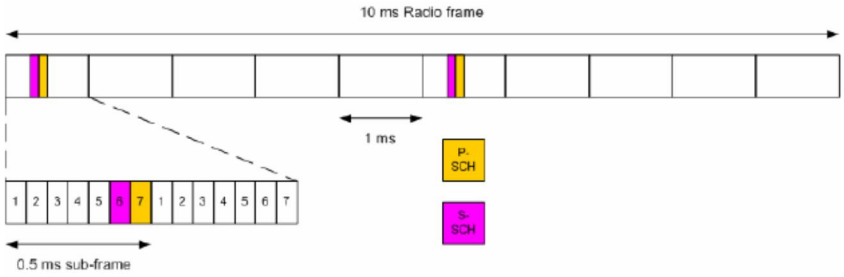

Figure 15: P-SCH and S-SCH.

This initial synchronisation procedure also gives information on cyclic prefix length and mode used (FDD or TDD). Primary Synchronisation Sequence is based on Zadoff-Chu sequences.

The following figure gives a summary of the mapping of logical channels on transport and then physical channels.

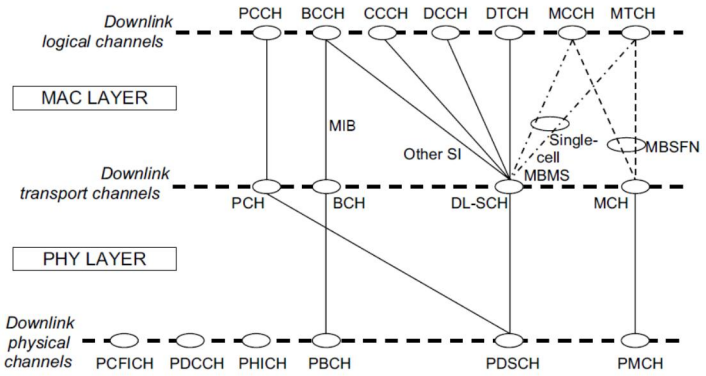

Figure 16: Summary of downlink physical channels and mapping to higher layers.

After synchronisation, a receiver decodes the data embedded in Physical Broadcast Channel (BCH). This channel carries MIB (Master Information Block), parameters required for initial access to the cell, and SIB (other System Information Blocks). MIB contains transmission bandwidth configuration (N_{RB} in downlink) while SIB gives information on MBMS frame allocation. Once BCH is decoded, there is still control information coming from MCCH (Multicast Control Channel), mapped on MCH (Multicast CHannel) transport channel (in MBSFN mode). MCCH gives information about mapping and coding rate used for transmission. Data can then be decoded thanks to all these information; data from MTCH (Multicast Traffic Channel) are mapped also to MCH in MBSFN.

2.4.3 Performance overview and comparison with DVB systems

2.4.3.1 Coverage

In a typical mobile DVB configuration, following parameters could be selected: GI = 1/8; FFT=8K in an 8MHz bandwidth. In such a case the typical coverage radius can reach 33.6kms.

With e-MBMS and maximum GI equal to 33.3us, maximum radius is “only” 10kms (typical: 5kms).

This significant difference can be explained by the different origins of both systems (small cells in 3GPP case).

2.4.3.2 Time interleaving

Maximum interleaving depth in DVB-T2 reaches 250ms while in E-MBMS case it is only 1ms. Latency constraint of unicast mode is clearly a limit for time interleaving here.

2.4.3.3 Doppler resistance

Sub-carrier spacing is clearly higher in 3GPP case (typically 15kHz versus 1.116kHz in DVB case); then it leads to a greater resistance to Doppler for DVB system (3kHz for 3GPP system versus about 220Hz for DVB).

2.4.3.4 Channel estimation limits

Nyquist limits in terms of Doppler and SFN can be defined with the following equations:

$$D_{Nyquist} = \frac{0.8 * F_s}{2 * (FFT * (1 + CP) * X)} \text{ and } T_{Nyquist} = 0.8 * \frac{FFT}{F_s} \frac{X}{Y}$$

Where:

- Fs: sampling frequency
- FFT: FFT size
- CP: CP value
- X: spacing between 2 pilot tones in time direction
- Y: spacing between 2 pilot tones in frequency direction

Comparison between DVB and 3GPP systems then gives following results:

BW=5MHz	**DVB-NGH (PP2)**	**E-MBMS (15kHz case)**
F_s (MHz)	5.71	7.68
FFT	8192	512
CP	1/8 (~180us)	¼ (16.67us)
Y	12	2
X	2	8
$D_{Nyquist}$ (Hz)	124	600
$T_{Nyquist}$ (us)	191	213

For the DVB case, pilot patterns are optimized in terms of SFN and delay spread but lead to quite “low” resistance to Doppler; for 3GPP case pilot pattern is over dimensioned (at least in frequency) and then density could be decreased.

2.4.3.5 Throughput

For this throughput comparison, the following configurations have been assumed (as many common parameters as possible even if scenarios are not realistic for network roll out):

BW=10 MHz	DVB-NGH	E-MBMS
Fs (MHz)	11.42	15.36
FFT	1K	1K
CP	1/4 (22.4us)	1/4 (16.67us)
Tu	89.6us	66.67us
MCS	QPSK 1/2	QPSK 1/2

In DVB case with PP1, 16 P2 symbols, a frame closing symbol, frame duration reaches 99.904ms (L_{data} = 874). Assuming 16K codewords, 83 LDPC blocks can be mapped on the frame, leading to a throughput of **5.57Mbps**. In a more realistic situation for DVB (8K, GI = 1/8, BW = 8MHz, PP2, frame size still ~100ms), throughput is slightly more than 5Mbps.

In 3GPP case, assuming an overhead of about 30%, throughput can be estimated to 4.8Mbps (5.49Mbps if only 20% overhead is considered).

Reachable throughputs are then comparable, even if the required signal to noise ratio is different due to far different time interleaver depths.

2.4.4 E-MBMS embedded in DVB-T2 FEF

2.4.4.1 Bandwidths

E-MBMS is not defined in usual DVB bandwidths 6, 7 and 8MHz. In order to cover these cases in an easy way, it is possible to start from 10MHz case, while modulating fewer carriers than in the original 10MHz case. The following figures can be derived:

FFT	1024						
BW (MHz)	Fe (MHz)	Symbols per Slots (Ext CP)	ExtCP (us)	Tsymb (us) Nfft/Fe	Delta_f (kHz)	Modulated sub-carriers	Transmission BW (MHz)
10	15.36	6	16.67	66.67	15	600	9
8	15.36	6	16.67	66.67	15	480	7.2
7	15.36	6	16.67	66.67	15	420	6.3
6	15.36	6	16.67	66.67	15	360	5.4

2.4.4.2 Frame size

An LTE radio frame has duration of 10 ms. DVB-T2 Future Extension Frame, likely to embed DVB-NGH standard, can have duration up to 250 ms. So it is possible to include multiple E-MBMS frame in a DVB-T2 FEF.

2.5 Proposal of a NGH satellite Super Frame structure

Based on the DVB-T2 structure, **CNES** studied and proposed an architecture based on a flexible position of NGH frames in the Super Frame to address terrestrial mixed T2/NGH transmission and NGH-only (or standalone) transmission. This super frame structure is compatible with both terrestrial and satellite requirements.

2.5.1 Future extension frame for the satellite component

First of all, satellite will not transmit DVB-T2 frames because they may not be used (because of either potential interference of the terrestrial network caused by a small guard interval or of degradation of satellite transmission spectral efficiency if T2 frames are not transmitted on the satellite).

Satellite will transmit only "future extension frames" or FEF. So we need to define a configuration of the FEF in order that they could be self-sufficient, allowing the transmission of FEF without DVB-T2 frames.

2.5.2 DVB-T2 Super Frame structure

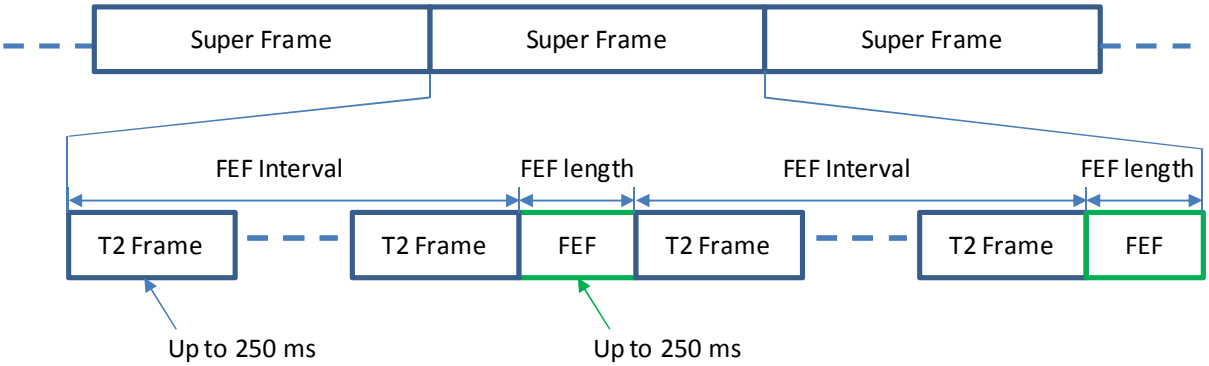

Figure 17: DVB-T2 Super Frame structure

DVB-T2 Super Frame structure is depicted in Figure 17.

The DVB-T2 Super Frame is composed of N_{T2} T2 frames and optionally N_{FEF} FEF, with N_{FEF} a divisor of NT2. T2 frames and FEF last each 250ms maximum. When present, FEF are "equidistributed" in the Super Frame and as there is less FEF than T2 frames, there is so never two consecutive FEF. Thus 2 T2 frames are at worst separate from 250ms. Besides, a mixed Super Frame always begins with a T2 frame and finishes with a FEF.

The DVB-T2 frame structure was used as starting point to build the proposal for NGH Super Frame structure.

2.5.3 Description of the proposed NGH Super Frame structure

The proposed NGH Super Frame structure is based on 3 criteria:

- one NGH frame lasts 250 ms maximum,
- the delay between two consecutive NGH frames is constant over one Super Frame and lasts 250ms maximum,
- the positions of NGH frames in the Super Frame are flexible.

First criterion guarantees that NGH frames may be included inside a FEF[1]. The goal of the second criterion is to limit zapping time (the longer the delay between two useful frames, the longer can be the zapping time). Finally, the third criterion allows addressing both terrestrial and satellite paths with a same Super Frame structure.

The proposed solution introduced the concept of segment which is the key element to enable terrestrial and hybrid scenario and to ensure the compatibility between DVB-T2 and NGH Super Frame structure. As depicted on Figure 18, the proposed Super Frame is composed of N_{NGH} segments that all have the same length and contain each one NGH frame. Position of the NGH Frame inside the segment is free but constant over all segment of the Super Frame. As a NGH frame lasts 250 ms and is separated from the next NGH frame from 250 ms at worst, a NGH segment lasts so 500 ms maximum. Apart from a maximum duration of 25 0ms, there is no constraint on the signal between two NGH frames (when present).

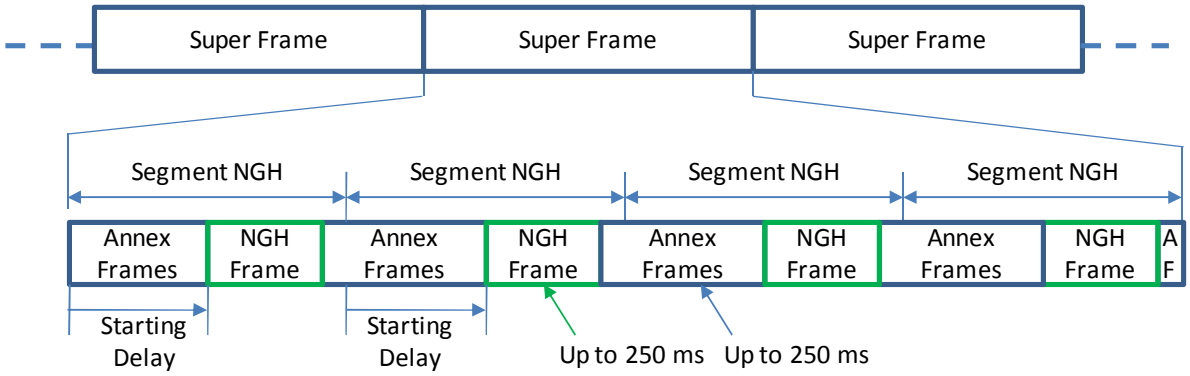

Figure 18 : proposed NGH Super Frame structure

In order to determine the positions of NGH frames, signalling should include the number N_{NGH} of NGH frames (equal to the number of segment), the length of a segment (or in an equivalent way, the delay between two NGH Frames) and the position (starting delay) of NGH frames in the segment.

The signal between two consecutives NGH frames (when present) is depicted as "annex frame" in Figure 18. These annex frames may have different definitions depending whether the NGH super frame structure is used for satellite or terrestrial transmission.

2.5.4 Mixed T2/NGH terrestrial Super Frame

Figure 24 depicts the super frame structure for a mixed T2/NGH transmission. One segment is composed of a T2 frame (or more if the total T2 part represents less than 250 ms) and a NGH frame. Due to the DVB-T2 Super Frame structure, NGH frames are necessarily inserted at the end of each segment.

[1] We consider here that NGH frames are introduced by a P1 preamble

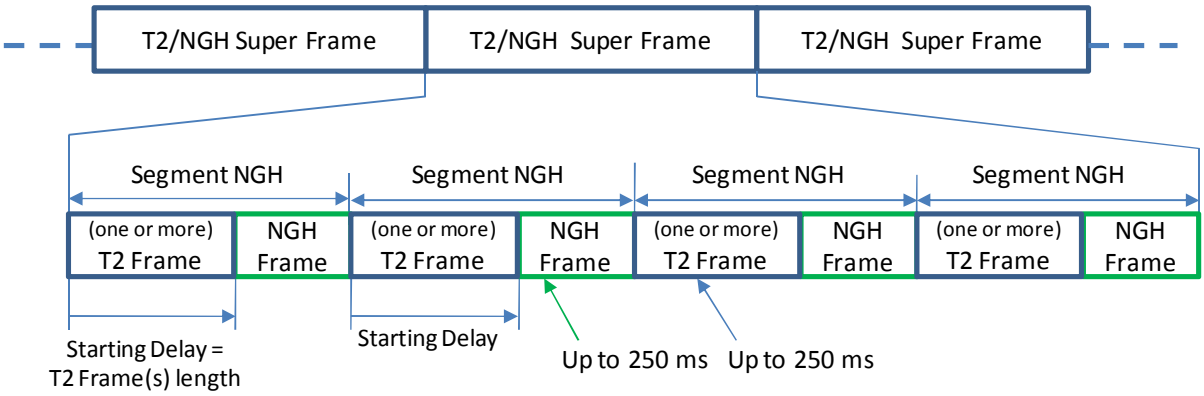

Figure 19: Mixed T2/NGH Super Frame

This example shows that T2 Frames insertion is considered by the proposed Super Frame structure but the solution is not restricted to mixed terrestrial transmission and we may consider a stand-alone NGH transmission.

2.5.5 NGH satellite Super Frame

Figure 20 depicts an NGH satellite Super Frame associated to a terrestrial T2/NGH Super Frame. On the satellite path, no T2 transmission is assured and all transmission time is allocated to NGH. In order to obtain the equivalence between both satellite and terrestrial Super Frame structures, we propose to enlarge the maximum Satellite NGH frame length to 500 ms. Besides, obtaining the same segment length on both paths may require some padding insertion at the end of each satellite segment. Consequently, the annex frame is reduced to these stuffing samples between two NGH frames.

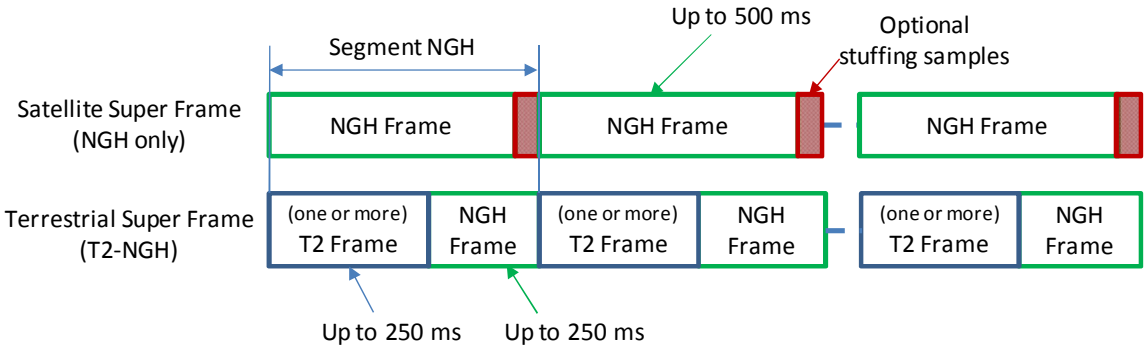

Figure 20: Terrestrial and satellite Super Frame for hybrid MFN transmission

Thus, the proposed Super Frame structure and the three associated signalling elements allow defining both satellite and terrestrial paths of a hybrid transmission. Here again, we may also consider a hybrid transmission that does not include T2 Frames.

2.5.6 Super Frame modification management

As described before, NGH segment parameters are fixed during the total duration of the Super Frame. We have however to consider the case of a modification of the configuration from one Super Frame to another and make sure that the NGH frame positions will always be known.

If NGH frames are inserted at the beginning of each segment, the determination of the position of the first NGH frame of the Super Frame N+1 requires only parameters of the Super Frame N as illustrated in Figure 21.

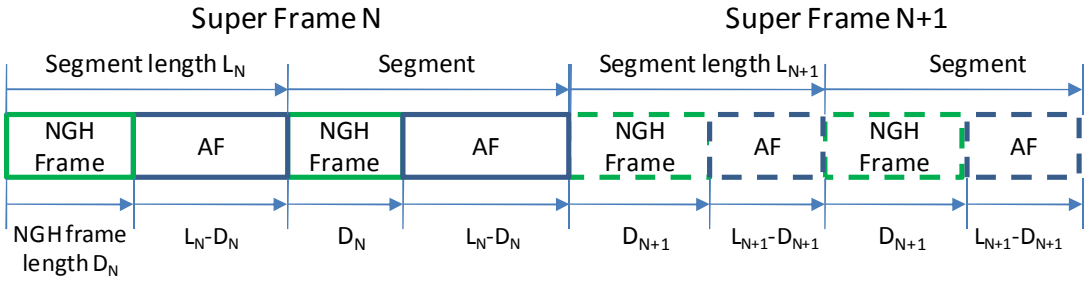

Figure 21: Super Frame modification, example 1

If NGH frames are not placed at the beginning of each segment, parameters of the Super Frame N are not sufficient to detect the position of the first NGH frame of the Super Frame N+1 (Figure 22). Thus, signalling of Super Frame N must also include parameters of Super Frame N+1.

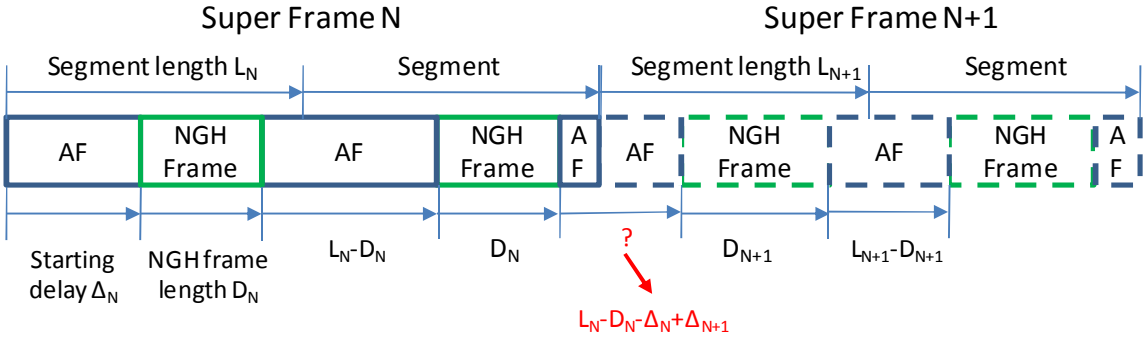

Figure 22: Super Frame modification, example 2

Consequently, in example 2, the signalling has to be aligned with the NGH Super Frame structure to enable the configuration changes in the Super Frame. New fields have to be defined to give information on the next frame (*i. e.* next frame start delay and next annex frame length). This additionnal signalling fields for the next frame are not required in example 1 when the NGH frames are located at the beginning or the end of the segment.

2.5.7 Conclusion

The solution proposed by CNES, based on DVB-T2 Super Frame, allows transmitting NGH frames and other signals (like DVB-T2 frames) inside a same Super Frame. More flexibility is offered for the position of NGH frames to address different kind of Super Frame sharing. In a DVB-T2/NGH Super Frame, NGH frames would always be transmitted after T2 Frames. In a stand-alone NGH frame, NGH frames will initiate the Super Frame. To facilitate NGH frames position management, the concept of NGH segment was introduced and specific signalling parameters were proposed.

3 ADVANCED COMPONENT TECHNIQUES FOR DVB-NGH

The second part of this document is dedicated to the studies related to advanced component techniques that have been devised or refined in order to solve fundamental issues for reaching required capacity and performance for DVB-NGH.

The contributions described in this document cover the following topics:

- Study of Forward Error Correction (FEC) coding techniques and constellations for data and signalling;
- Optimisation of channel interleaving;
- Study of advanced modulations techniques;
- Study of interference mitigation techniques, PAPR reduction for;
- Analysis of Time-Frequency Slicing (TFS) feasibility.

3.1 Forward Error Correction (FEC) coding techniques and constellations for NGH

This section covers the studies related to error correction coding and constellations that have been performed in the framework of ENGINES in order to increase the robustness of the transmission of data and signalling in the DVB-NGH context.

The first contribution, detailed in Section 3.1.1, investigates a double-binary turbo code, similar to the code recently adopted in DVB-RCS2, in order to challenge the DVB-T2 LDPC+BCH code. This FEC code offers high flexibility with respect to block size and coding rate. Therefore, it suits various conditions and environments and delivers better performance than the DVB LDPC codes at low error rates.

Section 3.1.2 studies the different techniques proposed for the robustness improvement of Layer 1 (L1) signalling in DVB-NGH. The goal is to investigate the feasibility of three new techniques for L1 signalling robustness and to study which configurations provide the best performance depending on the channel characteristics and operator's requirements.

In Section 3.1.3, a novel FEC and Time Interleaving scheme is proposed, known as BB-iFEC (Base Band - inter-burst FEC), which aims at providing long time interleaving with fast zapping support. It calls for a split FEC technique, particularly well suited for satellite transmissions but also proposed for the sheer terrestrial link in DVB-NGH.

Finally, Section 3.1.4 extends the principle of the rotated constellation technique, adopted in DVB-T2, to PSK and APSK constellations, widely used for satellite transmissions.

3.1.1 A double-binary 16-state turbo code for NGH

This study was carried out by **Telecom Bretagne**. The outcomes of this work have be presented to the DVB TM-H group, through 10 different contributions.

Due to the "family of standard" approach currently in force in DVB, the main second generation DVB standards (DVB-S2, DVB-T2 and DVB-C2) have adopted the same family of FEC codes, based on the association of a Low Density Parity-Check (LDPC) code with the addition of an outer BCH code, allowing the residual error floor to be lowered.

For DVB-NGH, two previous DVB standards could be taken as starting points: DVB-T2 and DVB-SH (Satellite Handheld). The former resorts to the above-mentioned LDPC+BCH code while the latter calls for a binary turbo code (TC), derived from the 3GPP2 standard. In order to challenge the DVB-T2 LDPC+BCH code, we have proposed a 16-state double-binary turbo code (DB-TC), similar to the code recently adopted in DVB-RCS2. This FEC code offers high flexibility with respect to block size and coding rate. Therefore, it suits various conditions and environments and delivers better performance than 3GPP2 code, especially at low error rates. It can also be associated with a BCH code if required.

Telecom Bretagne carried out an extensive study of the double-binary 16-state TC. It involves the search for code parameters (block sizes, interleaver parameters, puncturing patterns) and the comparison with the DVB-T2 code in terms of performance, hardware complexity and power consumption.

3.1.1.1 The turbo encoder structure

The structure of the proposed encoder is depicted in Figure 23. It is based on the parallel concatenation of two 16-state double-binary recursive systematic convolutional (RSC) encoders, fed by blocks of k bits (N = k / 2 couples). Internal permutation Π deals with blocks of N double-binary symbols. Both component encoders have identical features:

- 16-state double-binary convolutional code,
- polynomials 23octal (recursivity) and 35octal (redundancy),
- first bit (A) on tap 1, second bit (B) on taps 1, D and D3,
- circular termination for both component encoders.

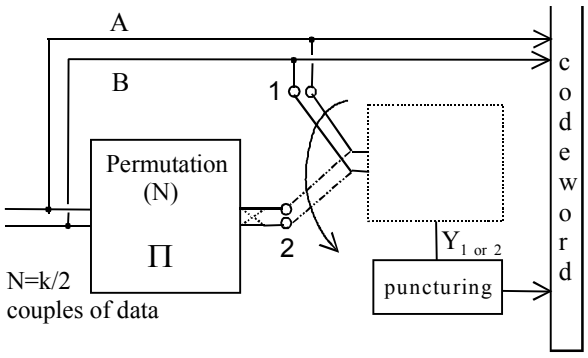

(a)

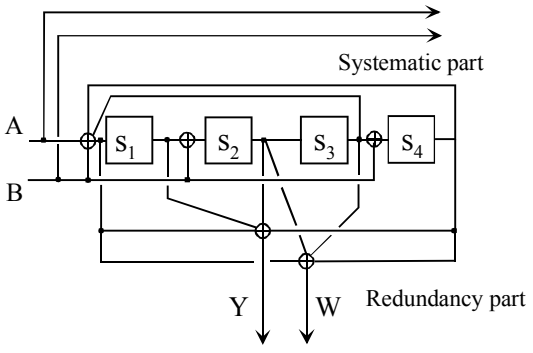

(b)

Figure 23: The proposed 16-state DB-TC (a) Global structure. (b) Component encoder: for R ≥ 1/2, redundancy W is not transmitted; for R < 1/3, input B is set to zero and is not transmitted.

The natural coding rate of the TC depicted in Figure 1 is R = 1/3. The usual way of increasing the coding rate of a TC consists of puncturing, that is to say not transmitting some redundancy bits. We have adopted the easiest way to perform puncturing through applying periodic puncturing patterns.

The permutation law Π

We proposed a two-layer permutation Π, as already adopted by the DVB-RCS and DVB-RCS2 TCs: the inter-symbol permutation is an Almost Regular Permutation (ARP) as described in [1][2]. In addition to the main inter-symbol permutation, intra-symbol permutation is also performed to increase the minimum Hamming distance of the code even further. In practice, the bits in the double-binary symbols are permuted once every other time before second encoding, the process beginning with the permutation of the first couple. The selection of the permutation parameters has been performed according to the method described in [3], which calls for an iterative combinatorial optimization on the correlation graph of the TC. Moreover, we have only kept permutation parameters providing low weight codewords with low input weights, thus making possible the association of the TC with an outer BCH code.

3.1.1.2 Performance comparison

The proposed double-binary turbo code was compared to the DVB-T2 LDPC for different coding rates and several transmission channels. The comparison was carried out in two steps:

- Comparison over static channels (Gaussian, Rayleigh, Rayleigh with erasures);
- Comparison over mobile channels (TU-6) for different Doppler frequency values f_d.

Both codes were compared for coding rates R=1/5, R=1/3 and R=2/3 and QPSK and 16-QAM constellations. The LDPC code was decoded using 50 iterations of the sum-product algorithm and the TC was decoded using 10 iterations of the BCJR algorithm.

Figure 24, Figure 25 and Figure 26 show some examples of performance comparisons for three different block sizes, coding rates and transmission channels.

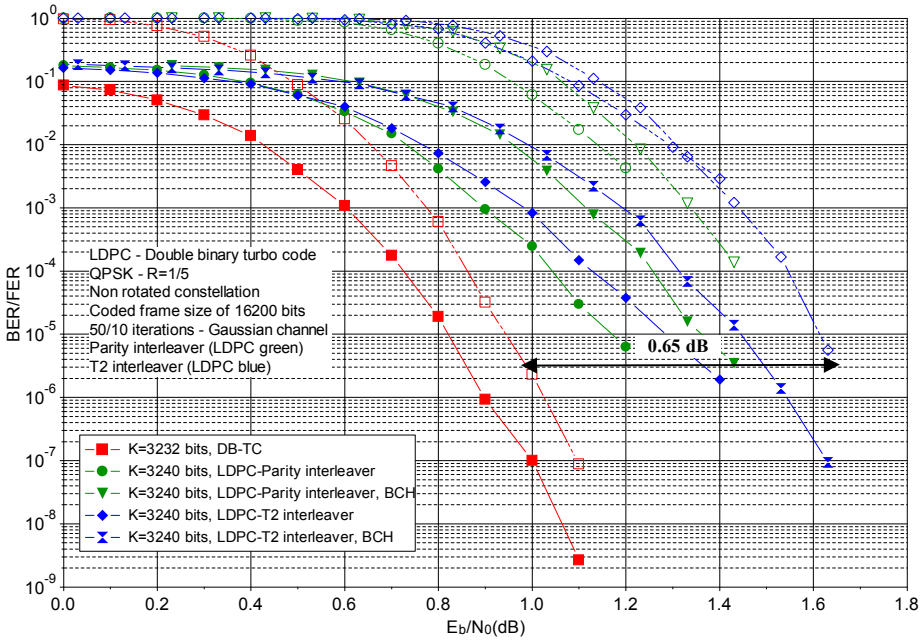

Figure 24: BER and FER comparison of the proposed DB-TC with the DVB-T2 LDPC+BCH. k= 3,232 bits for the DB-TC and k= 3,240 bits for the DVB-T2 code. Coding rate R = 1/5, QPSK constellation, Rayleigh channel.

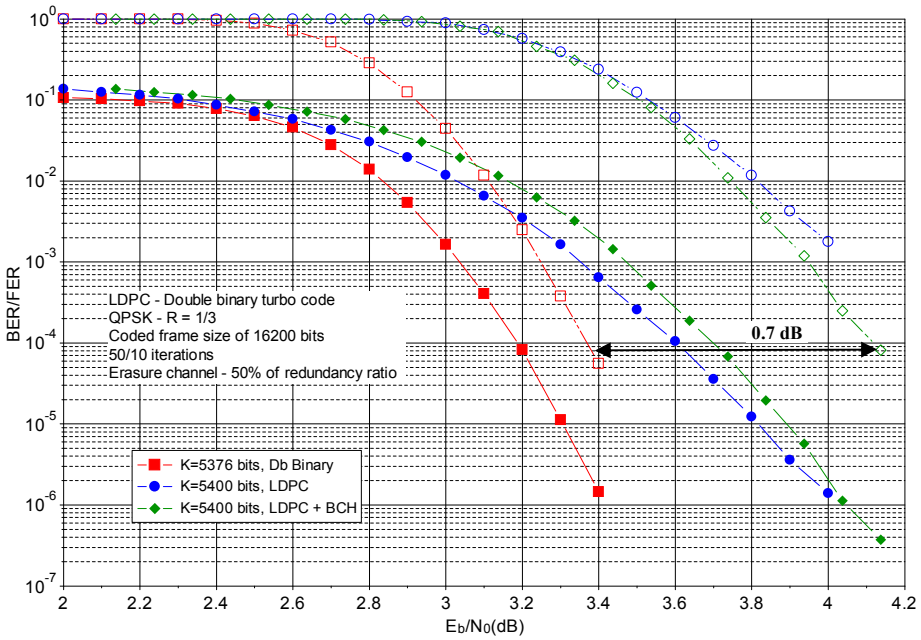

Figure 25: BER and FER comparison of the proposed DB-TC with the DVB-T2 LDPC+BCH. *k*=5,376 bits for the DB-TC and k=5,400 bits for the DVB-T2 code. Coding rate *R* = 1/3, QPSK constellation, Rayleigh channel with erasures.

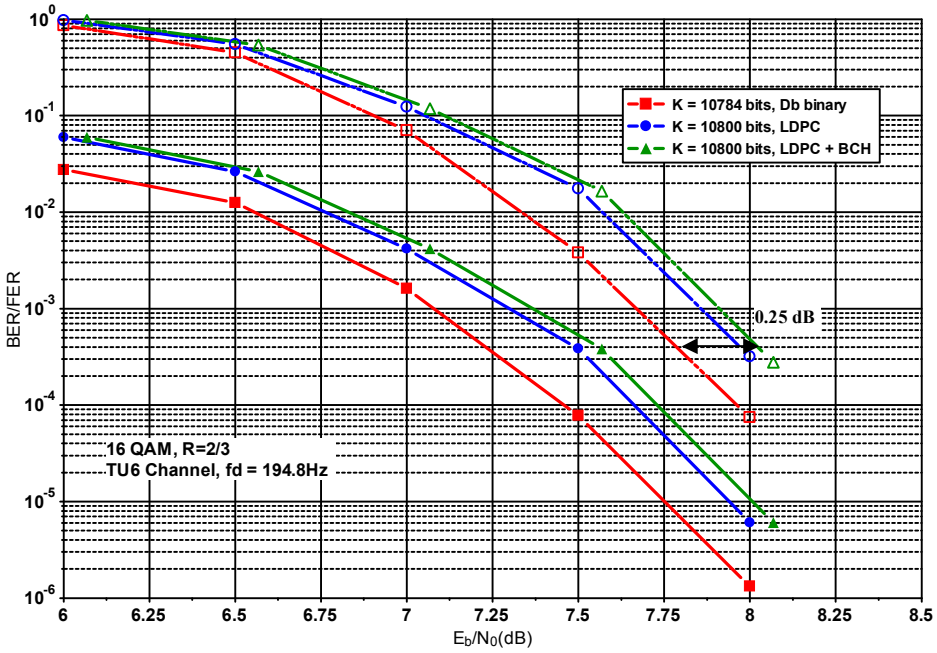

Figure 26: BER and FER comparison of the proposed DB-TC with the DVB-T2 LDPC+BCH. *k*=10,784 bits for the DB-TC and *k*=10,800 bits for the DVB-T2 code. Coding rate *R* = 2/3, 16-QAM constellation, TU-6 channel with Doppler frequency f_d=194.8 Hz.

Table 2 and Table 3 provide an overview of the gain in E_b/N_0 observed between the proposed DB-TC and the DVB-T2 LDPC+BCH code for the different simulated configurations.

		Coding Rate		
		1/5	1/3	2/3
AWGN	QPSK	0.6	0.3	0.25
	16QAM		0.3	0.35
Rayleigh	QPSK	0.55	0.4	0.3
	16QAM		0.4	0.25
Rayleigh with erasures	QPSK	0.5	0.7	0.2
	16QAM		0.45	0.0

Table 2: E_b/N_0 gain in dB observed between the proposed turbo code and the DVB-T2 LDPC+BCH code over static channels at FER = 10^{-5}.

		Coding Rate		
		1/5	1/3	2/3
TU-6 channel f_d=33.3 Hz	QPSK	0.75	0.3	0.25
	16QAM		0.5	0.25
TU-6 channel f_d=194.8 Hz	QPSK	0.7	0.5	0.25
	16QAM		0.4	0.25

Table 3: E_b/N_0 gain in dB observed between the proposed turbo code and the DVB-T2 LDPC+BCH code over mobile channels at FER = 10^{-4}.

3.1.1.3 Complexity comparison

A three-point complexity comparison of the two families of codes was carried out. The following criteria have been considered:

- Identify the required number of iterative decoder iterations for every family of codes to achieve a target error rate performance given a particular coding rate and constellation size.
- Complexity comparison, in terms of number of logic operations and memory accesses, based on realistic hardware architectures of LDPC and turbo decoders, given the number of identified iterations.
- Area estimate based on partial logic synthesis.

Figure 27 and Figure 28 illustrate some outcomes of the first point of the comparison. For coding rate 1/3 and QPSK constellation, the proposed turbo code, decoded with 5 iterations, outperforms the DVB-T2 decoder using 50 iterations, both over static and mobile channels.

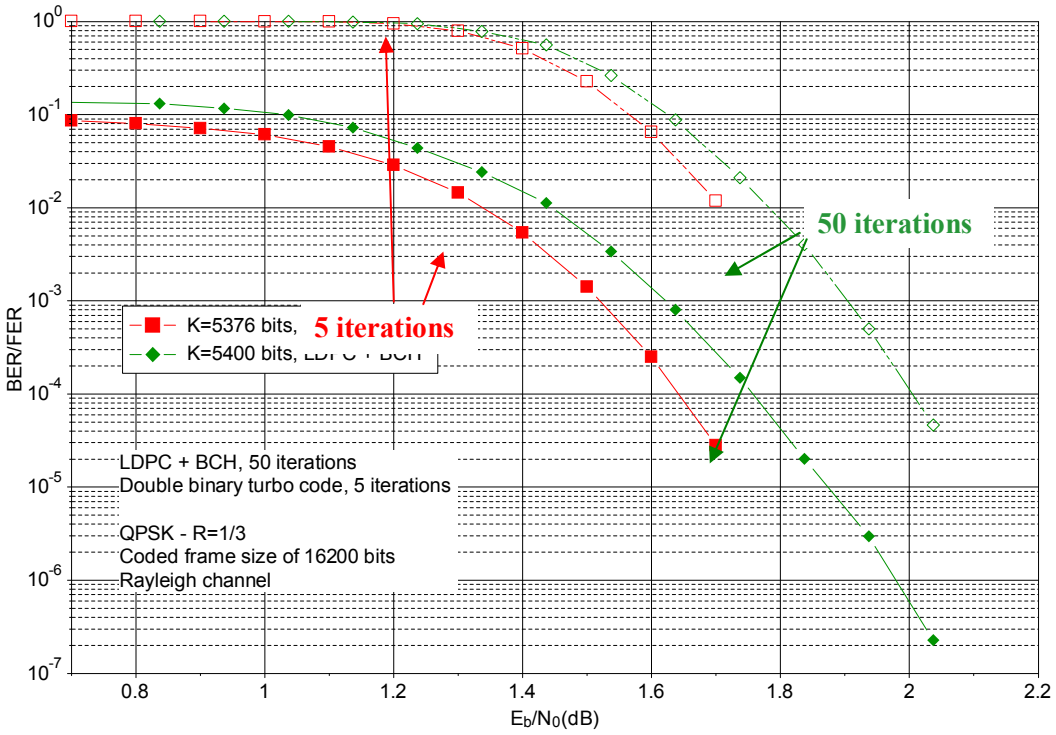

Figure 27: Comparison of the proposed DB-TC – 5 and 10 iterations – with the DVB-T2 LDPC+BCH code – 25 and 50 flooding iterations – over Rayleigh channel. QPSK constellation, coding rate 1/3.

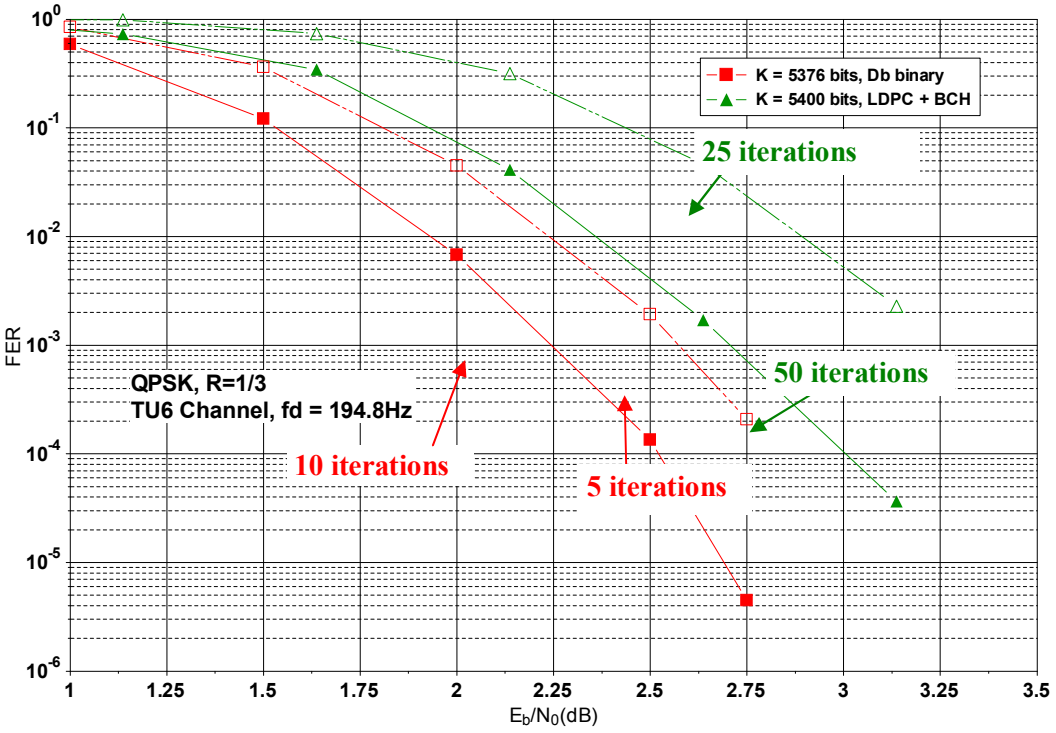

Figure 28: Comparison of the proposed DB-TC – 5 and 10 iterations – with the DVB-T2 LDPC+BCH code – 25 and 50 flooding iterations – over TU-6 channel with f_d = 33.3 Hz. QPSK constellation, coding rate 1/3.

It was finally shown that, for $R = 1/5$, 4 iterations of DB-TCs show better performance than 50 flooding or 25 layered of the LDPC code over static and mobile channels. For $R = 1/3$, 5 iterations of DB-TCs show quasi-identical performance to 50 flooding or 25 layered iterations of the T2 LDPC code over Gaussian and Rayleigh channels. For $R = 2/3$, 6 iterations of DB-TCs are needed.

A second stage of the comparison is based on a joint work with Panasonic Langen in Germany. Floating-point decoder models of the turbo and the LDPC decoders were elaborated. For the turbo decoder, both the Log-MAP and the Max-Log-MAP decoding algorithms were considered. For the LDPC decoder, the model was based on the sum-product algorithm using the Gallager computation of the hyperbolic tangent function (low-complexity but challenging for a real implementation, due to the detrimental effect of quantization on performance). Based on these models, a Graphical User Interface (GUI) application was developed in Matlab in order to compare both architectures in terms of number of logic operations and memory accesses. Table 4 shows the figures provided by the Matlab GUI for a target data throughput of 4 Mbit/s, as agreed in the DVB-NGH working group.

From these figures, the comparison of the logic requirement for both types of decoders is not straightforward: the number of required additions is higher for the TC decoder than for the LDPC code. However, in the GUI Matlab application, floating-point additions are considered for the LDPC decoder whereas the turbo decoder only needs integer additions. From the memory requirement point of view, for a decoder implementing coding rates from 1/5 to 2/3, the LDPC decoder memory requirement is 217% the TC decoder requirement. Concerning the total number of memory accesses, which is directly related to the decoder power consumption, the LDPC decoder requires from 320% to 570% more memory accesses than the TC decoder, depending on the coding rate. This important difference indicates that the LDPC decoder should logically be less power efficient than the TC decoder. This has an important impact on battery life since a mobile application is targeted.

	16K LDPC decoder			16K turbo decoder		
	R=1/5	R=1/3 @42Mhz	R=2/3 @48Mhz	R=1/5	R=1/3 @42Mhz	R=2/3 @48Mhz
Input memory size (LLRs)	16,200	16,200	16,200	16,200	16,128	16,176
Extrinsic memory size (LLRs)	48,600	54,000	54,000	3,240	8,064	16,176
Internal memory size	96	120	120	512	512	512
Input memory read	1,215,000	1,350,000	1,350,000	155,520	215,040	323,520
Extrinsic memory read	1,215,000	1,350,000	1,350,000	49,680	145,152	355,872
Extrinsic memory write	1,215,000	1,350,000	1,350,000	24,840	72,576	177,936
Internal memory read	1,215,000	1,350,000	1,350,000	414,720	430,080	1,035,264
Internal memory write	1,215,000	1,350,000	1,350,000	414,720	430,080	1,035,264
Number of additions (floating point additions for LDPC)	4,860,000	5,400,000	5,400,000	6,246,720 4,639,680	14,757,120 10,563,840	34,487,232 24,393,408
Number of LUT accesses	2,430,000	2,700,000	2,700,000	6,246,720 0	7,096,320 0	17,081,856 0
Number of adders	96	96	48	168 / 122	370 / 262	362 / 254
Number of LUTs	48	48	24	242 / 0	252/ 0	252 / 0
Info. throughput [Mb/s]	n/a	4.0	4.6	n/a	4.2	4.0

Table 4: Number of operations and memory accesses required for the implementation of an LDPC and turbo decoder, targeting a information data throughput of 4 Mbit/s. For the turbo decoder, both the Log-MAP (blue figures) and the Max-Log-MAP (red figures) algorithms are taken into account. Figures provided by Panasonic.

A third comparison point is based on an actual implementation performed by the technical university of

Kaiserslautern, taking into account the target throughput of 4 Mbit/s.

Table 5 shows the area estimate obtained from the logic synthesis results. It appears that the logic area represents less than one quarter of the overall area and cannot be used alone to compare the complexity of the two decoders. In a DVB-NGH context, the turbo decoder is shown to be 20% less complex than the DVB-T2 LDPC decoder and 30% less complex than the LDPC+BCH decoder while guaranteeing a higher efficiency.

	ASIC 65nm@300MHz after synthesis, real memory cuts	
	DB-TC decoder	**LDPC decoder**
Logic	**0.09**	**0.05**
Memories	**0.31**	**0.46**
BCH decoder		**0.08**
Overall area (mm^2)	**0.40**	**0.59**
Decoding algorithm	Max-Log-MAP+ ESF 8 iterations	Lambda 3-Min 40 iterations
Parallelism	1 ACS	8 CNs, serial CN
Payload throughput/iter	17 Mbit/s (R≥1/3) 10 Mbit/s (R<1/3)	15 Mbit/s (R= 3/4) 4 Mbit/s (R=1/5)
Efficiency [4] (**Mbit/s/mm^2**)	42.5 (R≥1/3), 25.0 (R<1/3)	29.4 – 7.8

Table 5: Area estimate of a 16-state double binary TC and a LDPC decoder for DVB-NGH block sizes and coding rates, targeting a information data throughput of 4 Mbit/s. Figures provided by the technical university of Kaiserslautern.

3.1.1.4 Conclusion

The 16-state DB-TC proposed for DVB-NGH was compared in terms of performance and decoding complexity with the reference DVB-T2 LDPC+BCH code. This work was carried out in the framework of the Constellation, Coding and Interleaving (CCI) working group in DVB-NGH. The performance and complexity superiority of the 16-state DB-TC was demonstrated and acknowledged by the TM-H group.

Finally a two-fold standardization approach was adopted by the group:

- T2-mobile and NGH-phase 1: following a strong request from broadcasters, a first version of the standard will be closely aligned with DVB-T2. Thus the DVB-T2 LDPC code is kept for this first version.
- NGH-Phase 2: a second version of the standard is under study, which should be more closely aligned with the broadcast mode of the mobile networks (LTE e-MBMS). Then a TC-based FEC solution should be adopted.

3.1.2 L1 signalling robustness improvement techniques

This section describes a study carried out by **Universidad Politécnica de Valencia/ iTEAM Research Institute (UPV-iTEAM)** on the different techniques proposed for the robustness improvement of Layer 1 (L1) signalling in DVB-NGH.

3.1.2.1 Introduction

The sheer terrestrial profile in DVB-NGH has adopted three new mechanisms in order to enhance the robustness of the layer 1 (L1) signalling: 4K LDPC codes (mini-codes), Additional Parity (AP), and Incremental Redundancy (IR). These mechanisms substitute the L1 repetition scheme from DVB-T2, being the use of In Band signalling optional in DVB-NGH.

The headers of Layer 1 have also been optimized (L1-Configurable and L1-Dynamic). New techniques have been adopted to reduce the overhead in the transmission such as the periodic transmission of L1-Pre and L1-Configurable and Self-decodable L1-Configurable.

The goal of this section is to investigate the feasibility of the new techniques for L1 signalling robustness and to study which configurations provide the best performance depending on the channel characteristics and operator's requirements. First, a summary of the L1 Robustness in DVB-T2 issue is given. Then, the abovementioned robustness mechanisms adopted are explained and, finally, the new techniques for reducing and optimising the L1 headers are argument.

3.1.2.2 Summary L1 Robustness in the Sheer Terrestrial NGH Profile

It is observed that L1 signalling in DVB-T2 does not have enough time diversity, and it is only spread in few OFDM symbols. In contrast, the data path is spread in time and it could be more robust than L1 signalling in mobile channels.

The L1 signalling robustness in DVB-T2 can be increased by transmitting in each frame the signalling related to the current frame and the following frame. This mechanism is known as L1 repetition. L1 repetition implies an increment in the zapping time in case the first frame is received erroneously. In addition, this mechanism increases the signalling information and less data can be signalled. Another technique that enhances the L1 signalling robustness is known as In-Band Signalling and consists of transmitting the signalling information though out the data path. This technique enhances the continual reception and provides the same robustness as data has. However, In-Band signalling introduces some problems in first synchronization and initial zapping. As a consequence, there is a need to improve the signalling robustness and an overhead reduction for mobile environments.

DVB-NGH improves L1 signalling robustness by adopting several mechanisms. These mechanisms are divided in two groups: 1) mechanisms that enhance the L1 signalling robustness by getting more time diversity in the signal and better performance in reception, and 2), those mechanisms which aiming at optimization and overhead reduction.

16K LDPC codes are used in DVB-T2 for L1 signalling with padding and puncturing methods in order to adapt the information to the code word, but robustness is reduced. DVB-NGH 4k codes were introduced to optimize the performance provided by the 16K codes used in DVB-T2, providing several advantages. The abovementioned mechanisms that enhance the time diversity of signalling are Incremental Redundancy (IR) and Additional Parity (AP). In IR 8K LDPC codes are used, the L1 repetition mechanism is replaced and more additional parity bits than 4K LDPC code are provided. AP enhances the robustness by transmitting the punctured bits and, optionally, adopting the In-Band scheme signalling from DVB-T2.

The signalling structure in DVB-T2 allows each PLP to have completely independent parameters and features. In contrast, in DVB-NGH this is unfeasible since the signalization has been re-structured. The PLPs are associated by configurations with the same features, optimizing the L1 headers. Moreover, in DVB-T2 transmissions, the properties of the channel signalled in L1-Pre and the configuration and features of each PLP signalled in L1-Configurable are transmitted in every T2 frame. The values of these two fields seldom change per super frame and can be considered constants. In DVB-NGH these fields are split in *n* frames, and

in every frame a portion will be sent at the same position reducing de L1 overhead.

These new mechanisms and methods adopted are detailed in the following points.

3.1.2.2.1 4KLDPC Codes

In DVB-T2, the L1 signalling is protected with 16K LDPC with a fixed code rate 1/5 for the L1-pre and a code rate 4/9 for the L1-post. The L1 signalling information of DVB-T2 does not generally fill one 16K LDPC code word. In order to keep the code rate effectiveness, the LDPC code word needs to be shortened and punctured, which degrades the performance. DVB-NGH adopts for L1 signalling new 4K LDPC codes of size 4320 bits.

The shrunk size of 4K LDPC codes is more suitable for signalling, and considerably reduces the amount of shortening and puncturing, see Table 6. The code rates adopted for L1-pre and L1-post in DVB-NGH are 1/5 and 1/2, respectively.

LDPC Codes	Code Rate	Information bits	Parity bits	NGH L1 Signalling	Shortening bits	Puncturing bits
4K	1/5	864	3456	640	224	896
4K	1/2	2160	2160	640	1520	1520
16K	4/9	7200	9000	640	6560	8200
16K	1/2	8100	8100	640	7460	7460

Table 6: 4K Codes vs 16K Codes

16K LDPC codes provide a better performance than 4K LDPC codes without padding and puncturing. However, due to the reduced size of the L1 signalling information, 4K LDPC codes actually outperform in the order of 1-2 dB 16K LDPC codes. The main benefits of 4k codes are fast convergence, lower power consumption and fast detection. 4k codes consume less power thanks to reduced number of padding and puncture bits, so less iteration is needed to obtain the L1 signalling information bits and get better performance in compare with 16K. Reduced number of padding and puncturing methods consume less power and L1 are detected faster (fast convergence).

3.1.2.2.2 Additional Parity (AP)

The technique of AP replaces the L1-Repetition mechanism in DVB-T2. AP consists of transmitting punctured LDPC parity bits on the previous NGH frame and exploiting the time diversity of the mobile channel, resulting in an increase of the L1 signalling robustness but reducing the effective code rate. This new technique obtains a better performance in comparison with just repeating the information in the frame (L1-repetition).

L1-post signalling is coded by an inner BCH and 4K LDPC outer code. Shortening and puncturing methods allow maintaining the global code rate according to the information length, as shown in Figure 29. The key issue of AP are the puncturing method and how to use profits of this method.

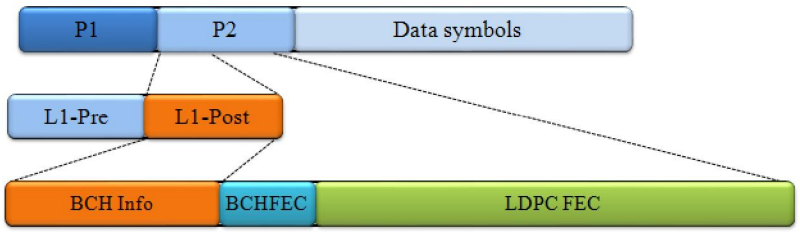

Figure 29: L1-Post codification.

Puncturing Method

This method is used to maintain the global code rate depending on the amount of signalling information bits. All LDPC parity bits denote by $\{p_0,p_1,\ldots\ldots,p_{Nldpc-Kldpc}\}$ are divided into Q_{ldpc} parity groups where each parity group is formed from a sub-set of the LDPC parity bits as follows:

$$\boldsymbol{P_j = \{p_k |\ k\ mod q = j, 0 \le k < N_{ldpc} - K_{ldpc}\} \quad for \quad 0 \le j < q}$$

Equation 1: Parity group calculation, where Pj represents the j-th parity group

Each group consists of 360 parity bits and the total number of Q_{ldpc} groups depends on the LDPC parity length. (Qldpc= LDPC parity length /360), as illustrated in Figure 30.

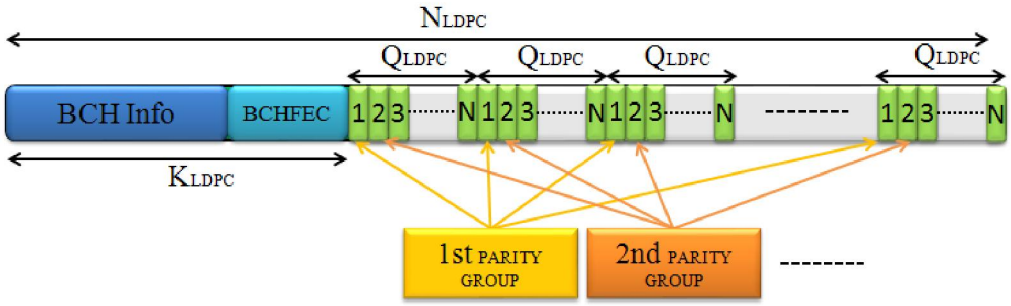

Figure 30: Parity bit groups in an FEC Block

Puncturing of LDPC parity bits is performed on a bit-group basis following the order predetermined by the standard, *i.e.* puncturing pattern. The puncturing pattern depends on the modulation and code rate employed, and shows which Qldpc groups have to be punctured depending on the signalling information length. As illustrated in Figure 31, specific parity groups have been punctured according to the puncturing pattern.

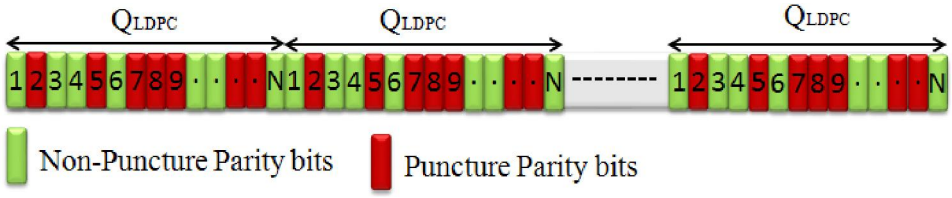

Figure 31: Puncturing of LDPC parity groups

AP Generation rule

AP extends the new 4k LDPC with additional parity bits to provide additional robustness. These additional bits are the punctured bits. When AP is applied, the new configuration of the codeword results as shown in Figure 32.

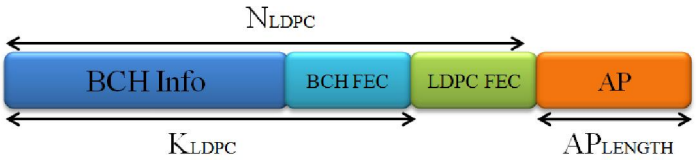

Figure 32: The resulting LDPC code word with Additional Parity bits

The length of this additional part is denoted AP length, and it is obtained from Equation 2, where K is defined as 1/3, AP_RATIO {0,1,2,3,..}, and p(L1_post) gives the number of parity bits corresponding to the L1_Post_block.

$$AP_{LENGTH} = K \cdot L1_{APRATIO} \cdot p(L1_{POST})$$

Equation 2 : Additional Parity length calculation

Advantages

The main advantage of using AP is that the effective coding rate for L1 signalling could be reduced without any LDPC matrix. The following table shows the effective code rate achieved for different configurations with parameter K=1/3.

Num PLP	CR	K_sig	Parity bits	AP bits			Code Rate Achieved		
				AP_Ratio=1	AP_Ratio=2	AP_Ratio=3	AP_Ratio=1	AP_Ratio=2	AP_Ratio=3
1	1/2	610	610	204	408	612	0,4284	0,3747	0,333
1	1/5	610	1830	610	1220	1830	0,2	0,1667	0,1429

Table 7 : Additional Parity benefits

Note that in the AP mechanism, punctured bits are transmitted first. For a given frame, its parity is sent in two consecutives frames. The additional parity is sent in the previous frame as incremental redundancy, and the basic FEC is sent with information at the same time, as depicted in Figure 33, where I, B, P and AP, are the information fields, BCH FEC bits, basic parity bits and additional parity bits, respectively.

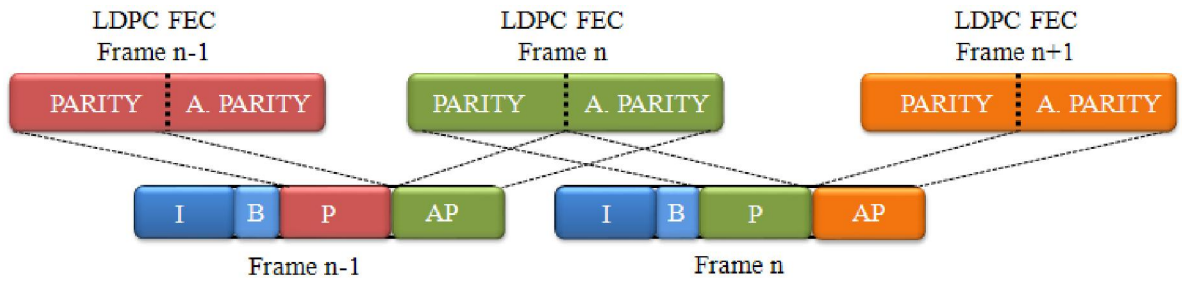

Figure 33: The resulting LDPC code word with Additional Parity bits

3.1.2.2.3 Incremental Redundancy (IR)

IR replaces the L1 repetition mechanism and introduces a new FEC scheme. Initially, IR is thought to get additional bits when are required. As a starting point, IR uses 4k LDPC mini codes in order to reduce latency and decoding complexity at a low code rate. The main idea behind IR is to extend this new 4k LDPC with additional parity bits (another 4k codeword) to provide additional robustness. IR only applies with 1/2 code rate, resulting an extended codeword at 1/4 code rate.

IR Generation rule

The basic FEC 4k is the conventional FEC, where the LDPC encoder code rate input is R_0=1/2, where R_0 = K_{ldpc}/ N_{ldpc}. K_{ldpc} are the output bits from the BCH encoder, and that output is a systematic codeword of length N_{ldpc}. The last N_{ldpc} - K_{ldpc} bits of this codeword are the LDPC parity bits, named as LDPC FEC at Figure 34.

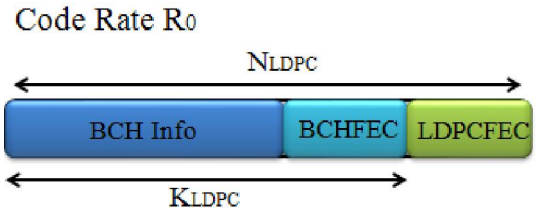

Figure 34 : Basic FEC 4K.

IR uses special 8K LDPC codes (8640 bits) for coding L1 signalling information bits. These codes have been created to obtain the same parity bits as 4k LDPC codes, taken into account the first 4K bits, and they have special properties.

The resulting codeword of applying the IR mechanism can be differentiated in two parts: the first part corresponds to the basic FEC and in the second part the additional parity bits are located. This basic FEC concerns as a 4K LDPC code has been used to code the signalling information bits, and the additional parity bits are going to be used as IR and named as MIR at Figure 35.

The codeword length is, thus, 8K bits, and it is composed by $N_{ldpc},1 = N_{ldpc} + MIR$. The LDPC encoding with IR can be considered as one encoder of code rate $R1 = K_{ldpc}/N_{ldpc},1$, initially $R_1 = 1/4$, where the output is split into two 4K codeword, basic FEC and an IR part. The relationship between original codeword and extended codeword can be seen in Figure 36.

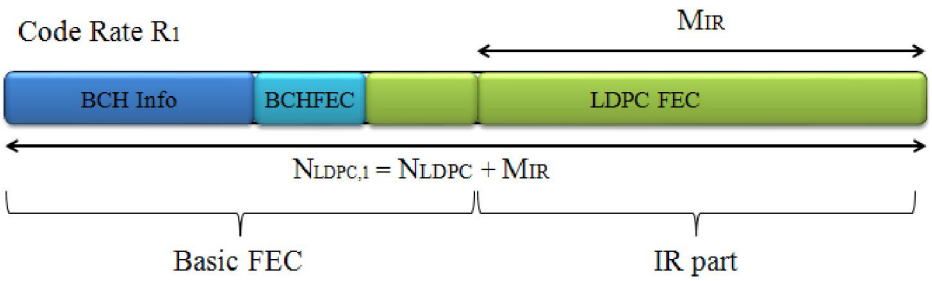

Figure 35 : Extended Codeword. Basic FEC+ IR part (8K codeword)

IR Method

When IR is applied, the amount of LDPC parity bits has increased to $N_{ldpc} - K_{ldpc}$+ MIR. However, the main property of the 8K LDCP code is that the first $N_{ldpc} – K_{ldpc}$ parity bits are identical to the parity bits of the 4K basic FEC with 1/2 code rate. In addition, the codeword is divided into two parts: the first Nldpc bits are the basic FEC part, while the remaining MIR bits are the IR part to be used as additional parity at the receiver. This IR part (MIR bits) is sent in different transmission times in the following way: first, the basic FEC is sent, and then, the IR part if it is needed. IR replaces L1 Repetition from DVB-T2, avoiding sending the same information in consecutives frames. IR sends a 4K codeword with new parity bits.

Thus, depending on the channel characteristics it is ensured that the decoding of the received codeword is possible in good channel conditions with a R_0–rate decoder, which only takes into account the basic FEC part, while the extended codeword, consisting of both basic FEC and IR part, permits the decoding with a R1-rate decoder in bad channel conditions.

The main advantage of IR is that the IR part can be ignored by the receiver unless it is needed.

The main objective of this section is to analyze the most effective transmission mode and which receiver parameters are the most suitable. Finally, the operator will decide the use of IR or not depending on the transmission characteristics.

3.1.2.3 L1 Signalling overhead reduction and optimization

3.1.2.3.1 L1-Configurable overhead reduction

In DVB-T2 the signalling mechanism allows each PLP to have completely independent parameters in the signalling process. In all realistic situations there will only be a very limited number of PLP configurations used in a given transmission. This means that several PLP will use exactly the same features as MODCOD. For this reason, DVB-NGH suggests a re-structure of the signalling method, associating the PLPs with the same features.

The PLP signalling loop in L1 Configurable from DVB-T2 defines all the features of each PLP. These features are the characteristics of each PLPs, as the name (ID) of each PLP, the modulation and codification used, the PLP location inside the NGH frame and its length. These features can be repeated in different PLPs. The properties that are the same are grouped in PLP configurations. With different configurations, each PLP is linked to its associated configuration. As a consequence, each PLP is not more independent form others, reducing the L1 signalling overhead.

For this reason, the signalling loop in L1 Configurable from DVB-NGH is split into two different loops. The first loop defines the different PLP configurations and associating each configuration with a short code (PLPMODE_ID). On the other hand, the second loop is a loop over PLP_IDs that defines the PLPs themselves. This second loop associates each PLP_ID with the code above.

In this way there are only 6 bits per PLP in the PLP loop and only a very limited number of PLP configurations are required inside the PLP configuration loop. This solution allows for a totally general case, with unique configurations for up to 255 PLPs, but in the typical use cases the required amount of L1-Config is radically reduced.

In addition, the L1-Config format from DVB-T2 is very general and supports a lot of features as aux streams, reserved fields, possibility to send a PLP only in certain frames, TFS, more than one PLP group, time interleaving over 255 frames, etc. However, in a particular use case, only a few of these features will be probably used and, hence, the others could be removed or reduced in size. In this case, the introduction of a flag field in the beginning of the L1-config can signal whether the feature is available or not. This flag field will be one bit per feature. The new L1-Config format is illustrated in Table 8.

The overhead savings for L1-Configurable and L1-Dynamic have been calculated. The study has been done assuming the number of required PLP modes or configurations are 1/4 of the total number of PLPs. The savings using this reduced overhead are ~0.85%, considering quite extreme cases in terms of number of PLPs (the more PLPs, the higher savings). Figure 36 shows the comparative of different overhead structures.

The main advantage of applying this signalling structure is that the zapping time is not affect; it is only about how the signalling structure is defined. [8][9].

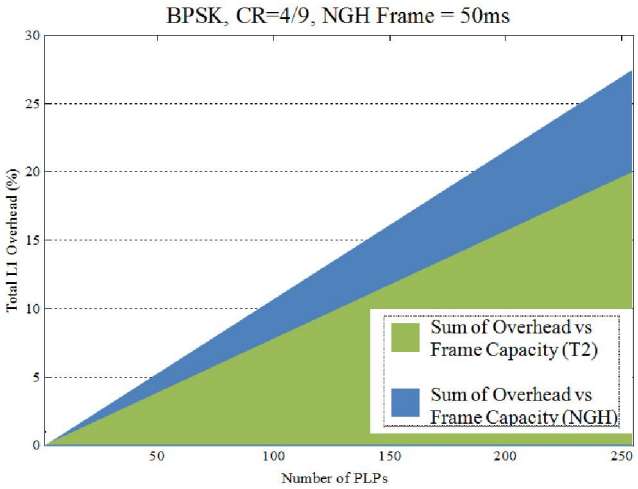

Figure 36 : Comparison between different overheads structures.

FIELD	SIZE (Bits)
L1_POST_OPTIONS	18
NUM_PLP	8
NUM_PLP_MODES	6
SUB_SLICES_PER_FRAME	10
NUM_AUX	4
AUX_CONFIG_RFU	8
NUM_NGH_FRAMES	8
NUM_CELLS_NGH_FRAME	22
for i=0:NUM_RF-1{	
L1_RF_FREQUENCY	32
}	
for i=0:NUM_PLP-1{	
PLP_ID	8
PLPMODE_ID	6
PLP_GROUP_ID	8
FIRST_FRAME_IDX	8
PLP_REP_INT	3
RESERVED_1	3
}	
for i=0:NUM_PLP_MODES-1{	
PLP_TYPE	3
PLP_PAYLOAD_TYPE	5
PLP_COD	3
PLP_MOD	3
PLP_ROTATION	1
PLP_FEC_TYPE	2
PLP_NUM_BLOCKS_MAX	10
FRAME_INTERVAL	8
TIME_IL_LENGTH	8
TIME_IL_TYPE	1
IN_BAND_A_FLAG	1
IN_BAND_B_FLAG	1
STATIC_FLAG	1
STATIC_PADDING_FLAG	1
PLP_MODE_REP_INTERVAL	3
RESERVED_2	10
}	
RESERVED_3	32
for i=0:NUM_AUX-1{	
AUX_STREAM_TYPE	4
AUX_PRIVATE_CONf	28
}	

L1_POST_OPTIONS	Bits
TYPE_2	1
AUX	1
L1_CFG_PERIODIC	1
L1_MODE_PERIODIC	1
DETERM_L1_SCHED	1
PLP_GROUPING	1
RSV_FLAG	12

Table 8 : The new L1-Config format for DVB-NGH

3.1.2.3.2 N-periodic L1-Pre and L1-Configurable transmission and Self-decodable L1-configurable

In T2 transmissions, L1-Pre and L1-Configurable are transmitted in every T2 frame. L1-Pre signals the properties of the channel (GI, PP, L1 ModCod...), it has a fixed length of 200 bits and it is fixed BPSK-modulated with a 1/4 code rate. L1-Pre is used for accessing L1-Config. On the other hand, L1-Config signals the configuration of the PLPs (ModCod, time, interleaver settings, frequencies..). The values of these two fields may change per superframe, but in practice only change when the multiplex of the RF-channel is reconfigured and this rarely happens.

As these values do not usually change, the transmission of L1-Pre and L1-Configurable can be split in *n* frames. The split part of L1-Pre and L1-Configurable will be at the same position but their length is reduced by a factor of *n*. A portion of these fields of every frame will be sent and the contents of L1-Pre and L1-Configurable will be completed after *n* frames.

The spreading of quasi static signalling contents to several frames, improves the time diversity, and reduces the signalling overhead by a factor *n*.

Figure 37 is meant to clarify the concept of n-periodic transmission, and illustrates the case when L1-Pre and L1-Configurable fields are spread by a n factor of 4.

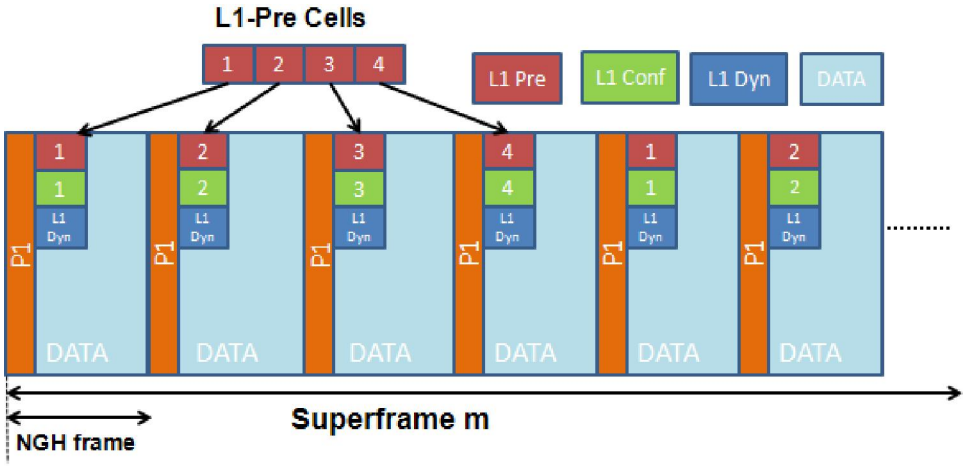

Figure 37 : Comparison between different overheads structures.

The selection of the parameter n is a trade-off between channel scanning time and signalling overhead.

Table 9 shows the results of the capacity savings with n-periodic signalling.

Capacity savings with n-periodic Signaling							
PLPs	**DVB-T2 Capacity**	**N-periodic Signaling**					
		L1-Pre + L1-Config		**L1-Config Only**		**L1-Pre Only**	
		n = 4	**n = 8**	**n = 4**	**n = 8**	**n = 4**	**n = 8**
1	1.28%	0.72%	0.8%	0.13%	0.16%	0.59%	0.64%
4	1.62%	0.89%	0.99%	0.30%	0.35%	0.59%	0.64%
8	2.07%	1.11%	1.25%	0.52%	0.61%	0.59%	0.64%
16	2.98%	1.56%	1.77%	0.97%	1.13%	0.59%	0.64%
32	4.78%	2.43%	2.79%	1.84%	2.15%	0.59%	0.64%

Table 9 : Parameters for overhead calculation: 8K FFT, GI 1/4, 50ms Frame duration, BPSK, CR 1/3 for L1-Pre and L1-Config [9]

However, the channel scanning time increases when the receiver is switched on for the very first time. Joint encoding for L1-Configurable and L1-Dynamic degrades the L1-configurable robustness since a single error makes all L1-Configurable parts useless. N-periodic transmission increases the initial acquisition delay by n factor. This is a major problem in case of TFS since the receiver will not be able to know which the next frequency is.

To mitigate these disadvantages, instead of splitting the L1-Configurable into n blocks based on the basis of guaranteeing the same length of L1-Configurable portions, the L1-Configurable has to be divided into fixed-length portions of self-decodable L1-configurable information.

Applying this fixed length of L1-Configurable new advantages appear. No delay can be obtained for the constant signalling information, which is desirable since signalling information cannot tolerate any delay (TFS info or FEF info). The PLP delays are also controlled: PLPs which cannot tolerate any delay can be sent with zero delay.

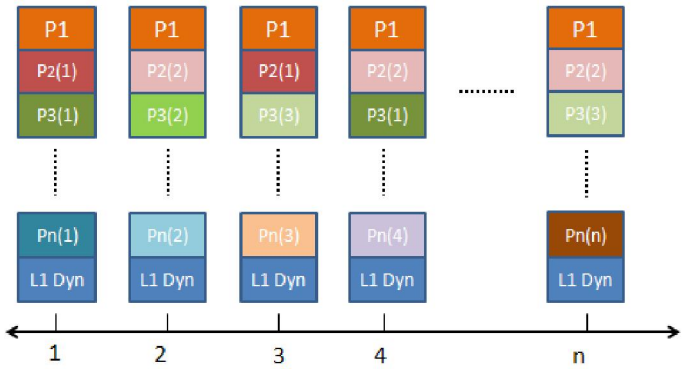

Figure 38 : Transmission mode of PLPs as a function of their repetition interval

The PLPs are sorted as a function of their repetition interval, i.e. PLPs with lower repetition interval are transmitted first. For the PLPs with the same repetition rate the PLP with the lower PLP_id is transmitted first. This sorting allows the receiver to know in advance some PLPs that will be signalled in the following frames.

The receiver starts decoding every portion of L1-Configurable. Figure 39 shows the signalling of the PLPs that are known before decoding.

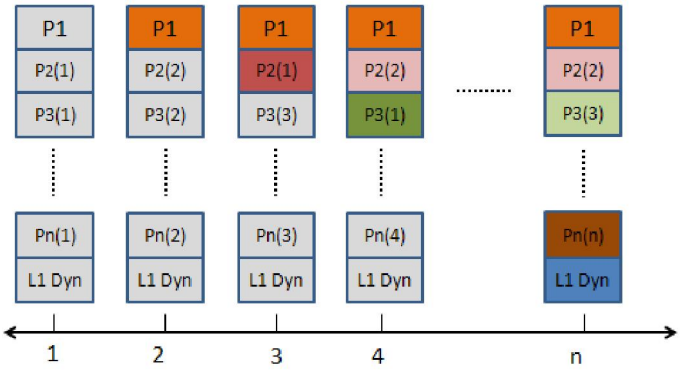

Figure 39 :Reception exemple, assuming L1-Configurable is decoded correctly in every frame

Using fixed portions of L1-Configurable, the probability of correct detection increases every time more information of L1-configurable is available. Zero delay is guaranteed for the constant signalling (e.g. TFS info or FEF info) and it is provided a better trade-off between overhead reduction and zapping delay,

controllable on a PLP basis according to the PLP's corresponding service requirement.

In addition, superposed correlation sequence is used to detect the portions and the order of the L1-pre portions. A virtual QPSK with superposed PRBS sequence is used to detect n sequences within a single NGH-frame and estimate the order of the L1-pre portions. As Figure 40 illustrates, both I and Q paths transmit the signalling data. The Q path is cyclically shifted and XOR connected with the PRBS sequence.

The detection can be possible even at negative SNR, and the decoding performance is not degraded compared to usual BPSK due to LLR combining of the I and Q path [5][6].

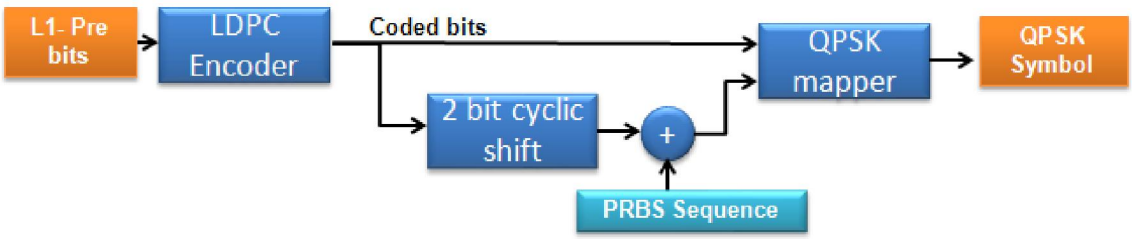

Figure 40 : The Q path is ciclically shifted and XOR connected with the PRBS sequence

3.1.2.4 Performance of L1 Robustness

The objective of the simulations is to check and validate the solutions adopted mentioned above for different channels. The following tables summarize the simulation conditions used to study the different mechanism adopted.

L1 Signalling	
Parameter	*Value (bits)*
L1conf_est	142
L1conf_var	34
L1conf_PLPCONF	61
Num_PLPCONFIG	4
L1dyn_est	49
L1dyn_var	8
CRC	16
BCH	100

A) **The signalling fields of Configurable L1-post signalling**

L1 Signalling length equations
L1conf = L1conf_est+Num_PLP*L1conf_var+ L1conf_PLPCONF*Num_PLPCONFIG
L1dyn = L1dyn_est+Num_PLP*L1dyn_var
K_post =L1conf+L1dyn+CRC
K_sig = K_post + BCH

B) **L1-post signalling length calculation as a function of the number of PLPs**

Table 10 : L1-Post Signalling Fields

Simulation Framework			
	Parameter		Value
L1 Robustness Mechanism	Additional Parity	L1_AP_RATIO	1
		L1_AP_K	1/3
	Incremental Redundancy		8K LDPC CR=1/4

Table 11 : Robustness Mechanism Simulations Framework

Code Rate 1/2

Additional Parity Mode

Num_PLP	K_post	L1_Conf	L1_Dyn	K_sig	Parity bits	Puncture bits	AP bits	Code Rate Achieved
1	510	420	57	610	610	1550	204	0,4283
4	636	522	81	736	736	1424	246	0,4284
8	804	658	113	904	904	1256	302	0,4284
-	-	-	-	2160	2160	0	0	0,5

Incremental Redundancy Mode

Num_PLP	K_post	L1_Conf	L1_Dyn	K_sig	Parity bits	Puncture bits
1	510	420	57	610	1830	4650
4	636	522	81	736	2208	4272
8	804	658	113	904	2712	3768
-	-	-	-	2160	6480	0

Code Rate 1/5 (1/4)

Additional Parity Mode

Num_PLP	K_post	L1_Conf	L1_Dyn	K_sig	Parity bits	Puncture bits	AP bits	Code Rate Achieved
1	510	420	57	610	1830	1410	610	0,2
4	636	522	81	736	2208	1032	736	0,2

3.1.2.4.1 AWGN Channel

	Parameter		Value
OFDM	FFT Size		8192 (8K)
	BW		8MHz
	NGH Frame		50ms
Channel	Channel Model		AWGN
L1 Signalling	Number of PLPs		1,4,8
	MODCOD	Constellation	BPSK, CR 1/2 1/5
		Coding	4K LDPC
		Decoding	50 iterations, Fabrice Decoder

Table 12 : AWGN channel simulations framework

3.1.2.4.2 TU-6 Channel

	Parameter		Value
OFDM	FFT Size		8192 (8K)
	BW		8MHz
	NGH Frame		50ms
Channel	Channel Model		TU6
	Doppler		10Hz, 33.3Hz, 194.8Hz
L1 Signalling	Number of PLPs		1,4,8
	MODCOD	Constellation	BPSK, CR 1/2 1/5
		Coding	4K LDPC
		Decoding	50 iterations, Fabrice Decoder

Table 13 : TU-6 Channel Simulations Framework

3.1.2.5 Future Work

The next step is to focus on the determination of the optimum parameters according to the use case and the settings of coding-interleaving parameters for data. Moreover, the evaluation of the overhead due to the L1 signalling and determine the use case of additional parity bits and Incremental redundancy mechanism for the different configurations.

3.1.3 BaseBand inter Frame FEC (BB-iFEC)

This section describes a study carried out by **Universidad Politécnica de Valencia/ iTEAM Research Institute (UPV-iTEAM)**. It presents a novel Forward Error Correction (FEC) and Time Interleaving (TI) scheme, known as BB-iFEC (Base Band - inter-burst FEC) [10], proposed for both satellite and terrestrial profiles of DVB-NGH. BB-iFEC aims at providing long time interleaving with fast zapping support. This feature is key for satellite transmissions, because the Land Mobile Satellite (LMS) channel is characterized by long signal outages (e.g., due to the blockage of the line of sight with the satellite caused by tunnels, buildings, trees, etc.), which can only be compensated with a long time interleaving duration (in the order of 10 s) [11]. But long time interleaving with fast zapping is also of interest for terrestrial transmissions, because it allows exploiting the time diversity of the mobile channel in high-speed reception scenarios (e.g., vehicles, trains). Although other technical solutions have been proposed in DVB-NGH to increase the diversity of the mobile channel in other dimensions (e.g., in the frequency domain with time-frequency slicing TFS, or in the spatial domain with multiple-input multiple-output MIMO antenna configurations), there is no doubt that in some scenarios and for some applications time diversity can provide very important gains (e.g., vehicles, trains) [12], [13] . One of the features of BB-iFEC is that it is backwards-compatible, in the sense that it allows the coexistence of terminals with and without BB-iFEC. Therefore, it is also proposed as an optional feature for the terrestrial profile of DVB-NGH.

3.1.3.1 BB-IFEC Overview

BB-iFEC is based on the link layer MPE-iFEC (Multi Protocol Encapsulation inter-burst FEC) scheme of DVB-SH [14]-[17]. The main differences are that it is integrated in the physical layer, that it allows for both soft and hard decoding at the receivers, and that it re-uses the 16K LDPC codes adopted in DVB-NGH instead of using a Reed-Solomon code. The time interleaving is similar to the time interleaving of MPE-iFEC with sliding window Reed-Solomon encoding, although it is not identical.

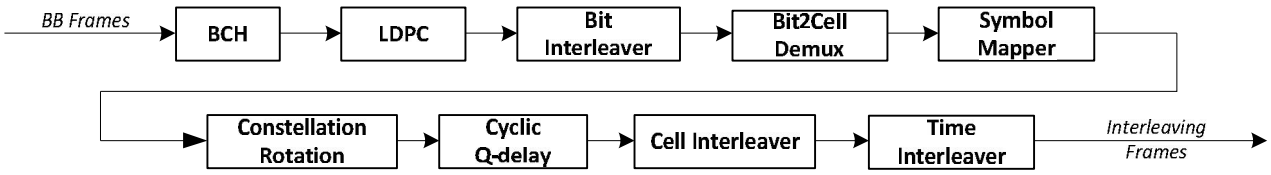

Figure 41: DVB-T2 BICM (Bit Interleaved Coding and Modulation) module at the transmitter.

Figure 41 shows the complete BICM (Bit Interleaved Coding and Modulation) module of DVB-T2. The FEC is based on the concatenation of an LDPC (Low Density Parity Check), which performance approaches within 1 dB the Shannon limit, and a BCH (Bose Chaudhuri Hocquenghem), that removes the error floor of the LDPC. The bit interleaver and the bit2cell demultiplexer compensate the unequal bit protection performed by the LDPC code, assigning the less protected bits to the more robust constellation points. Rotated constellations are used to provide additional robustness to the transmission, by transmitting in different instants (in time and frequency) the I and Q components of each constellation symbol [17]. The time interleaver is a block interleaver that operates with cells (constellation symbols). It allows inter-frame interleaving, but it does not provide fast zapping support [19]. The average zapping time is approximately 1.5 times the time interleaving duration [20].

BB-iFEC introduces an additional FEC and an additional time interleaver (TI). Therefore, there are two FECs and two TIs, denoted as inner and outer, respectively. Fig. 2 shows the modifications to the DVB-T2 BICM module of DVB-T2 at the transmitter to introduce BB-iFEC. Four new blocks are introduced: transmission delay block, data spreading block, outer FEC block, and parity spreading block. The main configuration parameters of each block are:

- Transmission delay block: data delay, D.
- Data spreading block: data spreading factor, B.
- Outer FEC block: outer FEC code rate, CR_{outer}.
- Parity spreading block: parity spreading factor, S.

The outer TI corresponds to the data and parity spreading blocks. It should be pointed out that each TI makes use of a specific time de-interleaver (TDI) memory. Hybrid satellite-terrestrial terminals require an external TDI memory to account for the long TI requirements at the physical layer. With BB-iFEC, the external TDI memory is managed by the Outer TI, and the on-chip memory is used by the Inner TI. The Outer TI interleaves bits/LLRs instead of cells like the Inner TI.

As shown in Figure 42, BB-iFEC generates an additional PLP, known as iFEC PLP. The proposed scheme is configurable on a PLP basis, and thus it allows different levels of protection (interleaving duration and/or code rate) for different data PLPs. Moreover, it allows co-existence of terminals with and without BB-iFEC.

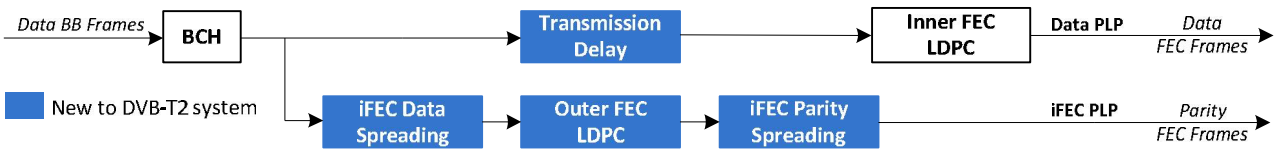

Figure 42: Modifications required at the DVB-T2 BICM module at the transmitter to include BB-iFEC. The iFEC PLP only transmits the parity generated by the Outer FEC. The only modification to the Data PLP is one buffer at the transmitter.

BB-iFEC operates on a burst basis, being possible to recover from completely erroneous bursts (i.e., it provides inter-burst FEC protection). The recommended cycle time is 1 sec, in order to provide fast zapping.

The Inner TI can be limited to intra-frame interleaving, but it can also perform inter-frame interleaving within 1 sec (typical trade-off between power saving due to time-slicing versus increased time diversity of continuous transmission). This way, the Outer TI does not interleave BB frames (packet data units of the DVB-T2 physical layer) which are already interleaved by the Inner TI. At the transmitter, after reception of a new data burst, all BB frames are first encoded with the BCH code, and then a parity burst is generated after data spreading, outer FEC, and parity spreading. Simultaneously, the original data burst can be encoded with the Inner FEC and subsequently transmitted.

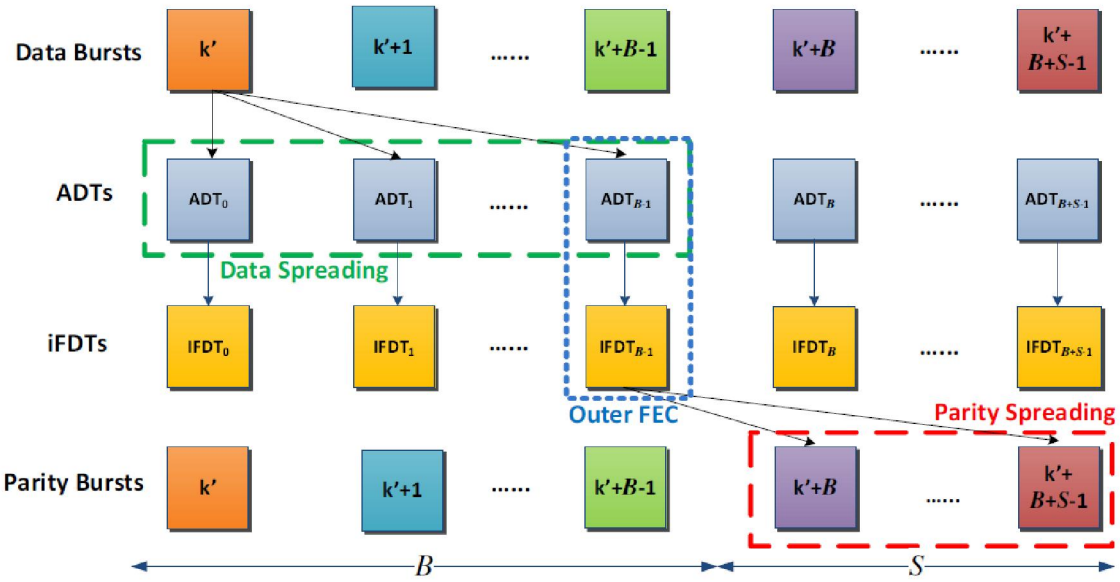

Figure 43: Inter-burst interleaving with BB-iFEC with the parity transmitted after the data ($D = 0$). The interleaving depth in number of interleaved bursts M, is equal to the data spreading factor, B, plus the parity spreading factor, S.

The interleaving depth in number of interleaved bursts, M, is given by both the data and parity spreading processes ($M = B + S$), with two possible values of D. Either $D = 0$, where the parity bursts are transmitted after the data bursts (see Figure 43), or $D = B + S$, where the parity bursts are transmitted before the data bursts. The two spreading processes employ a sliding window approach similar to sliding Reed-Solomon encoding in MPE-iFEC in DVB-SH [15]. In the data spreading process, the sliding window encloses B Application Data Tables (ADTs) which receive data BB frames from one data burst. At the transmitter, there are M ADTs. After reception of one data burst, one ADT is completely filled, and one iFEC Data Table (iFDT) is generated by the Outer FEC. In the parity spreading process, the sliding window encloses S parity bursts which receive BB frames from the generated iFDT. For each data burst, one parity burst is generated. Every burst the data and parity spreading sliding windows are shifted one element.

In Figure 42, it can be seen that with BB-iFEC there are three FEC encoding processes:

- BCH encoding of the data BB frames.
- Inner LDPC encoding of the Data PLP.
- Outer LDPC encoding.

Without considering the overhead introduced by the BCH, the overall code rate can be expressed as follows:

$$CR_{total} = 1/(1/CR_{inner} + 1/CR_{outer} - 1)$$

The code rate distribution for BB-iFEC represents a trade-off between fast zapping performance and overall performance. The protection after zapping is given by the Inner FEC of the Data PLP, whereas the Outer FEC exploits the long time interleaving. In general, it is recommended to put most of the protection in the outer FEC. BB-iFEC is a split FEC scheme, and there is a loss in performance with respect to single FEC

encoding in static channels, where the performance is given by the most robust code rate.

Table 14 shows typical examples of code rates for BB-iFEC.

CR_{total}	CR_{inner}	CR_{outer}
1/3	2/3	2/5
1/3	1/2	1/2
1/4	1/2	1/3
1/4	2/5	2/5
1/5	1/2	1/4
1/5	1/3	1/3

Table 14: Examples of code rate distributions for BB-iFEC.

For a given outer code rate CRouter and target interleaving depth *M*, the interleaving parameters of BB-iFEC *B*, *S*, and *D* can be derived as follows:

$$B = \lfloor M \times CR_{outer} \rfloor$$
$$S = M - B$$
$$D = B + S$$

where $\lfloor \cdot \rfloor$ denotes the *floor* function. This configuration minimizes the transition time between fast zapping mode and full protection mode, and guarantees a quasi-uniform time interleaving. This is elaborated in detail in the next section.

3.1.3.2 Main features of BB-IFEC

3.1.3.2.1 Transparency towards Upper Layers

BB-iFEC is not an upper layer FEC scheme but a physical layer FEC. Therefore, it is *fully transparent to the upper layers*, being compatible with any encapsulation protocol used. This feature is especially relevant in DVB-NGH, because two transmission protocol profiles are supported, in particular MPEG-2 Transport Stream (TS) and IP (Internet Protocol) [21].

3.1.3.2.2 Backwards-Compatibility

Since BB-iFEC generates an additional PLP, it *allows the co-existence of terminals with and without long time interleaving support without any drawback*. The only modification to the Data PLP is a delay in the transmission by an entire number of bursts. This feature is key in DVB-NGH, because the commercial requirements specify that the optional satellite component should not affect sheer terrestrial terminals [21].

Moreover, it also allows long time interleaving to be introduced as an optional tool in sheer terrestrial networks.

3.1.3.2.3 Soft and Hard Decoding Support

One of the main differences of BB-iFEC with respect to MPE-iFEC is that it allows to perform soft decoding, re-using the soft output of the Inner LDPC decoder. But BB-iFEC *allows both hard and soft decoding at the receivers*, being thus a scalable solution. There is a trade-off between memory consumption and performance. For hard decoding, two memory bits are required per information bit, since it is needed to denote three possibilities: 0, 1, or erased. For soft decoding, typically only four memory bits per LLR are required for satellite transmissions (e.g., in DVB-SH). Terminals with hard BB-iFEC decoding require thus half of the TDI memory than terminals with soft BB-iFEC decoding. However, in static conditions, the protection is only given by the Inner FEC. The Outer FEC protection is only useful in mobile conditions, and

there is also a degradation compared to soft decoding.

3.1.3.2.4 Reduced Signalling

BB-iFEC *requires very little signalling*. Only 12 bits are required to signal the value of the four BB-iFEC configuration parameters: outer FEC code rate CRouter (3 bits), data and parity spreading factors *B* and *S* (4 bits each), and data delay *D* (1 bit). The rest of the configuration parameters of the iFEC PLP would be the same than the parameters of its associated Data PLP.

3.1.3.2.5 Reduced VBR Signalling

For Variable Bit Rate (VBR) services, BB-iFEC requires to signal information about previously transmitted bursts to help the receivers to perform the time de-interleaving. The amount of signalling can be significant, especially for continuous transmission, since it is possible to interleave 40-50 frames. This information has to be transmitted in the dynamic field of the L1 (layer 1) signalling, which is very heavily protected for satellite transmissions (the data can be protected with QPSK 1/5). However, BB-iFEC *requires very little VBR signalling*. The reason is that the receivers only need help to perform the inverse of the parity spreading process (this is further elaborated in Section V). Furthermore, the combination of two levels of inter-frame interleaving with the Inner TI and Outer TI for the case of continuous transmission reduces the requirements for VBR signalling quite significantly, to a similar amount than for the case of discontinuous transmission.

3.1.3.2.6 Reduced BCH and BB Frame Overhead

In DVB-T2, each 16K LDPC BB frame carries 168 bits for BCH and 80 bits for the BB frame header [19]. This overhead is fixed, regardless the code rate, but lower code rates imply higher overheads because more BB frames are transmitted for the same amount of data. BB-iFEC can achieve very robust code rates with reduced overhead due to BCH and BB frame header. The reason is that the BB frames of the iFEC PLP do not carry BCH nor BB frame headers. The overhead is only due to the Inner FEC of the Data PLP.

3.1.3.2.7 TDI Memory Requirements

BB-iFEC is a very efficient solution from the TDI memory point of view due to two reasons. First of all, BB-iFEC requires less memory than a sheer block time interleaver like the one adopted in DVB-T2. The memory requirement is similar to a convolutional interleaver with uniform profile, and it is proportional to the factor (M + 1)/2 instead of M. Therefore, *the memory saving with respect a block interleaver tends to 50%.*

The second reason is that BB-iFEC *interleaves bits (LLRs) instead of cells (constellation symbols)*, like the DVB-T2 time interleaver. This is more efficient for the low order constellations considered for the DVB-NGH satellite profile (i.e., QPSK and 16-QAM). For cell interleaving, it is needed to store three components for each cell: real part, imaginary part, and channel state information. In DVB-T2, it is recommended to employ 10 memory bits for storing the real and imaginary parts [20]. BB-iFEC requires only 4 memory bits per bit/LLR (for soft decoding).

It should be pointed out that the required TDI memory in DVB-NGH with BB-iFEC is lower than the requirement in DVB-SH [17]. The reason is that BB-iFEC is applied on a PLP basis, not across the whole multiplex like in DVB-SH.

3.1.3.2.8 External TDI Memory Access

The power consumption when accessing the external TDI memory depends on the size of the Interleaving Units (IUs). The larger the IU size, the lower the power consumption. In DVB-SH, the IU length of the (bit) TI is 126 bits/LLRs [17].

The outer time de-interleaving of BB-iFEC operates with data BB frames after Inner LDPC decoding, which size depends on the code rate of the Inner FEC (e.g., for a code rate 2/3, the IU size is 10800 bits/LLRs [19]),

and with parity BB frames of constant size (the IU size in this case is 16200 bits/LLRs). Therefore, BB-iFEC *makes a very efficient access of the external TDI memory*, with IUs significantly larger than in DVB-SH.

3.1.3.2.9 Fast Zapping Support

The main feature of BB-iFEC is that *it allows fast zapping while providing long inter-frame interleaving* (e.g., 1 sec zapping time, 10 sec time interleaving). BB-iFEC has two operation modes as MPE-iFEC, known as early decoding and late decoding [15]. In early decoding mode, the data is protected only with the Inner FEC of the Data PLP, and the zapping time is given by the Inner TI. In late decoding mode, the protection is given by both Inner FEC and Outer FEC, but it cannot be achieved before receiving B + S bursts.

In a discontinuous transmission (time-slicing), if the Inner TI is configured to perform only intra-frame interleaving, it is possible to display the content after receiving the first burst if the reception conditions are good enough, such that the Inner FEC of the Data PLP correctly decodes the data. Assuming one burst per second, the average zapping time would be around 0.5 s. For continuous transmission, as mentioned before it is recommended to perform inter-frame interleaving with the Inner TI within 1 s, keeping the operation frequency of the Outer FEC and thus a fast zapping time.

Terminals in very good reception conditions would stay always on early decoding, but otherwise at some point terminals need to do a transition from early to late decoding to achieve full protection. The transition time from early decoding to late decoding is $B-1$ bursts when the parity is transmitted before data (i.e., $D = B + S$), and $B + S - 1$ bursts when the parity is transmitted after the data (i.e., $D = 0$).

The solution adopted to perform this transition for MPE-iFEC in DVB-SH is based slowing down the audio and video display rate, see [22] and [23]. For BB-iFEC, other solutions are currently under investigation, based on simply buffering and replaying. The key is that the transition time is much lower than in DVB-SH, because with BB-iFEC most of the protection is in the outer FEC. When the parity is transmitted before the data, the lower the code rate, the lower the transition time between early and late decoding. For 10 sec time interleaving, the transition time is only 1 sec for CR_{outer} 1/4, which can be considered to directly provide fast zapping, and 3 sec for CR_{outer} 2/5.

3.1.3.3 BB-IFEC Transmitter Implementation

3.1.3.3.1 Data Delay Buffer

The transmission delay block is the only modification to the Data PLP. This block is just a buffer, which delays the transmission of the data bursts an entire number of T2 frames, denoted with the parameter D, in analogy to the MPE-iFEC specification in DVB-SH [17]. It should be pointed out that there is no need for a buffer at the receivers.

Two values of D are possible. $D = 0$, where the parity data is transmitted after the source data (as shown in Figure 43); and $D = B + S$, where the parity data is transmitted before the source data. The latter configuration increases the end-to-end latency, but reduces the transition time from early decoding mode to the late decoding mode. In particular, for $D = 0$, the transition period is $B + S - 1$ bursts, and for $D = B + S$, the transition period is reduced to $B - 1$ bursts.

3.1.3.3.2 B. Data Spreading

The data spreading process is the responsible for assigning the BB frames of each data burst to its corresponding B ADTs (Application Data Table) enclosed by the data spreading sliding window, see Figure 44. Data bursts are split into B subblocks, in such a way that the maximum difference between one sub-block and the rest is only one BB frame. Each subblock contains an entire number of consecutive BB frames (i.e., BB frames are not split into several ADTs). Each subblock is then assigned to one ADT.

It should be noted that for Constant Bit Rate (CBR) services, the number of data BB frames per burst is

constant, and the size of the ADTs is the same than the size of the data bursts.

For Variable Bit Rate (VBR) services, the number of data BB frames per burst changes over time, and thus the size of the ADTs is not constant. The size of each ADT depends on the size of the B bursts that generate the ADT, but always corresponds to an entire number of BB frames.

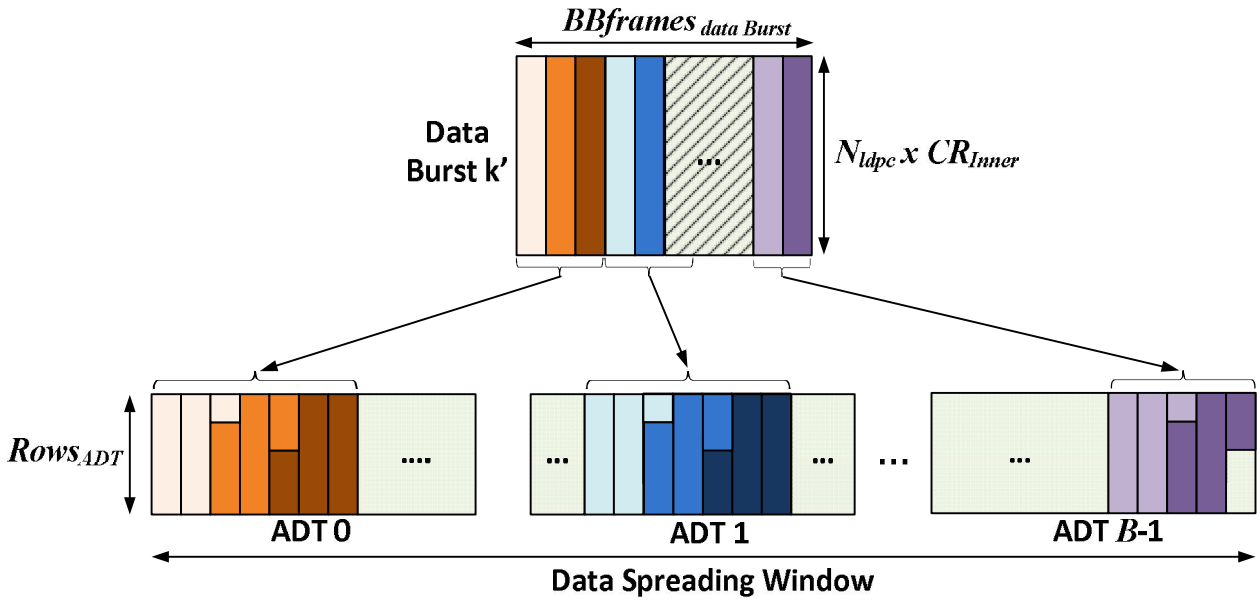

Figure 44: Illustration of the data spreading process. The data spreading process is performed from one data burst to B ADTs (Application Data Tables). The parity spreading process is performed from one iFDT (iFEC Data Table) to S parity bursts. Each ADT/parity burst contains an entire number of consecutive BB frames of the data burst/iFDT. The maximum difference between ADTs/parity bursts is one BB frame.

3.1.3.3.3 Outer FEC

The Outer FEC process generates the parity data to fill one iFDT (iFEC Data Table) taking as input data one filled ADT. Figure 45 shows the BB-iFEC encoding matrix (ADT + iFDT). The total number of columns is constant, and it is given by the size of the outer LDPC (i.e., N_{ldpc} = 16200). The number of columns of the ADT, $Columns_{ADT}$, and iFDT, $Columns_{iFDT}$, depend on the code rate of the outer LDPC:

$$Columns_{ADT} = 16200 \times CR_{outer}$$

$$Columns_{iFDT} = 16200 \times (1 - CR_{outer})$$

The number of rows of the ADT and iFDT, $Rows_{ADT,iFDT}$, is adjusted in such a way that the amount of padding in the ADT is minimized. The number of padding bits in the ADT is at most $(16200 \times CR_{inner} - 1)$ bits. That is, it depends on the code rate of the Inner FEC, since it determines the size of the data BB frames. It should be pointed out that the padding bits of the ADT table are not transmitted, and thus they do not reduce the effective capacity. The number of rows is fixed for CBR services and dynamic for VBR services. Once known the number of data BB frames in the ADT, BBframesADT , the number of rows can be computed as:

$$Rows_{ADT,iFDT} = \lceil BBframes_{ADT} \times CR_{inner}/CR_{outer} \rceil$$

where $\lceil \cdot \rceil$, denotes the *ceiling* function.

Once the ADT is filled (including padding), LDPC encoding is performed row by row. Before encoding one

row of the ADT, bit interleaving of the data is performed, as depicted in Figure 46. After decoding, the generated parity bits are also interleaved before writing them into one row of the iFDT. The bit interleaving is based on a block interleaver, with the number of columns equal to the data or parity spreading factor (*B* for data interleaving, and *S* for parity interleaving). Data is written by columns and read by rows, in a similar way than the bit interleaver of DVB-T2 [19].

Once the iFDT is written, it may be possible that some padding bits need to be included in the last parity BB frame. These padding bits need to be transmitted in order to avoid puncturing at the receivers. One interesting alternative is to use those bits to transmit in-band signalling, see [19] and [20]. In DVB-T2, there are two types of in-band signalling: type A (with updated L1 and L2 signalling information), and type B (with information related to the input processing of the Data PLP). In DVB-NGH, type A in-band signalling is optional, whereas type B is mandatory.

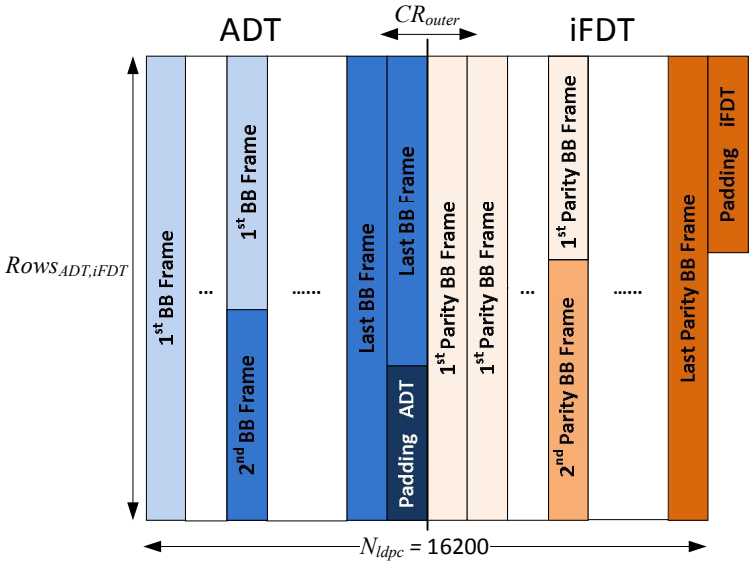

Figure 45: BB-iFEC encoding matrix. ADT (Application Data Table) and iFDT (iFEC Data Table). The padding bits of the ADT are not transmitted. The padding bits of the iFDT can be used to transmit in-band signalling.

Figure 46: Outer FEC process with bit interleaving of the ADT row before LDPC encoding and bit interleaving of the generated parity bits before writing them into one row of the iFDT. The bit interleaver is simply a block interleaver with the number of columns equal to the data spreading factor B and parity spreading factor S, for data and parity interleaving, respectively.

3.1.3.3.4 Parity Spreading

Once the iFDT is filled, a second spreading process is performed to distribute the parity BB frames to the S parity bursts enclosed by the parity sliding window. The number of parity BB frames in the iFDT can be easily derived from the number of rows of the ADT and iFDT, and the code rate of the Outer FEC:

$$BBframes_{iFDT} = [Rows_{ADT,iFDT} \times (1 - CR_{outer})]$$

The spreading process from the iFDT to the parity bursts is exactly the same than the spreading process from one data burst to the ADTs, depicted in Figure 44. The only difference is the number of elements enclosed by the sliding window (*B* ADTs in the data spreading process and *S* parity bursts in the parity spreading process). The iFDT is split into *S* sub-blocks. Each sub-block contains an entire number of consecutive parity

BB frames. Each sub-block is then assigned to one parity burst.

3.1.3.4 BB-IFEC Receiver Implementation

3.1.3.4.1 Decoding Process

Figure 47 shows a block diagram of a BB-iFEC receiver. In early decoding mode, the protection is given only by the Inner FEC of the Data PLP, and therefore the decoding process is the same than in DVB-T2 (inner LDPC first, and then outer BCH). The decoding process in late decoding mode, when the protection is given by both Inner and Outer FEC, is the following (recall that BB-iFEC operates in a burst basis):

1) Perform Inner LDPC decoding to all data BB frames of the burst of the Data PLP.
2) Send the decoded data, either soft or hard LLR values2, to the Data De-Interleaver block, which performs exactly the same spreading process than the Data Spreading block at the transmitter (see Fig. 2). In case of soft decoding in the Outer FEC, it is possible to store hard values (i.e., +/- 1 LLRs) when the Inner FEC detects that all parity check nodes are correct. This improves the performance and reduces the number of iterations required by the Outer FEC to converge.
3) Send the LLRs, either soft or hard values, of the parity BB frames of the iFEC PLP to the the Parity De- Interleaver block, which performs the inverse spreading process than the Parity Spreading block at the transmitter (see Fig. 2).
4) Perform the Outer FEC process, including bit deinterleaving of the data and parity.
5) Perform BCH decoding to all data BB frames.

From the decoding sequence above, it is clear that the receiver needs help in case of VBR services for doing the inverse of parity spreading process, but not for the data spreading process. For each parity burst, the receiver needs to know the amount of BB frames that correspond to each of the S iFDTs enclosed by the parity sliding window. This information should be transmitted in the dynamic field of the L1 signalling. It should be pointed out that the complete decoding process can be performed sequentially with only one LDPC hardware chain. BB-iFEC increases the number of LDPC decodings per burst with respect to a single FEC scheme. However, assuming 50 LDPC iterations per codeword as reference, the overall number of iterations can be kept without impacting the performance. For example, during early decoding mode, the outer FEC is not performed, and thus the Inner FEC can perform as many iterations as for single FEC. The Outer FEC is also not used in good reception conditions. In late decoding mode, in static conditions the overall performance is given by the FEC with more robust code rate, and thus this FEC should perform more iterations. On the other hand, in mobile conditions, it is possible to benefit when the Inner FEC is correct to speed up the convergence of the Outer FEC.

3.1.3.4.2 Receiver Implementation with Memory Pointers

One possibility for implementing BB-iFEC at the receivers is to use a double pointer structure, as described in the DVB-SH Implementation Guidelines for VBR memory management with MPE-iFEC [14]. The first pointer level would point to M encoding matrixes, the memory requirements of a sheer block interleaver. The second pointer level would point only to $(M + 1)/2$ encoding matrixes (optimized memory requirements, similar to a convolutional interleaver with a uniform profile). BB-iFEC only needs to manage M pointers per level (B pointers for the data and S pointers for the parity), much less than in MPE-iFEC, which requires M times the total number of columns of the ADT plus iFDT (i.e., 255) [17].

3.1.3.4.3 Receiver Implementation with Ring Buffers

Because of the regular structure of the BB-iFEC encoding process, the time de-interleaving at the receivers can be also implemented with ring buffers like traditional convolutional interleavers. Two convolutional interleavers are needed for the data and for the parity. The IU size of the convolutional interleaver for the

data depends on the code rate of the Inner FEC (i.e., 16200 × CR_{inner} bits/LLRs), whereas the IU size of the convolutional interleaver for the parity is constant and equal to 16200 bits/LLRs. The number of delay lines equals the number of BB frames of the data PLP and the iFEC PLP. The delay values range from 0 to $M-1$, with several lines having the same delay value (there are only M different values). Different interleaving configurations can be seen as different profiles of the convolutional interleaver. For the VBR case, the memory management is similar to one convolutional interleaver with dummy cells.

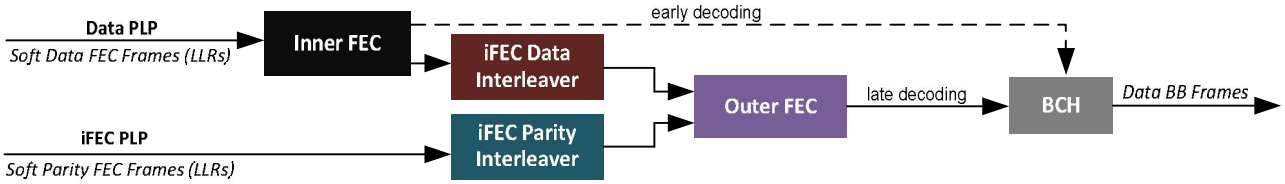

Figure 47: BB-iFEC receiver block diagram. In early decoding mode the protection is given only by the Inner FEC. In late decoding mode the protection is given by both Inner FEC and Outer FEC.

3.1.4 Rotated PSK and APSK for the satellite component of NGH

In this study, **Telecom Bretagne** investigated the application of the signal space diversity (SSD) technique called rotated constellation [24] to a constellations such as PSK and APSK, widely used in satellite transmissions. This technique allows the diversity order of the coded modulation in order to improve the transmission robustness over severe channels. It is based on applying a rotation to the constellation and introducing interleaving between the in-phase (I) and quadrature (Q) components of the transmitted signal. This method has been shown to perform well over fading channels with or without erasures [25]. In DVB-T2, Telecom Bretagne's main contribution to this technique was the proposal of new criteria for the rotation angle search. The technique and the rotation angles proposed for 4 to 256 QAM constellations were adopted in the standard. In DVB-NGH, a hybrid terrestrial/satellite coverage is considered. For mobile satellite transmissions, the Land Mobile Satellite (LMS) channel model, calling for a 3-state (line of sight, shadowing, blockage) Markov model, is widely used. The blockage state of the channel infers some erasure events in the transmission. Consequently, the rotated constellation technique is likely to improve significantly the robustness of satellite mobile transmissions. PSK and APSK constellations, widely used for satellite transmissions, have been investigated in this study.

3.1.4.1 The rotated constellation approach

The transmitter and receiver structure of the proposed SSD scheme is presented in Figure 48.

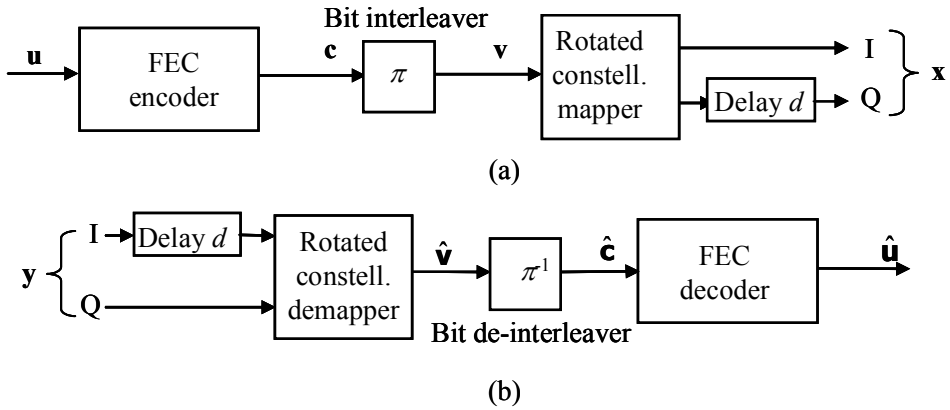

Figure 48: Structure of the proposed coded modulation SSD scheme: (a) transmitter and (b) conventional receiver.

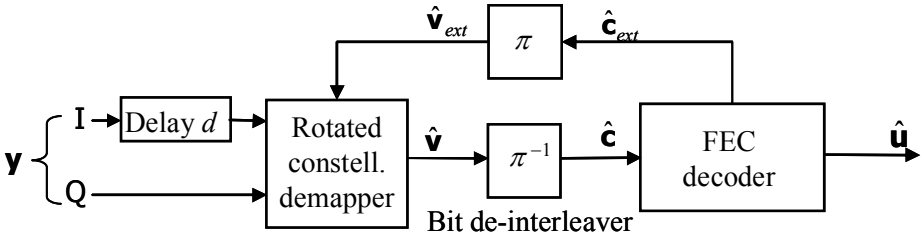

Figure 49: Iterative receiver structure for the proposed scheme.

Due to the constellation rotation and the delay insertion, the binary information contained in each constellation point is transmitted twice over the channel. Consequently, the rotated constellation can be seen in a way as a repetition code proceeding at the constellation symbol level.

From this point of view, the BICM transmitter of Figure 48(a) becomes a serial concatenation of two codes separated by an interleaver. Therefore, at the receiver side, the conventional structure presented in Figure 48 (b) can be beneficially replaced by an iterative structure, as described in Figure 49 in order to get additional gains. Extrinsic information related to every coded bit is then computed by the FEC decoder and fedback at the demapper input as *a priori* information.

The SSD principle had been originally devised for fading channels. However, in the DVB-T2 and DVB-NGH context, some additional erasure events have to be taken into account. Actually, in light of the presence of erasure events, some aspects of the original SSD had to be reconsidered in order to benefit from greater gains. In previous studies, the choice of the rotation angle α was based on maximizing the so-called *product distance* (PD) in order to minimize the pair-wise error probability between two different transmitted sequences. Unfortunately, this criterion is only valid for asymptotical performance, that is for very high values of Signal-to-Noise Ratios (SNR). In practice, actual operating SNRs can be rather low, especially when powerful FEC coding is considered. Consequently, the PD criterion turns out to be suboptimal for the SNR region of interest and the corresponding angles do not lead to the best actual coded performance. Moreover, for erased constellation signals, the distances are measured on the projection of the point on the non-erased axis, I or Q. In this case, a criterion based on a one-dimensional distance had to be introduced.

In order to find rotation angles suited to transmission over fading channels with and without erasure events, the following design criteria were proposed [25]:

- Maximizing the *minimum product distance* (PD), as already mentioned, in order to minimize the asymptotical Bit Error Rate (BER) at the output of the demapper over fading channels without erasures;
- Maximizing *the minimum 1-dimensional distance* ($1D_{min}$) between any two constellation points after their projection onto I or Q, in order to minimize the asymptotical BER at the output of the demapper in the presence of erasures;
- Minimizing the *average Hamming distance* between any two adjacent constellation symbols ($d_{H,avg}$) and the Hamming distance between any two adjacent constellation symbols at distance 1Dmin ($d_{H,1D}$) after their projection onto I or Q: these mapping-related distances play a role in the presence of erasures. In order to minimize the number of bits in error when a wrong constellation symbol is chosen, $d_{H,avg}$ and $d_{H,1D}$ should be kept as low as possible.

Unfortunately, in practice, these criteria are in conflict and their simultaneous application leads to different values of the rotation angle. Thus, a compromise has to be found.

3.1.4.2 Optimizing the rotation angle for PSK and APSK constellations

In the context of DVB-NGH, these design criteria have been applied to 8-PSK, 16- and 32-APSK. For instance, Figure 50 displays the different distance curves for the 8PSK constellation.

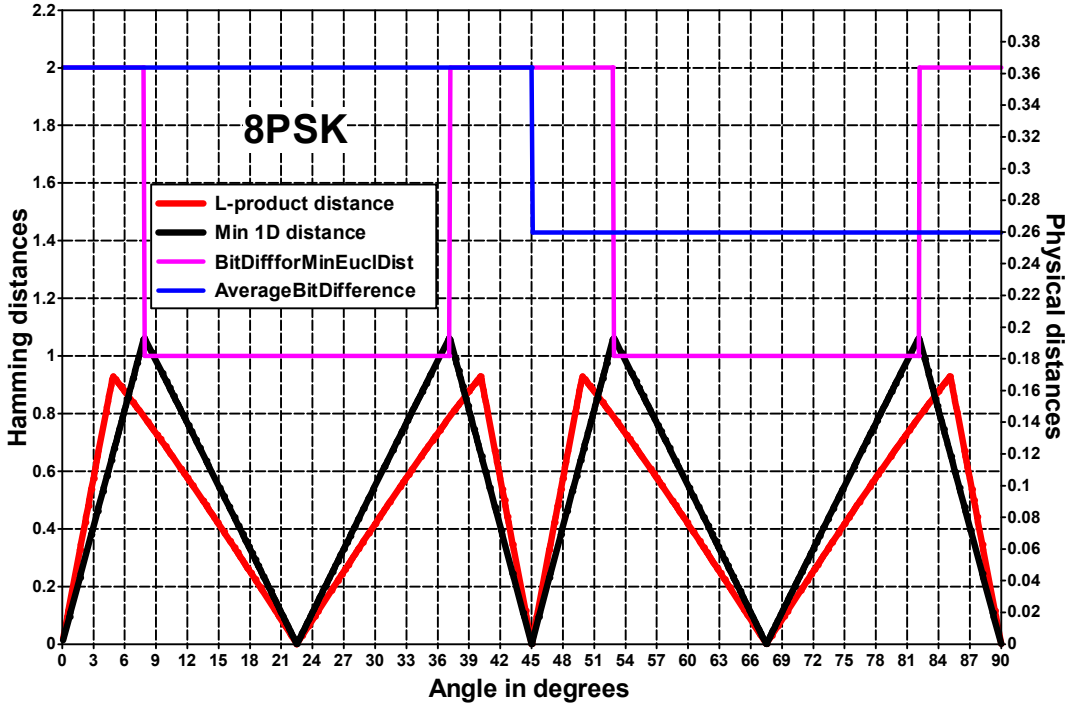

Figure 50: distance values as a function of the rotation angle α for constellation 8-PSK. Red curve: minimum product distance PD. Black curve: minimum 1-dimensional distance $1D_{min}$. Blue curve: average Hamming distance $d_{H,moy}$. Magenta curve: average Hamming distance $d_{H,min}$.

From this figure, we kept the rotation angles such that $1D_{min}(\alpha) \geq 1D_{min}(\alpha)$, where α□□ is the angle corresponding to the nearest peak of the product distance: $49.9° \leq \alpha \leq 58.5°$ and $76.5° \leq \alpha \leq 85.1°$.

The same procedure was applied to 16-APSK and 32-APSK constellations.

3.1.4.3 Simulation results

For each constellation under study, simulations have been carried out over two different channel types: the Rayleigh fading channel and the Rayleigh fading channel with 15% of erasures.

Figure 51 and Figure 52 compare the Bit Error Rate (BER) at the output of the non-rotated and rotated 8-PSK demappers for different acceptable values of angle α. One can observe a performance gain in favour of the rotated 8-PSK constellation for all values of signal to noise ratios (SNR) considered. In the presence of erasures, this gain is greater than 1 dB even for very lows SNRs.

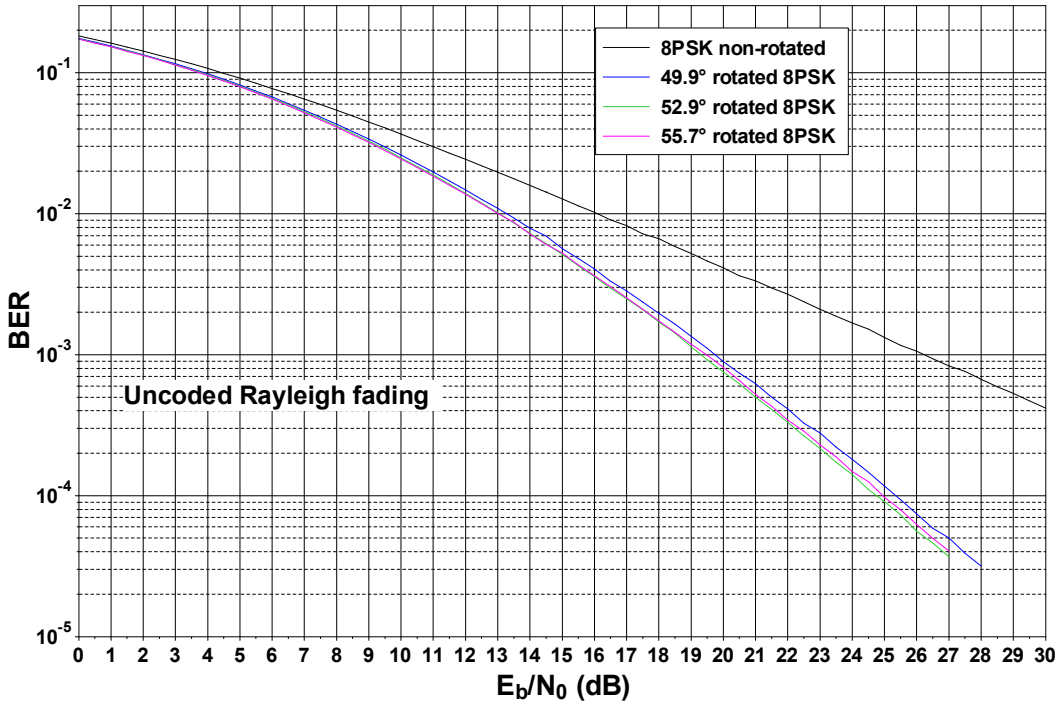

Figure 51: BER comparison at the output of a non-rotated and of a rotated 8-PSK demapper. Uncoded transmission over a flat fading Rayleigh channel.

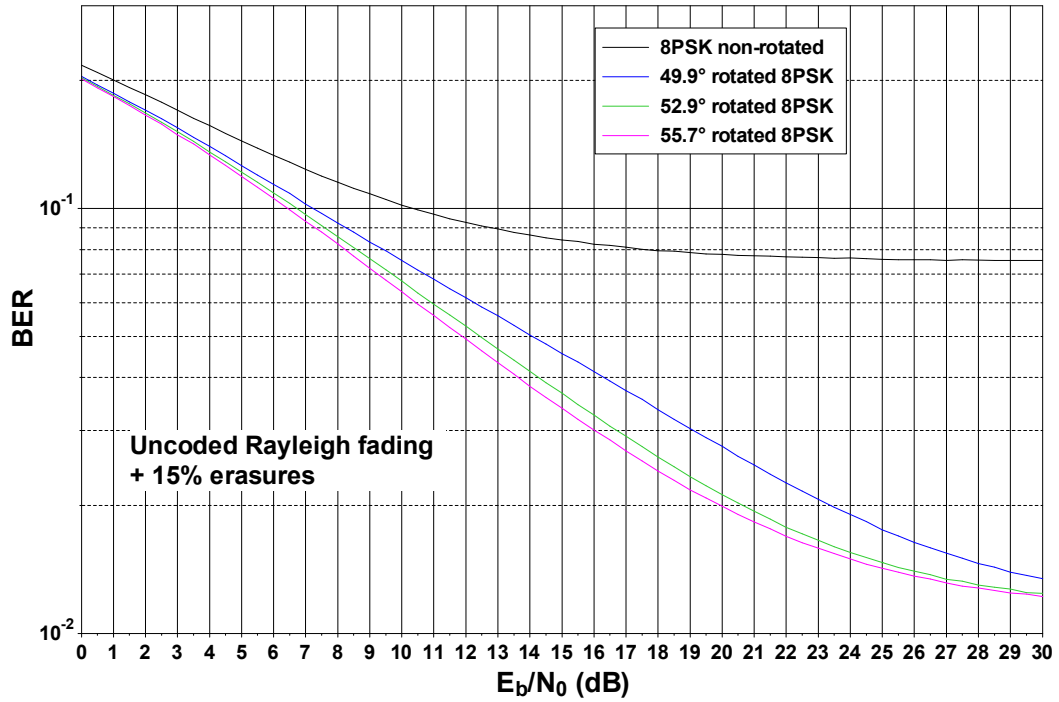

Figure 52: BER comparison at the output of a non-rotated and of a rotated 8-PSK demapper. Uncoded transmission over a flat fading Rayleigh channel with 15% of erasures.

3.1.4.4 Proposed angle values

The distance curve analysis combined to subsequent simulations led to the proposal for DVB-NGH of the angle values provided by Table 15.

Angle recommendations		
8-PSK	16-APSK	32-APSK
$\alpha = 55.7°$	$9.9° \leq \alpha \leq 10.3°$	$\alpha = 94.4°$

Table 15: Angle recommendations for rotated 8-PSK and APSK constellations in DVB-NGH.

3.2 Time interleaving

DVB-NGH being dedicated to mobile applications, some research has been undertaken to optimize the DVB-T2 channel interleaver in order to reduce the time interleaver memory in the receiver and to take into account the hybrid satellite/terrestrial mode of NGH.

Section 3.2.1 presents the results of the studies that led to the adoption of a combination of block and convolutional interleaving in the DVN-NGH baseline. Section 3.2.2 gives the summary of an analysis of time interleavers in Land Mobile Satellite conditions, which is presented in details deliverable TR4.1 [26].

3.2.1 Time interleaving proposal for NGH

Teracom was deeply involved in the design of a time interleaver structure appropriate to DVB-NGH. This section presents a synthesis of their work.

3.2.1.1 Introduction

The time interleaving (TI) proposal for NGH was originally heavily based on the block interleaving (BI) used in the DVB-T2 standard, including the possibility to interleave over several frames. For complexity reasons it was however found desirable to reduce the TI memory by 50%. This would however severely limit the possible time interleaving depth, especially since lower order constellations like QPSK, which are quite likely to be used for NGH, allows a shorter interleaving depth for a given number of cells in the TI memory and for a given PLP bit rate. For these reasons, but also to allow for shorter zapping time (especially in connection with the hybrid satellite/terrestrial mode of NGH) convolutional interleaving (CI) was suggested as an alternative to block interleaving. CI had however already been studied and rejected for DVB-T2, due to certain problems (e.g. TFS and VBR). However, after some analysis a solution was agreed: to combine BI and CI in such a way that BI is done internally in an NGH frame in a similar way as for T2, but the interleaving across NGH frames is done by CI. In this way the previously known problems with CI would vanish but there would still be significant memory gains and gains in zapping time.

3.2.1.2 I/Q shift for rotated constellations

When rotated constellation is used it is important for the original I and Q components of a cell to be transmitted with large separation in time and frequency, so that e.g. a bad RF channel or a badly received NGH frame (due to fading or interference) will not contain both components. In T2 this was not ensured, but for NGH it has been suggested to use a shift of one Interleaving Unit (IU) for the Q component before cell interleaving. This will ensure that the I and Q are always transmitted in different NGH frames, see Figure 53:

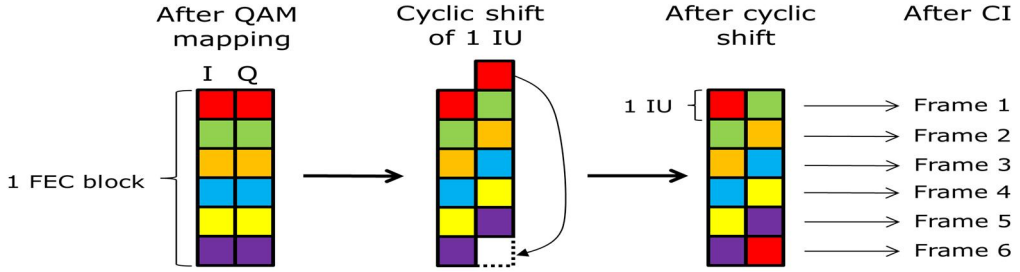

Figure 53: Proposed I/Q shift for DVB-NGH

3.2.1.3 Hybrid convolutional/ block time interleaver structure

With CI each FEC block needs to be spread over several frames. The way this is achieved is to divide each FEC block into a number of so-called Interleaving Units (IUs), with number of IUs equal to the time interleaving depth expressed in number of NGH frames. In order to minimise power consumption the highest possible IU size should be used.

Figure 54 shows the way the CI works. The upper figure shows the situation before CI and the lower figure after CI. There is one column per NGH frame and four IUs per FEC block. There are two PLPs – one "red PLP" and one "green PLP".

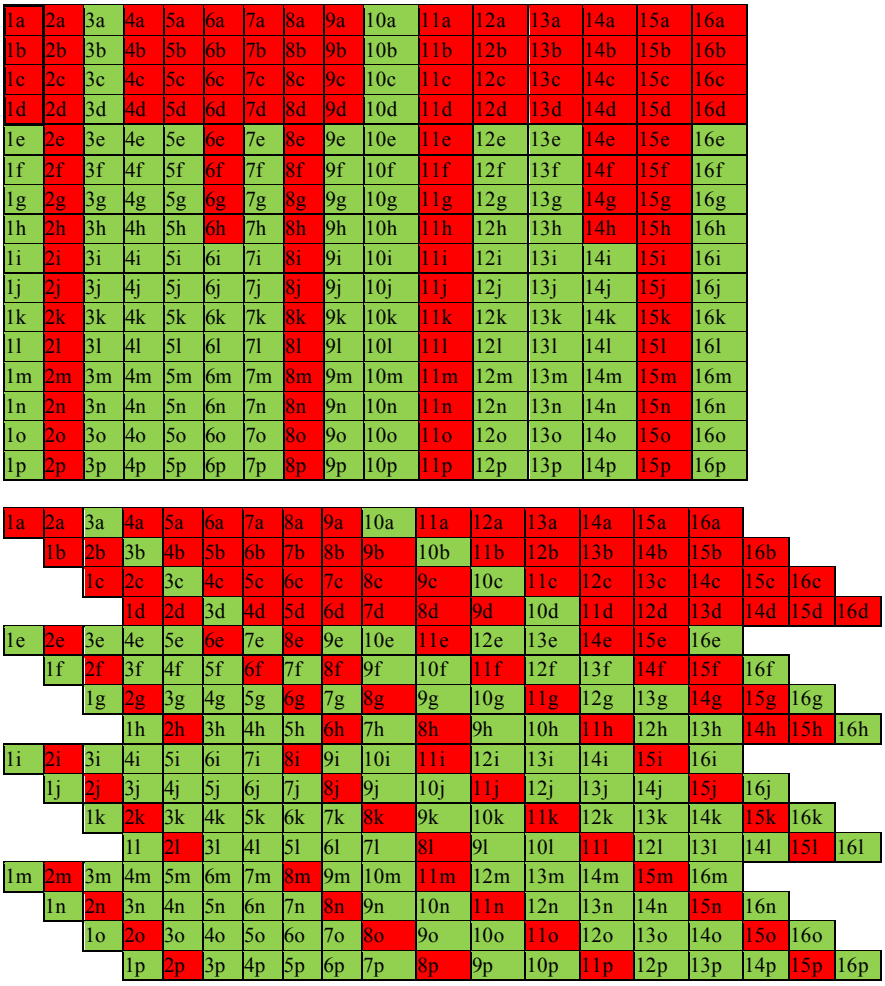

Figure 54: Illustration of the proposed IU-based CI process

The starting point for the interleaving process is that we have an integer number of 16200 bit FEC blocks per PLP for each NGH frame.

Unfortunately it is not always possible to divide a FEC block into equally large IUs using all the constellations QPSK, 16-QAM, 64-QAM and 256-QAM. In some combinations of constellation and interleaving depth (number of NGH frames N) some IUs get one cell more than the others (these cases are: 16-QAM N=4, 256-QAM, N=2, 4, 6) . This does not have any effect on the CI as such, but will affect the number of cells per frame for a given PLP.

In each NGH frame BI is performed for each PLP individually. The BI is shown in

Figure 55.

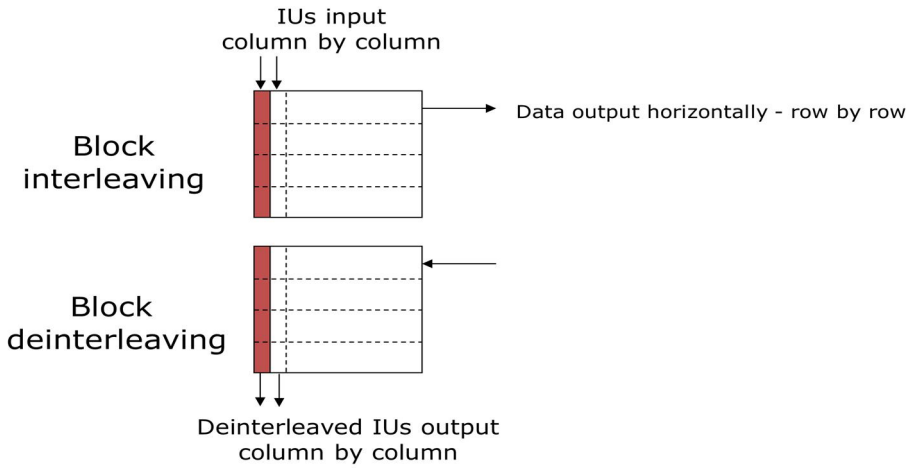

Figure 55: IU-based BI

For a given PLP each IU is inserted vertically in a column. The result is read out horizontally, row-by-row. Due to the slightly different IU lengths (for a given configuration) the IUs will in general not perfectly fit a column – some IUs will, but others will be "one cell short". There will thus be some empty space at the end of the BI. These empty positions are simply discarded when the data is read out, as can be seen from Figure 56.

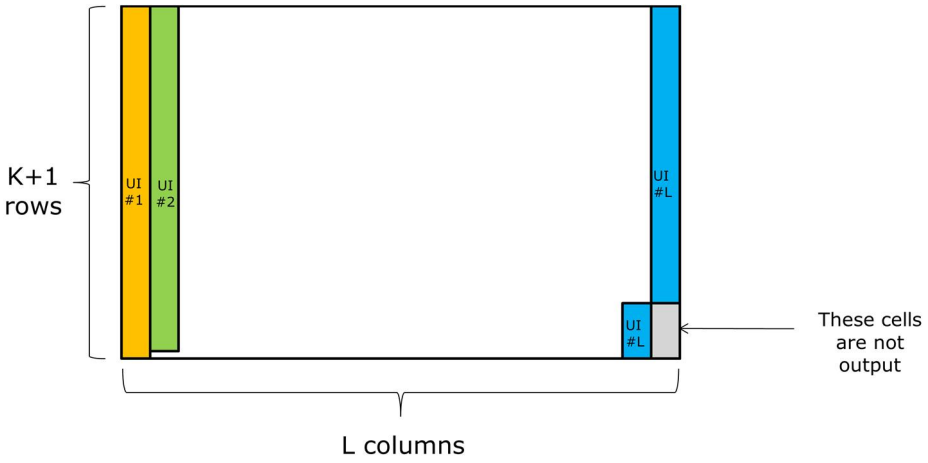

Figure 56: Insertion of IUs into the BI

3.2.1.4 Scheduling of PLPs

After the BI the PLPs are put on top of each other in a cell-based matrix, according to Figure 57.

Figure 57: PLP arrangement after the BI

The number of columns in the matrix equals “number of RF channels” multiplied by “number of sub-slices per RF channel”. When this condition is fulfilled (including any necessary padding cells in the top row), a deterministic scheduling of the cells into the NGH frame can be done in the way outlined below.

First step: Divide the matrix into "number of sub-slices per RF channel" (here two) and put one half on top of the other, see Figure 58:

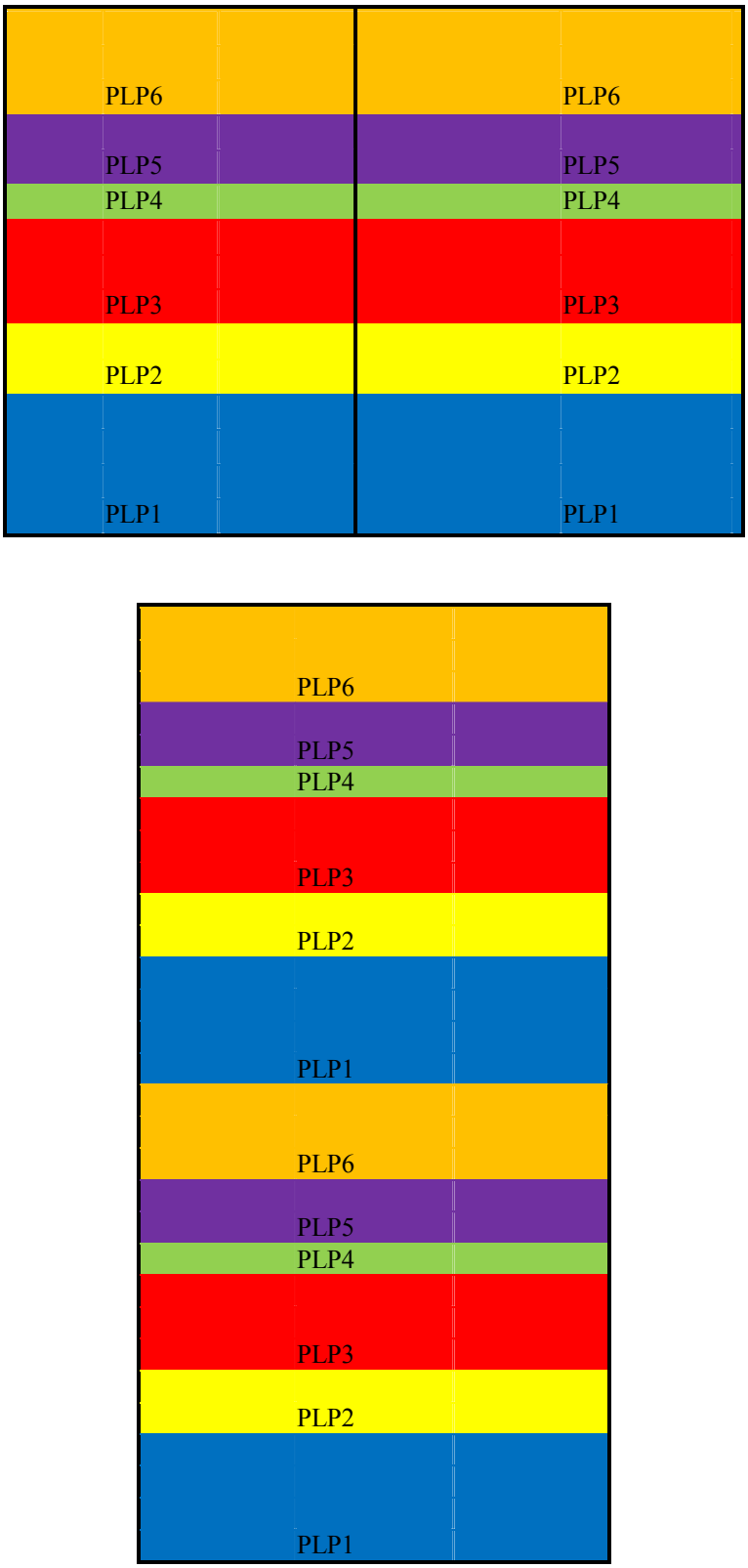

Figure 58: Result of the first scheduling step

Second step: Divide the resulting structure into "number of RF channels" (here three in Figure 59):

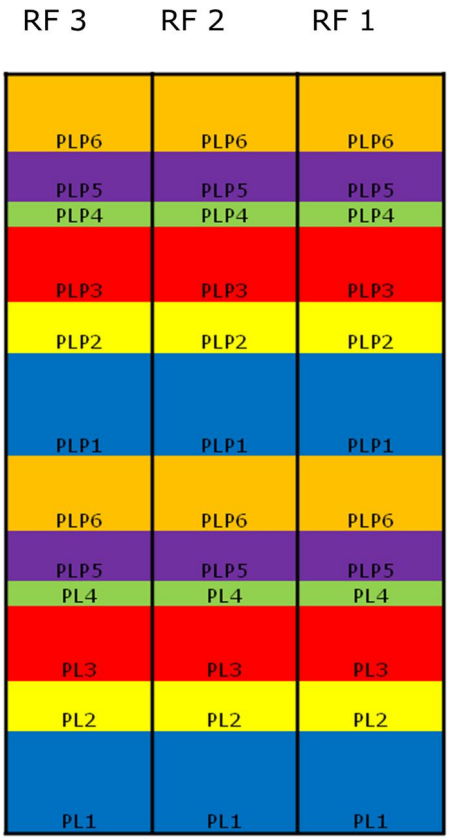

Figure 59: Result of the second scheduling step

Third step: Perform time shifting and folding back, according Figure 60. The time shift makes the PLPs evenly distributed in order to allow for good time diversity and time/frequency hopping.

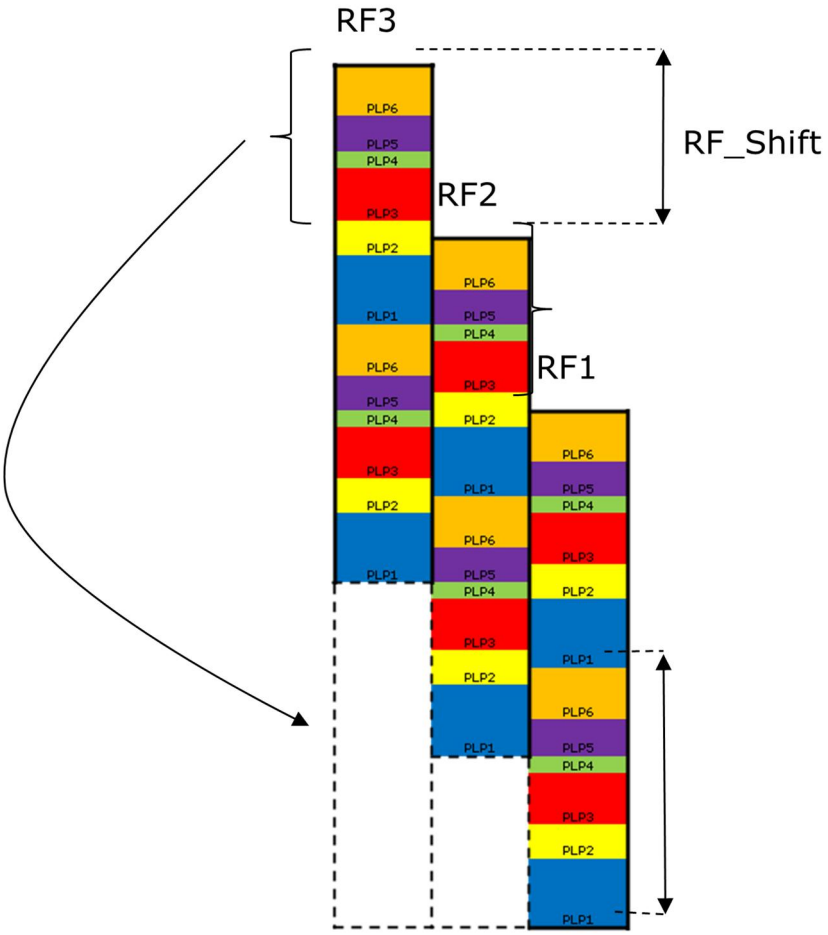

Figure 60: Result of the third scheduling step

End result of scheduling process

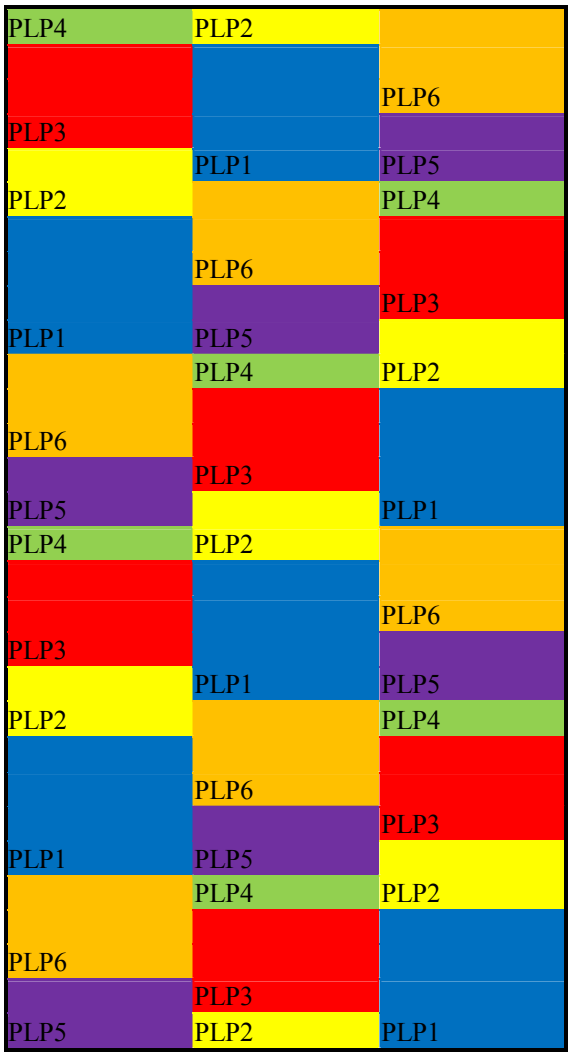

Figure 61: End result of scheduling

It should be noted that the previous process has not yet filled the scheduled cells with data – only allocated the positions in the frame.

Time interleaved PLP cells are introduced into sub-slices in the natural time sequence, independently of RF channel

The first time interleaved cell is therefore introduced in the first cell position of the first sub-slice of the PLP (in whichever RF channel it appears). A receiver performing the frequency hopping will therefore receive the time interleaved cells in the right order.

3.2.1.5 Frequency Interleaving

Frequency interleaving is performed in each symbol using a time varying frequency interleaver. This allows for each OFDM symbol to be differently frequency interleaved and therefore spreads the IUs to potentially all OFDM carriers in the frame to maximize frequency diversity. This allows also for a simpler BI since there is no need to use the approach adopted for T2 of splitting an input block (a FEC block in T2) into five columns.

3.2.2 Performance analysis of time interleavers in Land Mobile Satellite conditions

This study was carried out by **CNES**. It can be viewed as a common task of Task Forces 1 and 4, since TF4 deals with hybrid access technologies. Thus, this report only contains an executive summary of this study. For an extensive description, please refer to **Technical Report TR4.1: "Interim report on hybrid access technologies" [26]**.

For a satellite part, a long interleaver is needed to cope with the fluctuation of the shadowing effect seen by the mobile receivers while the code rate is tightly tuned to the optimisation of the satellite link budget and the compromise with data throughput.

Two solutions have been introduced in DVB-SH: one solely on the physical layer with the class 2 physical time interleaver, and the other one on the link layer with the class 1 physical time interleaver.

The class 2 interleaver must be implemented at the physical layer. This solution leads to the best performance in terms of decoding capability but it has zapping and service access times higher than those expected with NGH standards. The class 2 interleaver is a good compromise between robustness and zapping time.

The interleaver added with MPE-IFEC on top of class 1 physical interleaver is less performing but it allows lower zapping and service access time.

The use of a return channel may improve the performance of this solution as well in a compromise to be done with the additional use of the forward link it will trigger.

3.3 Study of advanced modulation techniques for NGH

DVB-T2 multi-carrier modulation is based on a classical Cyclic Prefix (CP) Orthogonal Frequency-Division Multiplexing (OFDM). Two ENGINES members, Orange Labs/France Telecom and MERCE studied and proposed two alternative solutions for DVB-NGH. **Orange Labs/France telecom** investigated the so-called OFDM-OQAM modulation, particularly efficient against frequency distortions such as Doppler Effect. This study is detailed in Section 3.3.1. Besides, MERCE proposed Single-Carrier (SC)-OFDM modulation for the satellite component of the DVB-NGH system. This contribution is summarized in Section 3.3.2. For an extensive description, please refer to **Technical Report TR4.1: "Interim report on hybrid access technologies" [26]**.

3.3.1 Terrestrial link: OFDM-OQAM modulation

The most common OFDM scheme transmits QAM symbols thanks to the use of a basic Inverse Fast Fourier Transform (IFFT) at the transmitter and an FFT at the receiver. Because of the sensitivity of such a scheme to multipath channels, a Cyclic Prefix (CP) is usually inserted at the transmitter side and removed at the receiver side. This procedure can cancel inter-symbol interference (ISI) if the length of the CP is larger than the largest echo of the channel. This scheme referred to as CP-OFDM has the advantage to provide good performance for a reasonable complexity. Nevertheless several issues are pending. The CP does not fight against frequency distortions such as the Doppler Effect; so inter-carrier interference (ICI) remains and the cyclic prefix may be seen as redundancy leading to a spectral efficiency loss. Finally the use of a simple IFFT at the transmitter, *i.e.* modulating the symbols over each sub-carrier by a rectangular function, leads to non negligible out-of-band radiations. This latter item implies that in practical systems consequent filtering has to be applied to meet spectrum masks requirements. In this document we focus on an OFDM scheme, proposed for DVB-NGH, that can solve, partially or completely, the aforementioned issues. In this

document, this specific OFDM modulation scheme often referred as OFDM/OQAM is described (where the OQAM term stands for Offset-QAM).

In OFDM/OQAM no cyclic prefix is inserted between the symbols but a specific pulse-shaping (prototype function) is introduced that in the meantime satisfies some orthogonality constraints. Among the OFDM/OQAM prototype function, we can find the Isotropic Orthogonal Transform Algorithm (IOTA) that has been proposed in 1995 by France Telecom in the case of a transmission over a time-frequency dispersive channel. However, since this date, other prototype functions either optimized in continual-time such as the Extended Gaussian function (EGF), or in discrete-time using the Time-Frequency Localization (TFL)[28] criterion have also been proposed. Some of the basic features of these main functions are presented in this document. In order to illustrate the hardware feasibility of OFDM/OQAM, we also present the France Telecom OFDM/OQAM demonstrator.

3.3.1.1 Time-frequency representation

Time-frequency representations are particularly appropriate for multi-carrier modulation schemes that can indeed have different features in the time and frequency domains. Figure 62 represents the time-frequency lattice for the OFDM and OFDM/OQAM modulations. In this scheme the lattice density is measured by the inverse of the product of the distance between two elements on the vertical and horizontal axis.

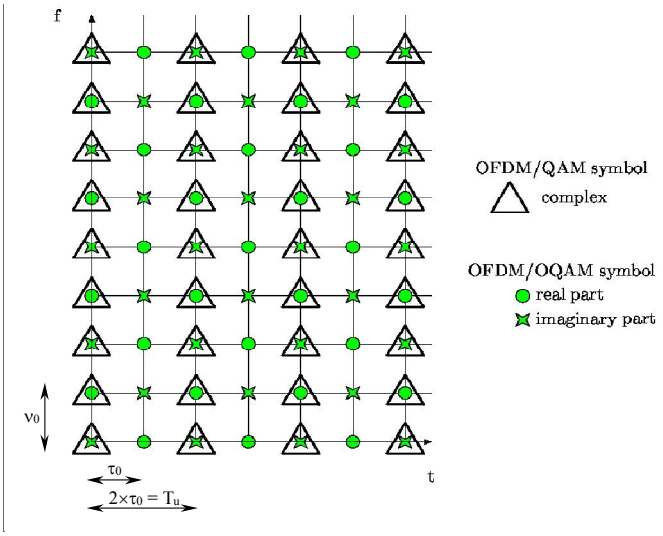

Figure 62: Time-frequency lattice for OFDM and OFDM/OQAM.

It can be seen that, if the frequency spacing, denoted here by $\upsilon_0 (= F_0)$, is identical for both modulation schemes, it is not the case for the time spacing. Indeed, as previously mentioned, the real OFDM/OQAM symbols have a duration τ_0 that is half the one of the useful time duration, denoted here $T_u (= T_0)$, of complex OFDM symbols. So, in theory, both modulation schemes can achieve a similar maximum bit rate. In practice OFDM is always less efficient with a guard time interval (also called cyclic prefix), T_g that introduces a loss of spectral efficiency. Otherwise stated the OFDM/OQAM spectral efficiency is, in theory, $(T_g + 2\tau_0)/2\tau_0$ times higher than the one of OFDM.

3.3.1.2 Continual time formulation

In the OFDM/OQAM scheme, instead of transmitting a QAM symbol, $s_{m,n} = s_{m,n}^{\mathrm{Re}} + j.s_{m,n}^{\mathrm{Im}}$ at a given rate T_0, on each sub-carrier, the real (Re) and imaginary (Im) are transmitted separately at rate $\tau_0 = T_0/2$, with a

time-offset of τ_0 (m: sub-carrier index, n: symbol index). That means either the real or the imaginary part is delayed of one half-symbol duration. The constraint is to keep a phase difference of $\pi/2$ between adjacent symbols in time and frequency. This so-called staggering rule, which is summarized in Table 16 leads to the OQAM transmission scheme. As the sub-carriers have to be grouped by pairs, we naturally have *M* (total number of sub-carriers) even.

	$(2m-1)F_0$	$(2m)F_0$	$(2m+1)F_0$
$nT_0 - T_0/2$	$s^{\mathrm{Re}}_{2m-1,n-1}$	$j.s^{\mathrm{Im}}_{2m,n-1}$	$s^{\mathrm{Re}}_{2m+1,n-1}$
nT_0	$j.s^{\mathrm{Im}}_{2m-1,n}$	$s^{\mathrm{Re}}_{2m,n}$	$j.s^{\mathrm{Im}}_{2m,n}$
$nT_0 + T_0/2$	$s^{\mathrm{Re}}_{2m-1,n}$	$j.s^{\mathrm{Im}}_{2m,n}$	$s^{\mathrm{Re}}_{2m+1,n}$

Table 16: Coding scheme for OQAM symbols.

Based on this coding principle we get the modulator scheme that is depicted in Figure 63.

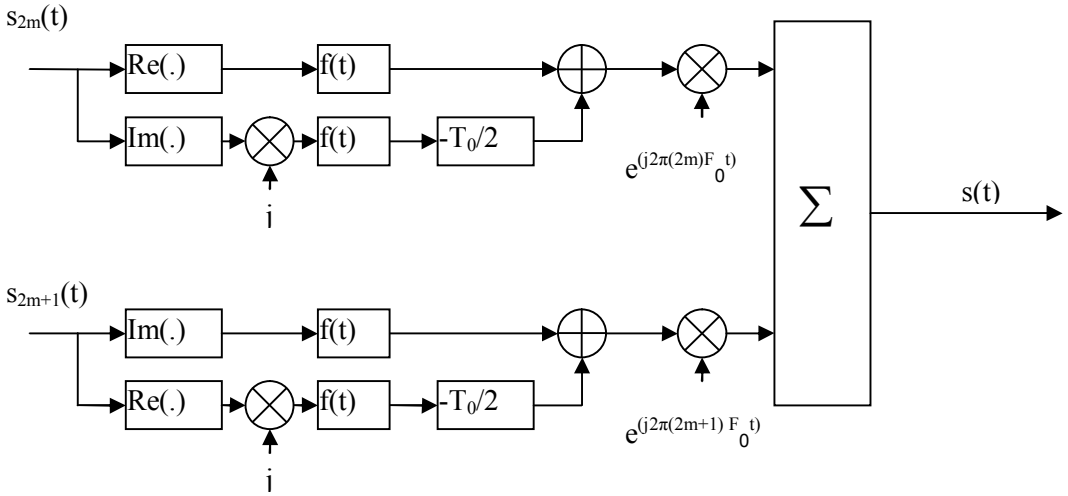

Figure 63: OFDM/OQAM modulator in its analog form (continual-time).

From Figure 63, it can be seen that the baseband OFDM/OQAM signal $s(t)$ is obtained as the combination of 4 signals that are shifted in time by τ_0, the duration of one real symbol, and in frequency by F_0, the spacing between two successive carriers. With a direct formulation it can be seen that $s(t)$ is obtained as a summation in time and frequency of 4 terms. This expression can be simplified in order to get the following unified formulation where the baseband OFDM/OQAM signal is written as follows:

$$s(t) = \sum_{n=-\infty}^{\infty} \sum_{m=0}^{M-1} a_{m,n} f_{m,n}(t)$$

Where the base of modulation can be expressed as a Gabor family:

$$f_{m,n}(t) = f(t - n\tau_0) e^{j2\pi m F_0 t} e^{j\varphi_{m,n}} \quad (1)$$

The phase term $\varphi_{m,n}$ is directly related to the OQAM staggering rule so it has to be such that:

$$\varphi_{m,n} = \begin{cases} 0 & \text{if } m \text{ and } n \text{ have the same parity} \\ \frac{\pi}{2} & \text{if } m \text{ and } n \text{ have a different parity} \end{cases} \quad (2)$$

It is important to note that the family of functions in (1) does not form an orthonormal basis for a lattice with $F_0 T_0 = 1$. Therefore the Balian theorem which states that is not possible to get an orthonormal basis for $L^2(R)$ for a Gabor system with $F_0 T_0 = 1$ and a bounded time-frequency localization product does not hold for OFDM/OQAM. So if for OFDM it is not possible to get a prototype function being well-localized in time and frequency the situation is different for OFDM/OQAM.

But, in this latter case, the demodulation basis, the same as the modulation one, has to be based on the **real** scalar product of $L^2(R)$. Then at the receiver side the real symbols are recovered by:

$$\hat{a}_{m,n} = \left\langle f_{m,n} \middle| s \right\rangle_R = \mathrm{Re}\left\{ \int_{-\infty}^{+\infty} f_{m,n}^*(t) s(t) dt \right\}$$

Then the orthogonality condition can be checked with the following relation:

$$\mathrm{Re}\left\{ \int_{-\infty}^{+\infty} f_{m,n}^*(t) f_{m',n'}(t) dt \right\} = \delta_{m,m'} \delta_{n,n'}$$

With this expression it can be checked that a phase rotation has a direct impact on this orthogonality condition which means that indeed the phase term cannot be arbitrarily chosen. In the case of continual-time OFDM/OQAM, the definition used by Hirosaki was the one given in (2). As $\varphi_{m,n}$ may be defined modulo π, in fact we need $\varphi_{m,n} = \varphi_0 + \frac{\pi}{2}(m+n)$. To simplify we can only choose $\varphi_{m,n} = \frac{\pi}{2}(m+n)$.

3.3.1.3 Discrete time formulation

Sampling the continual-time signal at the Nyquist rate T_0/M, we get the discrete-time version of OFDM/OQAM:

$$s[k] = \sum_{n \in Z} \sum_{m=0}^{M-1} a_{m,n} \underbrace{f[k - n\frac{M}{2}] e^{j\frac{2\pi}{M}(k-L-1)} e^{j\varphi_{m,n}}}_{f_{m,n}[k]}$$

Where L is the length of the so-called prototype filter f [k].

Then the orthogonality of the family of discrete-time functions $f_{m,n}[k]$ can be checked using again the real scalar product for this discrete-time function, i.e.:

$$\mathrm{Re}\left\{ \sum_{k \in Z} f_{m,n}^*[k] f_{m',n'}[k] \right\} = \delta_{m,m'} \delta_{n,n'}$$

This discrete-time formulation naturally leads to filter-bank-based realization schemes.

3.3.1.4 OFDM/OQAM prototype functions

Among the main prototype functions that could have been candidates in DVB-NGH standard, we can list:

- The IOTA function that constitutes a remarkable case of OFDM/OQAM modulation by many

specific aspects. Probably the most surprising is the double orthogonalization procedure which, to the best of our knowledge, was never used before. However, the IOTA prototype function is time-continual and defined in an infinite interval that is not very convenient for burst transmission.

- The EGF prototype function that is a variant of the IOTA one. The EGF is given by a closed-form expression and it keeps the parameter, i.e. it is possible to favour with value, the time or the frequency dimension.
- The TFL prototype function that results from an optimization of the waveform carried out directly in discrete-time. Its main advantage is the possibility to get short prototypes, with duration (T_0) less than for CP-OFDM, that are well suited for transmission over time and frequency dispersive channels.
- The Frequency Selective (FS) prototype is also designed directly in discrete-time and is particularly appropriate for channels that are only selective in frequency.

Note also that some other prototype filters are available from the state-of-the-art on OFDM/OQAM[29]or on filter banks [30].

3.3.1.5 PAPR

It has been shown in [31] that OFDM/OQAM has a similar Complementary Cumulative Density Function (CCDF) as OFDM, as long as its prototype is orthogonal (TFL, FS) or nearly orthogonal (IOTA, EGF). Otherwise stated, the PAPR values and impact are identical with an OFDM or an OFDM/OQAM modulation scheme.

3.3.1.6 Main key points of CP-OFDM and OFDM/OQAM modulations

Table 17 gives a general idea of the main difference between CP-OFDM and OFDM/OQAM modulations.

Parameters	CP-OFDM	OFDM/OQAM
Symbols	Complex (QAM)	Real (PAM)
CP	Yes	No
Symbol rate	T0+CP	T0/2
Prototype function	Rectangular	IOTA, EGF, TFL …
Equalization	One tap	One tap
Implementation	FFT (T0)	FFT (T0/2) + polyphase filter
Orthogonality	Complex	Real
PAPR	0	0
Robustness to Doppler	+	++
Robustness to band limited interferers	+	++
Robustness to SFN	++	-

Table 17: List of the main key points of OFDM and OFDM/OQAM modulations

3.3.1.7 Hardware implementation

Figure 64 shows the hardware implementation block diagram that reflects what has already been prototyped by France Telecom; this hardware implementation has allowed the comparison of the main differences between CP-OFDM and OFDM/OQAM modulation in terms of complexity.

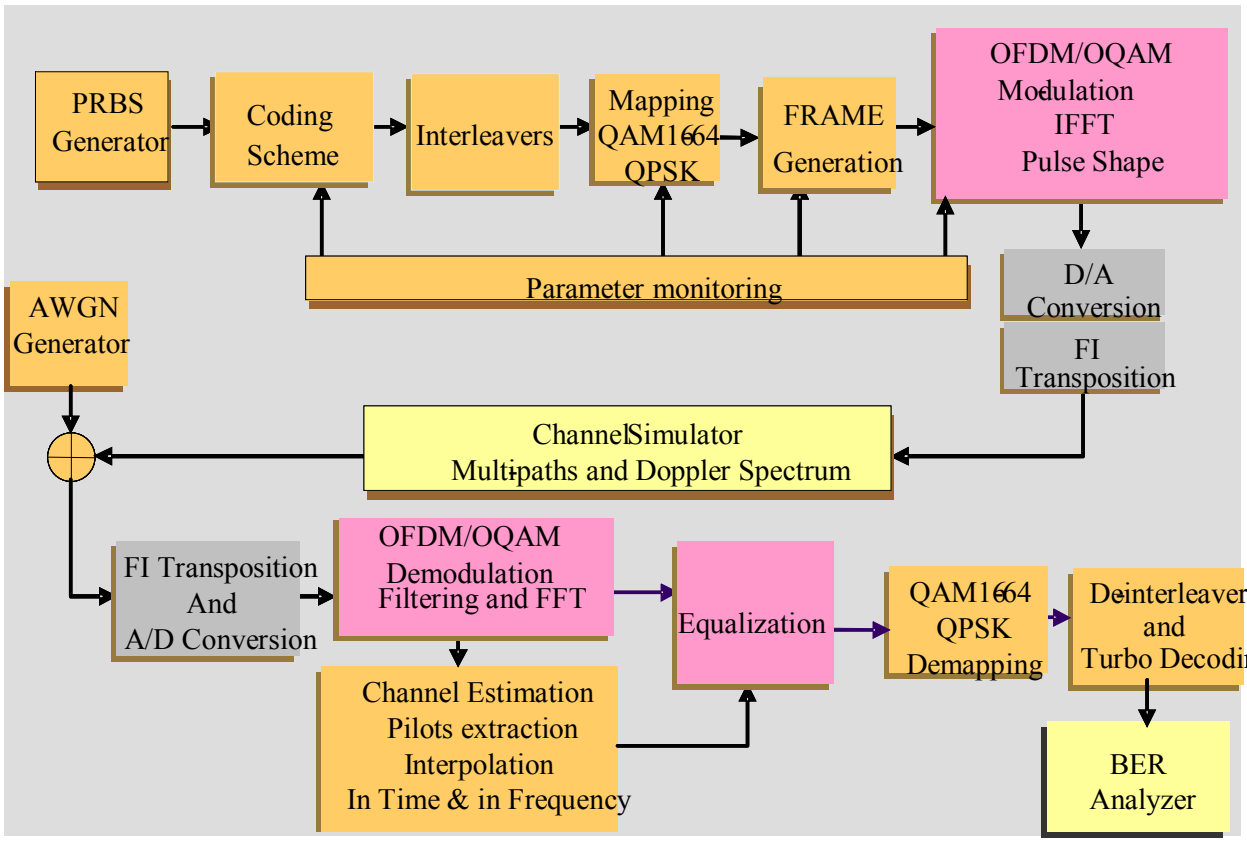

Figure 64: Example of hardware implementation block diagram

3.3.1.8 Implementation considerations

This section aims at introducing main differences between CP-OFDM and OFDM/OQAM at the hardware level.

Except the synchronization techniques using CP for correlation process, all the other synchronisation methods, which don't use the cyclic prefix, i.e. based on pilot sequence correlation known by the receiver, can still be used.

The hardware implementation impact, with regard to conventional OFDM, is mainly due to the prototype function pulse shaping. The complexity of this process greatly depends on the type of the chosen prototype function (e.g. IOTA, EGF and TFL).

The modulation requires some additional processing:

- OFDM/OQAM pulse shaping requires a set of 2L real multipliers (where L is the length of the truncated prototype function, e.g. L = 1,2 or 4) and 2L FIFO symbol memories.
- Inverse FFT requires doubling the process speed but still remains equivalent to OFDM IFFT because data are real.

The choice of the OFDM/OQAM prototype function can be carried out in relation with the propagation channel characteristics. This flexibility can be considered in hardware implementation by changing the waveform according to the scenario (fixed / portable / mobile).

3.3.1.9 OFDM/OQAM modulator

This section gives the implementation guidelines of an OFDM/OQAM modulator.

In a first step a complex symbol is split in real and imaginary parts; the $\pi/2$ rotation is added on each cell $a_{m,n}$ by (i^{m+n}) ("m" for frequency index). This modulation is performed in the Real domain.

The modulator uses the inverse fast Fourier transform, which is similar to OFDM. The prototype filter is applied, in time domain, to the symbol; then after the $\tau 0$ offset applied on the imaginary part, both parts are added at the end of the process.

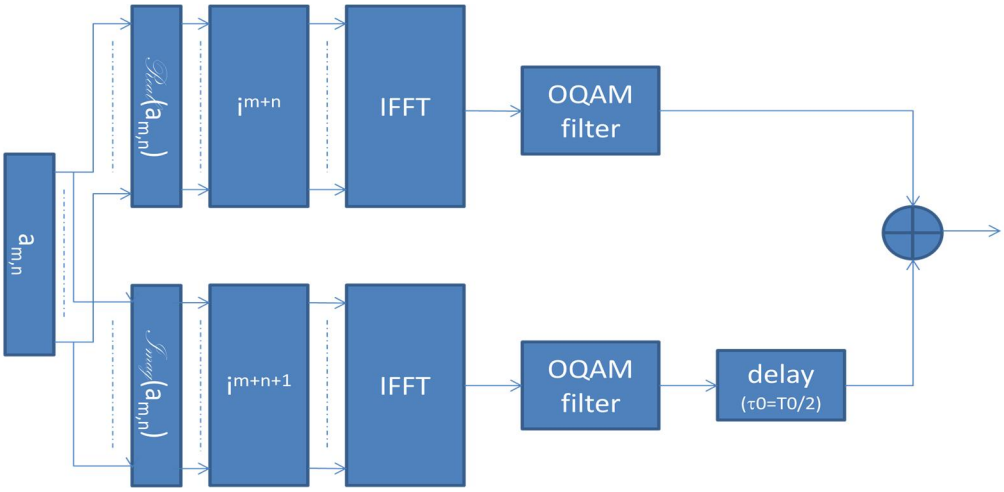

Figure 65: OFDM/OQAM Modulator

3.3.1.10 OFDM/OQAM demodulator

In this section, OFDM/OQAM demodulator is described. The blocks are the dual functions of those included in the modulator. The algorithm of "OQAM filtering" is equivalent to a windowing function of FFT (Fast Fourier Transform).

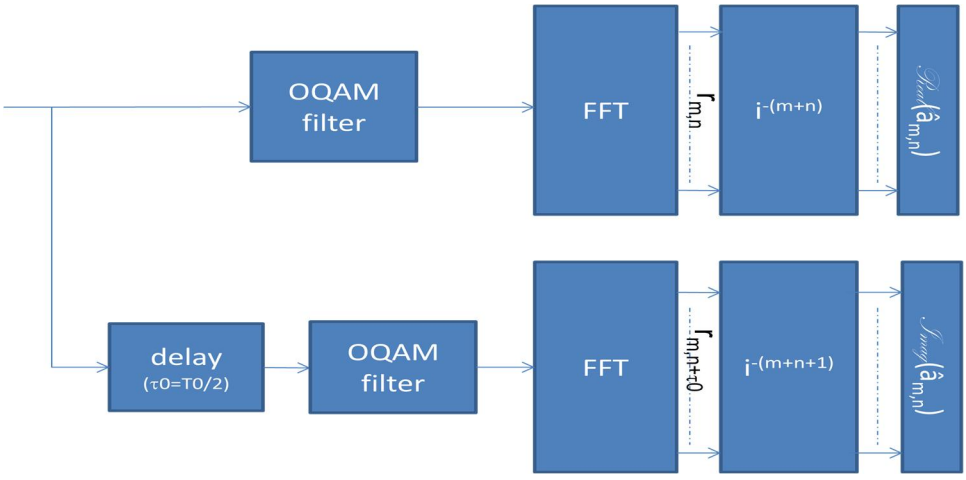

Figure 66: OFDM/OQAM demodulator

3.3.1.11 Complexity issue

A compared analysis of the hardware complexity of the CP-OFDM and OFDM/OQAM modulators and demodulators led to the results shown in Table 18 and Table 19.

CP-OFDM Mod (clk/2)	Logic cells		LC registers		Memory	
	Nb	%	Nb	%	Nb bits	%
CP insertion	204	1.90	69	0.84	262144	39.71
Time interleaver	1522	14.19	685	8.48	65536	9.93
IFFT (mode burst buffered)	7500	69.93	6518	80.67	262144	39.71
Framing	182	1.70	96	1.19	0	0.00
Mapping	447	4.17	188	2.33	0	0.00
Turbo encoder	870	8.11	524	6.49	70304	10.65
total	10725	100	8080	100	660128	100
	Logic cells		LC registers		Memory	
OFDM/OQAM Mod	Nb	%	Nb	%	Nb bits	%
TFL1 Filtering	223	1.52	175	1.59	106496	10.38
IFFT (streaming)	7238	49.38	6208	55.91	327680	31.98
Framing	405	2.76	257	2.31	0	0
Interference Matrix	3768	25.71	2916	26.26	393216	38.38
Rephase	212	1.45	112	1.01	0	0
Time interleaver	1549	10.57	712	6.41	65536	6.4
Mapping	386	2.63	197	1.77	61440	6
Turbo encoder	876	5.98	526	4.74	70240	6.86
total	14657	100	11103	100	1024608	100
Increase (%)	36.66		37.41		55.21	

Table 18: Result of the complexity analysis of the CP-OFDM and OFDM/OQAM modulators

CP-OFDM Demod	Logic cells		LC registers		Memory	
	Nb	%	Nb	%	Nb bits	%
CP Cancellation	295	0.70	133	0.48	155648	8.08
IFFT	7453	17.70	6301	22.58	327680	17.02
Equalization	7336	17.42	3712	13.30	1024	0.05
Time Interpolation	667	1.58	479	1.72	360496	18.72
Freq. Interpolation	1970	4.68	1344	4.82	375792	19.51
Time de-interleaver	1204	2.86	768	2.75	262144	13.61
DeMapping	108	0.26	85	0.30	0	0.00
Turbodecoder	23076	54.80	15087	54.06	442880	23.00
total	42109	100	27909	100	1925664	100
	Logic cells		LC registers		Memory	
OFDM/OQAM Demod	Nb	%	Nb	%	Nb bits	%
TFL1 Filtering	334	0,83	202	0,75	245776	9,68
FFT	7209	17,93	6201	22,90	327680	12,90
Rephase	257	0,64	132	0,49	0	0,00
Equalization	4563	11,35	2636	9,74	1024	0,04
Time Interpolation	1688	4,20	735	2,71	942080	37,10
Freq. Interpolation	2108	5,24	1343	4,96	375792	14,80
Time de-interleaver	1204	3,00	768	2,84	262144	10,32
DeMapping	231	0,57	139	0,51	0	0,00
Turbodecoder	22604	56,23	14919	55,10	384708	15,15
total	40198	100,00	27075	100,00	2539204	100
Increase (%)	-4.54		-2.99		31.86	

Table 19: Result of the complexity analysis of the CP-OFDM and OFDM/OQAM demodulators

According to the reported comparison tables we find that the OFDM/OQAM receiver needs 31.86% extra memory compared with CP-OFDM system but less logical cells and registers. It is worth mentioning that the reported values are obtained from the basic implementation VHDL without any sophisticated design from the efficiency point of view by the experts.

3.3.1.12 Performance description

3.3.1.12.1 Presentation of TFL1 OQAM filter, proposed for DVB-NGH

For DVB-NGH, France Telecom proposed the so-called **TFL1 filter**, among the large family of OFDM/OQAM filters. This filter exhibits better performances against Doppler effect and its length is equal to the FFT length; the complexity is proportional to the length of the filter (L=1). The coefficients of this filter, in 2K FFT mode, are represented in Figure 67.

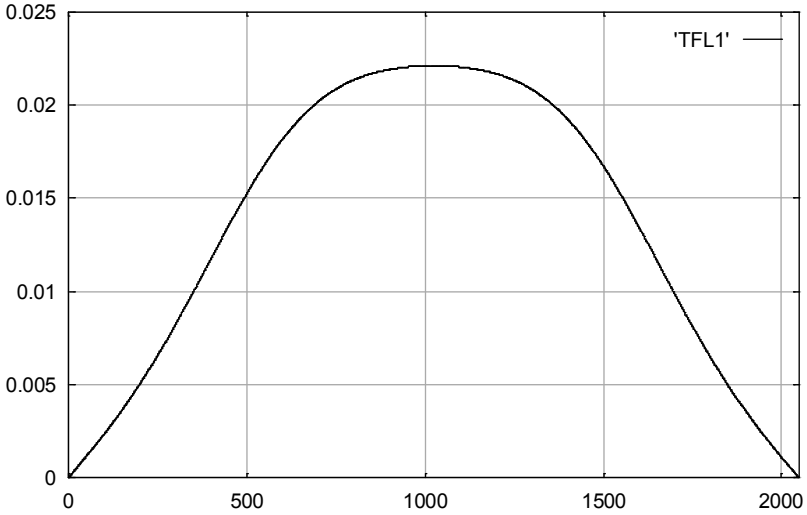

Figure 67: Coefficients of TFL1 OQAM filter for 2K FFT case

3.3.1.12.2 Performance of OFDM/OAQM against SFN and Doppler

Performance of OFDM/OQAM modulation in an SFN scenario and its robustness to Doppler effect induced by speed of the receiver (mobile scenario) has been obtained in France Telecom simulation chain with the following components:

- A random data generator;
- A double- binary turbo encoder of 1504 info size bits (mother code rate 1/2);
- A bit interleaver of the same size for both systematic and redundancy parts;
- A puncturing component in order to achieve the 1/2, 7/12, 2/3, 3/4, 5/6 and 11/12 coding rates;
- A pre-mapping block that optimizes the results for low SNR values (LSB and MSB bit partitioning);
- A mapping component allowing QPSK, 16QAM, 64QAM and 256QAM mappings to be generated;
- DVB-T framing in 2K mode;
- A framing module that inserts the scattered pilots (and that will allow to process the intrinsic interference produced on the pilot by the neighbouring data);
- A phase component that corresponds to the ambiguity function of the OFDM/OQAM filters;
- A 2K FFT modulation;
- The OFDM/OQAM prototype filter: TFL1.

Figure 68 and Figure 69 present the performance results of OFDM/OQAM-TFL1 filter and CP-OFDM for a target BER=10^{-4}, the first figure corresponding to the resistance to a Doppler shift and the second figure corresponding to the performance in an SFN channel (two paths with 0dB).

The parameters of the simulation chain are : 64QAM, coding rate 1/2, no time interleaver, 2K FFT mode.

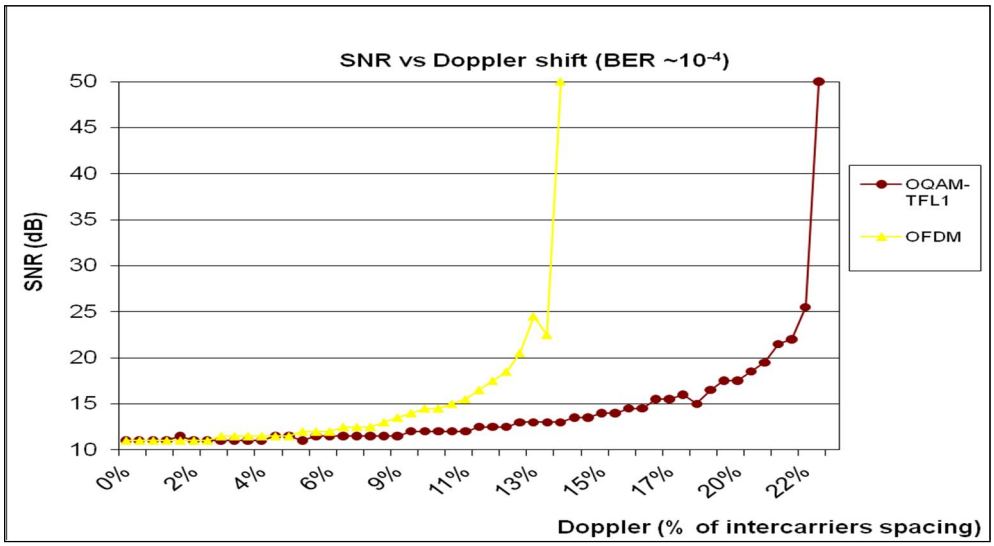

Figure 68: Performance of OFDM and OFDM/OQAM-TFL1 against Doppler shift.

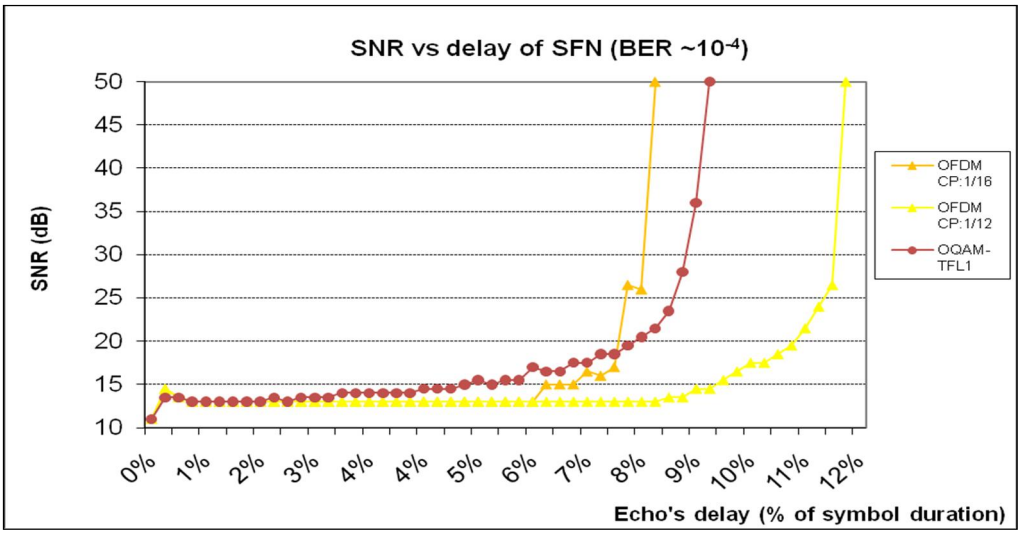

Figure 69: Performance of OFDM and OFDM/OQAM-TFL1 against SFN channel

It is possible to improve the performance of the OFDM/OQAM chain in an SFN channel with a shift of the window on receiver side, searching for a synchronisation around the barycentre of the channel impulse response. Figure 7Figure 70 shows the performance improvement for this chain as a function of the window shift, keeping a target BER=10^{-4}. Figure 71 shows the effect of the delay value on Doppler performance (single path, no SFN).

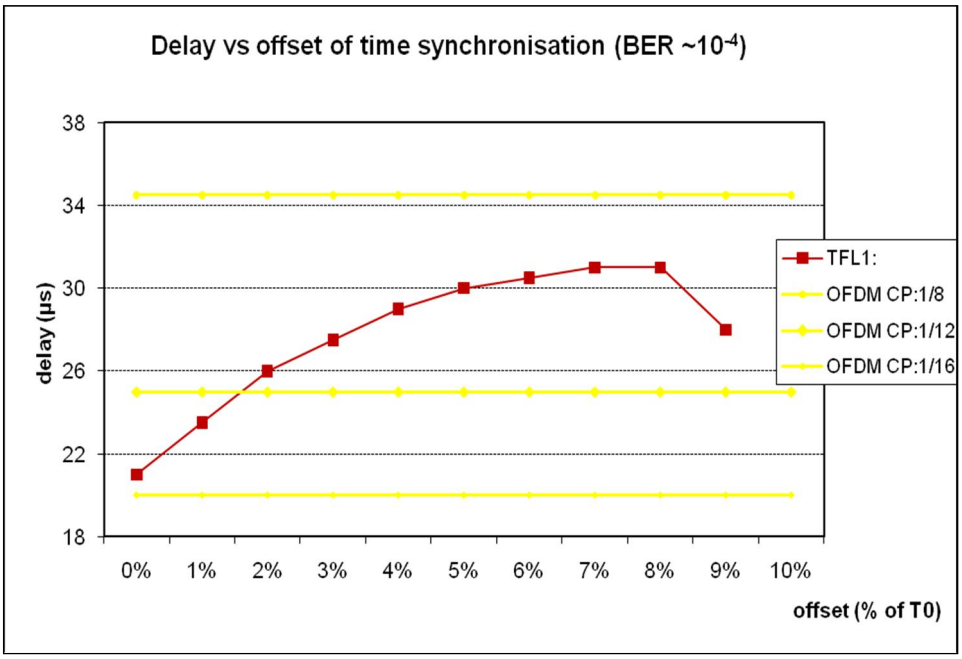

Figure 70: Performance of OFDM and OFDM/OQAM-TFL1 against SFN channel with window offset.
Comment: the maximum robustness of the OFDM/OQAM receiver, with this window offset, is close to the OFDM case with a cyclic prefix equal to 1/8.

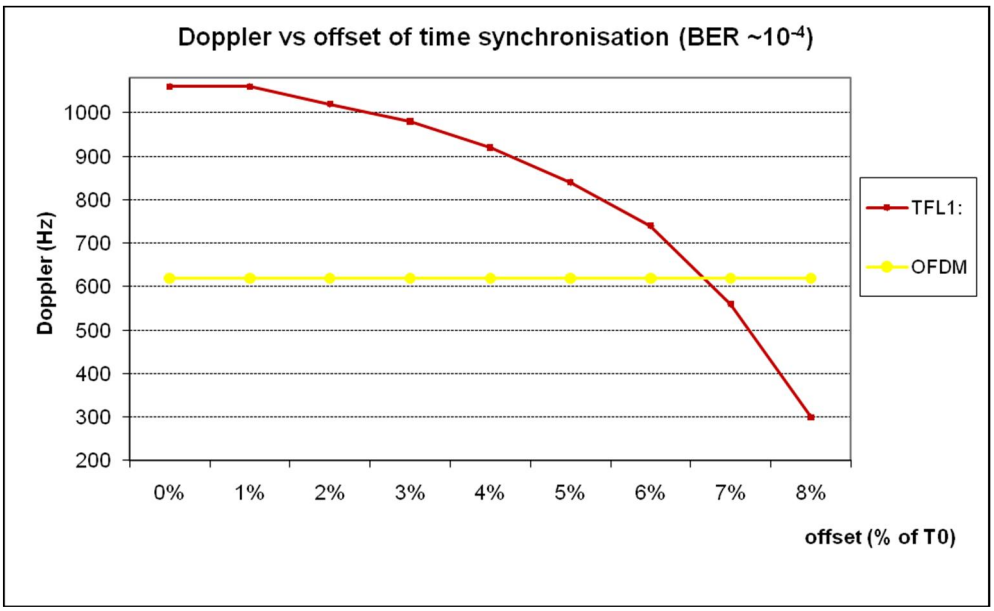

Figure 71: Performance of OFDM and OFDM/OQAM-TFL1 against Doppler with window offset

With a window shift less than 7% of T0 (symbol duration), OFDM/OQAM modulation still outperforms classical CP-OFDM modulation.

3.3.1.12.3 Extension of these results for different FFT sizes

The performance for "OFDM-OQAM-barycentre" corresponds to a shift of the windows filter, in this case the shift is equal to 5% of symbol duration. The results displayed in Figure 72 arise from the interpolation of the performance of FFT-2k.

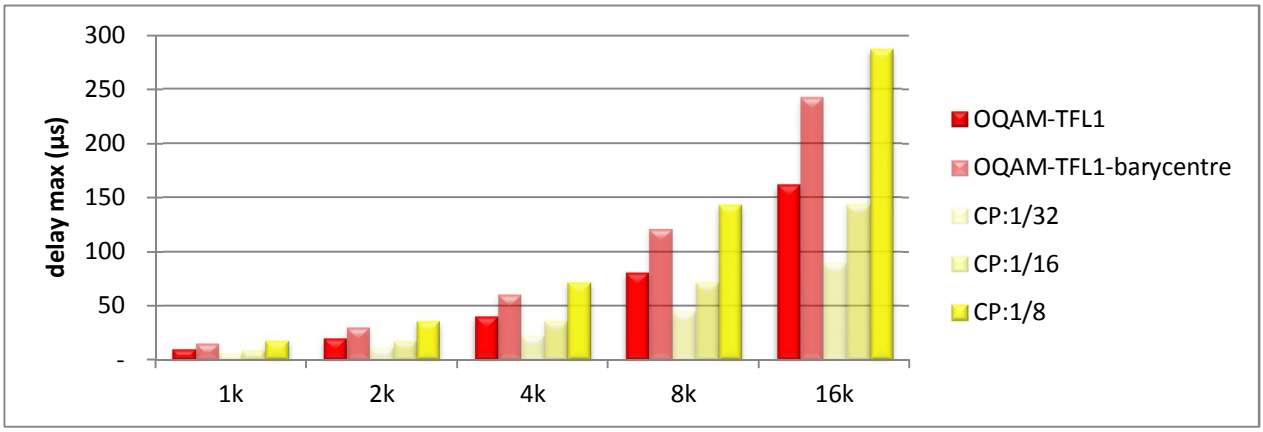

Figure 72: Performance comparison of CP-OFDM and OFDM/OQAM-TFL1 for different FFT sizes (window shift = 5% T0)

3.3.1.13 Specific framing for DVB-NGH with OFDM/OQAM

In this section we describe some specific adaptations in terms of framing through some cases:

- Association between OFDM and OFDM/OQAM.
- Cancellation of intrinsic interferences for scattered pilots and continual pilots.
- Scattered pilot patterns as a function of the performance of OFDM/OQAM-TFL1 and as a function of channel estimation.

3.3.1.13.1 Cancellation of intrinsic interferences

OFDM/OQAM modulation is orthogonal only in the real domain; but the propagation channel is complex and for this reason it is necessary to cancel the intrinsic interference of the scattered pilots "P". This operation is possible directly on modulator side. To do so, it is necessary to compute the intrinsic interference coming from TFL1 filter.

For example if "P" is the position of the scattered pilot, the intrinsic interference noted "I" is dependent of the value of the data near the pilot tone on one side and of the coefficients "$Ci_{m,n}$" on the other side, coefficients described in the table below:

m

0,007	0	-0,007
-0,022	0,040	-0,022
-0,112	0	0,112
-0,228	0,538	-0,228
-0,281	P	0,281
-0,228	-0,538	-0,228
-0,112	0	0,112
-0,022	-0,040	-0,022
0,007	0	-0,007

n

Table 20: Coefficients of the intrinsic interference of the OFDM/OQAM-TFL1 filter

For example, considering the scattered pilot $P_{m,n}$, the position of the specific element "I" used to cancel

interference on "P" will be in coordinates (m+1,n) and the value of this element will be :

$$I_{m+1,n} = -\frac{1}{Ci_{m+1,n}} \sum_{n-1}^{n+1} \sum_{m-4}^{m+4} Ci_{m,n} \cdot d_{m,n} \quad \text{with} \quad Ci_{0,0} = 0$$

The performances of intrinsic interference cancellation scheme on imaginary part of scattered pilot depends on the number of the coefficients (described in Table 20) used.

The couple of pilots scattered "P" and interference cancellation "I" is equivalent to a complex scattered pilot in OFDM system.

3.3.1.13.2 Insertion of pseudo continual pilots

In broadcasting system it is necessary to evaluate the common phase error (CPE) between two successive symbols. This evaluation will be carried out by continual pilots in OFDM system.

For OFDM/OQAM system we use "pseudo" continual pilots to achieve this function, because intrinsic interferences cannot be easily cancelled with continual pilots (similar to conventional OFDM). However if the framing provides a couple of pilots, it is possible to evaluate the CPE between this pilots. The typical related framing will be presented below.

With "d" for data, "C" for pseudo continual pilot and "Ic" pilot for cancellation of intrinsic interferences on imaginary part of pilot "C".

This framing allows the estimation of the common phase error (CPE) every OFDM/OQAM symbol under τ0 (T0/2) sampling.

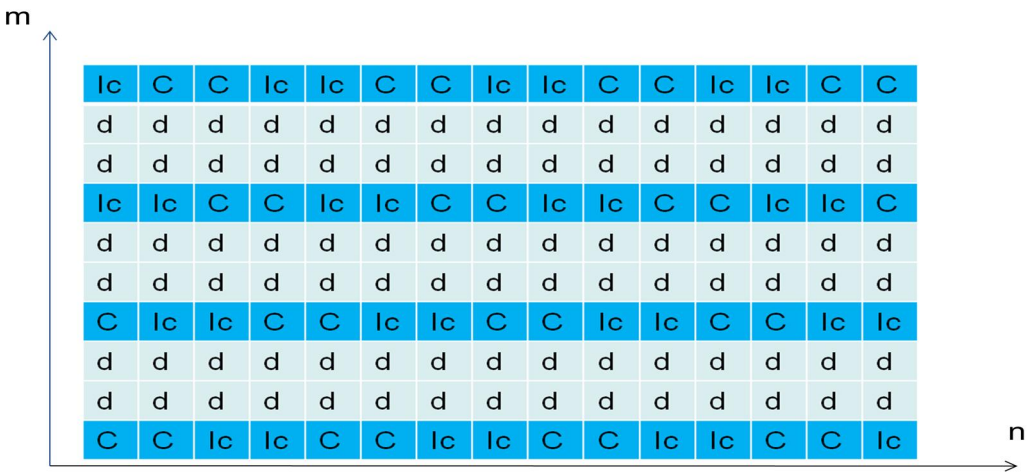

Figure 73: Framing for pseudo continual pilots

3.3.1.13.3 Association between OFDM and OFDM/OQAM symbols

DVB-NGH system could be transmitted in DVB-T2 Future Extension Frame. One constraint already exists at the beginning of this FEF: a P1 symbol will be the first symbol of the frame. This symbol is an OFDM modulated symbol.

Nevertheless it is possible to associate OFDM symbols with OFDM/OQAM symbols. One possible configuration is presented in Figure 74.

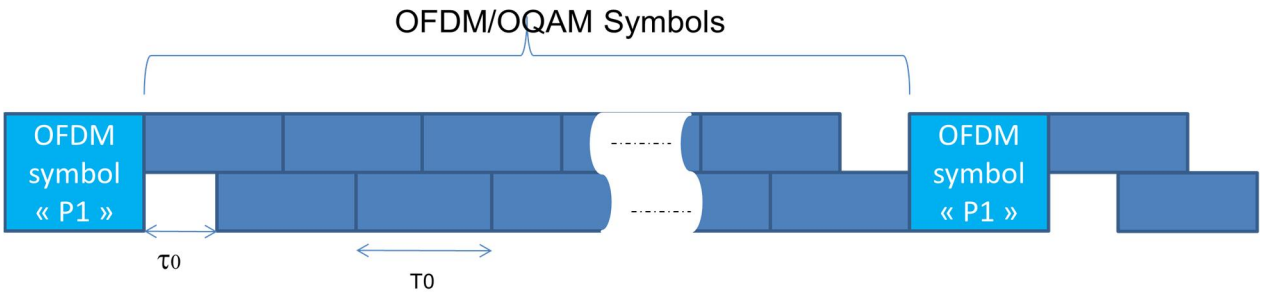

Figure 74: Framing for OFDM and ODFM/OQAM symbols

Only half a symbol is wasted at the end of the frame because an overlap-add operation is done between real and imaginary parts of a symbol, so the loss in spectral efficiency is really not significant considering realistic frame lengths. It is possible to define a synchronization symbol looking like P1 but using ODFM/OQAM modulation.

3.3.1.14 Scattered pilot insertion

The scattered pilot patterns must be adapted to the performances of OFDM/OQAM-TFL1 filter in regards to the channel variations in time and frequency domains.

The scattered pilots are used to estimate the propagation channel. The periodicity in time allows following the Doppler effect and the periodicity of scattered pilots in frequency domain allows to estimate the variation due to the multiple echoes.

The periodicity in time is D_y=4, where "D_y" corresponds to the OFDM/OQAM sampling D_y=4*τ0.

The periodicity in frequency domain is equal to X=12*f0 with f0=1/T0.

This means that after time interpolation there is one pilot each "D_x=6" sub-carrier in frequency domain. Figure 75 gives this repartition of scattered pilots optimized for OFDM/OQAM/TFL1 filter.

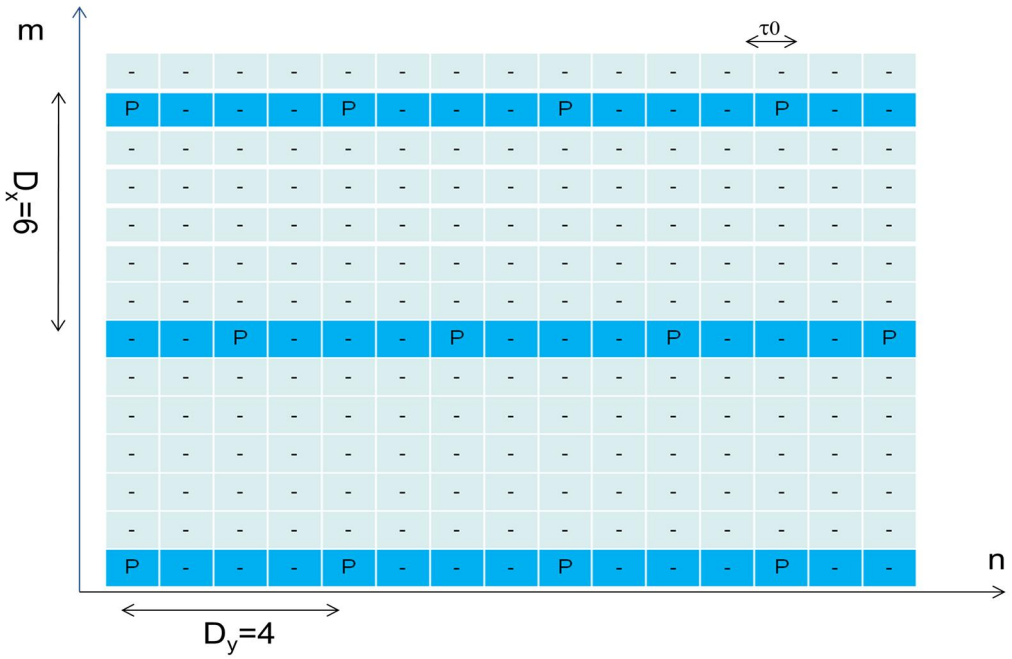

Figure 75: Scattering pilots for ODFM/OQAM framing

3.3.1.15 Alamouti coded OFDM/OQAM

One of the major problems for the OFDM/OQAM system is its intrinsic interference, which causes a difficulty in operating Alamouti encoding. The conventional Alamouti coding scheme cannot work properly with OFDM/OQAM. The most recently published research, i.e. [31], gives a possiblilty for OFDM/OQAM using Alamouti block encoding at the cost of memory increase on the receiver side or spectral efficiency lost by zero padding.

3.3.1.16 Conclusion

In this document, we have described the multicarrier OFDM/OQAM modulation and the way we have adapted it for DVB-NGH. We have listed the main difference of this modulation compared to conventional CP-OFDM modulation. The main advantage of using OFDM/OQAM modulation is the no cyclic prefix insertion leading to significant gain in terms of spectral efficiency. The performance results have shown that the OFDM/OQAM modulation exhibits better robustness against Doppler than CP-OFDM modulation. In terms of delay spread, TFL1 is better than OFDM with CP equal to 1/12 and with an offset in receiver, it is possible to be close to the performances of OFDM with CP equal to 1/8. In addition we heve propose a framing including scattered pilots, pseudo continual pilots and the association between OFDM and OFDM/OQAM symbols.

3.3.2 Satellite link: SC-OFDM modulation

MERCE proposed a modulation scheme, called Single Carrier-Orthogonal Frequency Division Multiplexing (SC-OFDM) modulation, suitable for the satellite component of the DVB-NGH system.

One of the key components in a satellite is the power amplifier (PA) that is due to bring the incoming signal at a level compatible with the receivers sensibility over large areas. In order to guarantee the durability of the satellite, it is critical to keep low the power consumption of the system and thus to optimize the amplifier power efficiency, i.e. to drive the amplifier with small input back-offs. Single Carrier modulations have long been the reference scheme for satellite transmissions for their suitability to achieve low power fluctuations compatible with small input back-offs. However, OFDM modulation is taking over SC schemes thanks to a better flexibility and a comparatively lower complexity when it comes to compensate for high channel degradations. However, the more sub-carriers are added together the more the signal behaves like a Gaussian noise with large power fluctuations. This means either the use of costly power amplifiers with a large linear region at the expense of a poor power efficiency or significant performance degradations due to the saturation of the peaks in the signal when driving the PA with a small input back-off. As its name stands for, the Single Carrier-Orthogonal Frequency Division Multiplexing (SC-OFDM) modulation was derived to combine the best of the two underlying waveforms and more precisely to preserve a lot of commonalities with pure OFDM while significantly reducing power fluctuations. As shown in [26] that depicts the relationships between the OFDM, SC-FDE and SC-OFDM schemes, this is achieved by applying a Discrete Fourier Transform (DFT) on the symbols to be transmitted prior the actual OFDM modulation. A comprehensive description of the SC-OFDM modulation is given into the TR4.1 technical report that specifically addresses the topics related to satellite transmission Figure 76. It is shown in this document that the SC-OFDM appears as a sensible solution when it comes to transmit over power amplifier with very small input back-offs.

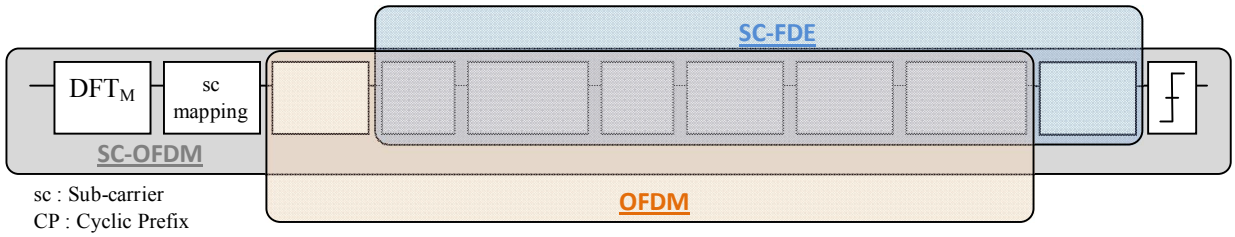

Figure 76: General architecture of an SC-OFDM system.

3.4 Study of interference mitigation and PAPR reduction techniques

Multi carrier communications play a key role in digital communications industry but they suffer from a serious drawback from their high Peak to Average Ratio (PAPR) because it reduces the efficiency of the power amplifier.
Two contributions related to PAPR reduction techniques are reported in this document. In Section 3.4.1, **Thomson Broadcast** investigates the comparison between several Peak to Average Ratio (PAPR reduction techniques for DVB-NGH, especially Tone Reservation and Active Constellation Extension. Section 3.4.2 presents the results of a study carried out by **INSA-IETR** on the optimization of the phase and amplitude of the channel estimation pilots, used jointly for PAPR reduction process.

3.4.1 System considerations

Multi carrier communication is playing a key role in digital communications industry but they are suffering of a serious drawback from their high PAPR. It is impacting the design to cost of transmitters and the power efficiency of the High Power amplifier on the transmitter site. Indeed, in one hand, network operators are requiring higher Modulation Error Ratio of the signal being transmitted to the end user and in the other hand they need better power efficiency of their systems to improve the operating expenditure of the entire network. In the past years, it is commonly accepted that the output of transmitter used in the broadcast UHF bandwidth exceeds 35dB but these requirements are clearly made against the efficiency of the transmission system. However, techniques enabling to reduce the PAPR are helping to maintain good performances while improving the efficiency of the transmitter. Moreover, like standard clipping techniques, PAPR techniques help to protect the HPA against overdriving the amplifier.

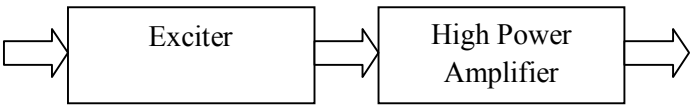

Figure 77 : System under consideration

Choosing a technique is not an easy task and a figure of merit of the techniques has been put in place in order to estimate the gain for the system. Techniques are being also checked for their impact on the receiver design trying to put the complexity of the signal processing into the transmission system and not on the receiver chipset.

Measurements made on Tone Reservation techniques applied to fixed transmission have shown that:

- Power may be increase up to 10% or 0.4dB as well as power effciciency
- MER is increased by 2dB for operating the transmitter at operational transmission

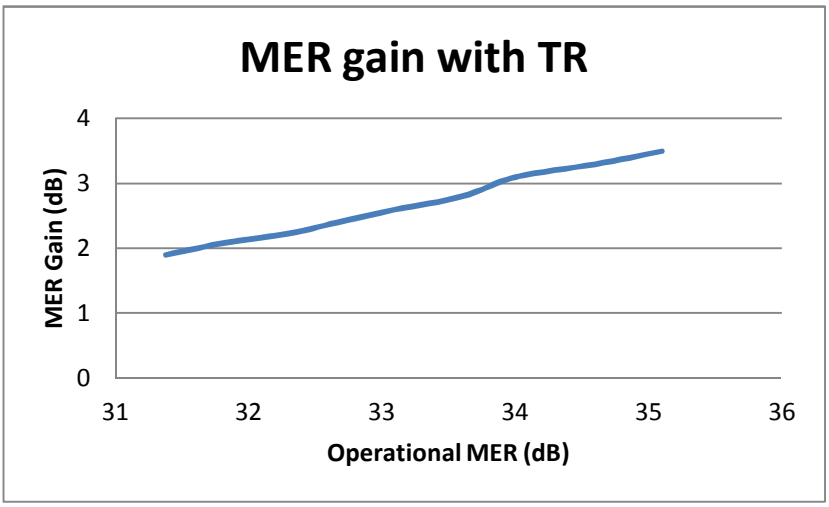

Figure 78: MER gain(dB) versus operational MER(dB) for TR implementation

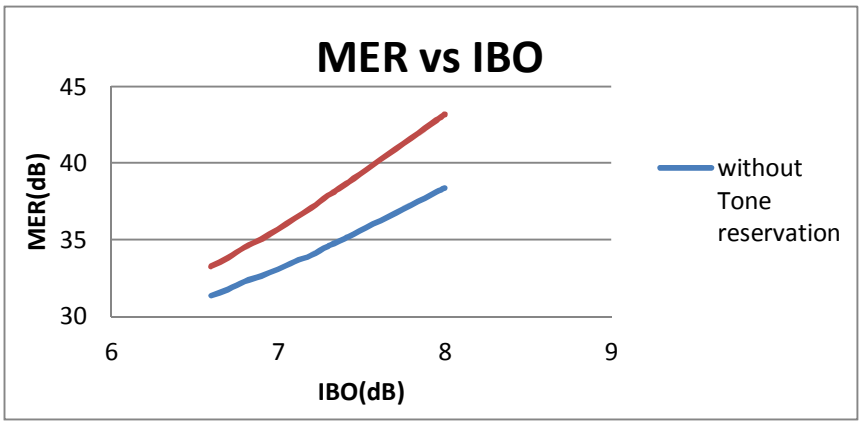

Figure 79 : MER verus HPA IBO

From the chart above, we observe that the gain in MER of tone reservation technique is linearly increasing with the the input back off of the transmitter HPA resulting with higher MER performance for higher MER operatioanl requirements. For instance, in a system requiring a MER of 35dB , an HPA with a back off inferior to 0.4dB can be used improving system efficieny by 10%.

Tone reservation technique is matching the needs for fixed transmission but better gain can be achieved where lower constellations order are available. Better results for mobile transmission with Active Constellation Extension are achieved in QPSK mode (1.5dB power gain has been achieved in previous B21C project). Other techniques (SC-OFDM or Joint PAPR) are being investigated in the project may potentially show superior efficiency for a mobile system.

Input Back Off IBO dB	MER operation dB	MER gain dB	MER with PAPR dB	Out Of Band products (oob) dB	Figure Of Merit Fom
6.6	31.38	1.9	33.28	1.87	0.156875
6.7	31.78	2.07	33.85	2	0.2164375
6.8	32.3	2.23	34.53	2.1	0.2254375
6.9	32.66	2.4	35.06	2.2	0.235
7	33.1	2.6	35.7	2.3	0.24625
7.1	33.6	2.8	36.4	2.4	0.2575
7.2	34	3.1	37.1	2.48	0.274375
7.3	34.6	3.3	37.9	2.5	0.285625
7.4	35.1	3.5	38.6	2.7	0.296875
8	38.4	4.8	43.2	2.9	0.37

Figure 80: Performance table for Tone Reservation

Input Back Off IBO dB	MER operation dB	MER gain dB	MER PAPR dB	Oob dB	Fom
6.7 (QPSK)	33.1	15	48.1	2.3	1.54375
6.7 (16QAM)	33.1	5	38.1	3.3	0.68125

Figure 81: Performance table for Active Constellation Extension on QPSK – 16 QAM

3.4.2 Joint PAPR and channel estimation

Various approaches have been proposed as summarized in [34][35] to mitigate the PAPR of an OFDM signal. Among them, clipping and filtering technique is easy to implement. However, these schemes yield a broken system performance since clipping is a nonlinear process [36] leading to a signal distortion. An alternative method based on coding was proposed in [36], in which a data sequence is embedded in a longer sequence and only a subset of all these possible sequences is used to exclude patterns generating high PAPR. Moreover, other methods such as partial transmit sequence [37], selected mapping [38] and interleaving [38] are also proposed. The main drawback of these methods is the necessity to transmit side information (SI) to the receiver, resulting in some loss of throughput efficiency.

Some methods recently proposed do not need this SI transmission [39][40]. Indeed, the active constellation extension (ACE) method proposed in [40] reduces the PAPR by changing the constellation of the signal without modifying the minimum distance. However, this technique has some gain limits when the constellation size of the signal increases. Moreover, this technique is not suited for rotated constellation schemes, which have been selected for the second generation digital terrestrial television broadcasting system (DVB-T2). The Tone Reservation (TR) method, proposed by Tellado [40] and adopted in DVB-T2 also, uses allocated subcarriers to generate additional signal that minimizes the PAPR value. However, TR technique reduces the spectrum efficiency since it requires some dedicated pilots for PAPR reduction issues. In DVB-T2, 1% of the subcarriers are dedicated for PAPR. Moreover, an iterative process should be implemented at the transmitter with a special need for a smooth control of the transmitted power on the dedicated subcarriers in order to respect the DVB-T2 spectrum mask requirements (the dedicated pilots should be at a power level less than 10 dB with respect to the data subcarriers power).

With the limitations of ACE technique for rotated constellation schemes and those of TR by spectral

efficiency loss, an innovative technique which could be implemented for rotated constellation and without efficiency loss is clearly needed. In this work, we adopt, as in [34], the TR technique by using the pilots of channel estimation for both PAPR reduction and channel estimation issues. The novelty of our proposition is based on the optimization of the phase and amplitude of the channel estimation pilots, used jointly for PAPR reduction process. Indeed, instead of using orthogonal pilots sequences (OPS), we optimize the transmitted sequence for PAPR issue in terms of phase and amplitude. Using a predefined law between different sequences, the receiver could easily utilize a blind detection of the transmitted sequences.

The proposition of this work is multifold. First, instead of using dedicated pilots for PAPR reduction, we expend the idea of [34] which consists in utilizing existing pilots dedicated for channel estimation for both channel estimation and PAPR reduction issues. In this way, we avoid the use of reserved pilots as proposed in DVB-T2 standard improving thus the spectral efficiency of the system. Second, in order to allow their recovery serving for channel estimation process at the receiver, these pilots have to follow particular laws. Multiplicative law in frequency domain is then proposed and investigated in this work. At the receiver, this law is applied to detect and estimate transmitted pilots in frequency domain. As the detection and estimation of multiplicative law's parameters in continuous frequency domain, i.e., in real space, cause degradations, we propose to operate this law in the discrete frequency domain, i.e., in a predefined discrete set. Third, we show by simulations the validity of our technique using DVB-T2 [1] parameters. Its performance is compared to the DVB-T2 PAPR Gradient algorithm and to the second order cone programming (SOCP) technique proposed in [40][41][43].

3.4.2.1 OFDM signal and PAPR value

Let $\mathbf{X} = [X_0, \dots, X_{N-1}]$ be a sequence of complex symbols and $\mathbf{x} = [x_0, \dots, x_{N-1}]$ be its discrete inverse Fourier transform. The OFDM baseband signal; in continuous time domain, is expressed as:

$$x(t) = \frac{1}{\sqrt{N}} \sum_{k=0}^{N-1} X_k e^{\frac{j2\pi kt}{TN}} \qquad 0 \le t < NT \tag{1}$$

where $j = \sqrt{-1}$, N denotes the number of subcarriers and T is the original complex signal duration. In practice, only NL equidistant samples of $x(t)$ are considered, where L represents the over-sampling factor [40] used to make the signal as close as possible to the continuous signal. The over-sampled signal is then given by:

$$x_{[n/L]} = \frac{1}{\sqrt{N}} \sum_{k=0}^{N-1} X_k e^{\frac{j2\pi kn}{LN}} \qquad \forall n \in [0\ NL-1] \tag{2}$$

When the over-sampling factor L is large enough, the PAPR value of the OFDM signal is defined as the ratio of its maximum power divided by its average power. It is expressed as [44]:

$$PAPR\{x(t)\} \approx PAPR(\mathbf{x}_L) = \frac{\max_n \left|x_{n/L}\right|^2}{E\left\{\left|x_{n/L}\right|^2\right\}} \tag{3}$$

where $\mathbf{x}_L = \mathbf{Q}_L \mathbf{X}_L$, $\mathbf{X}_L$ is the zero-padded over-sampled vector of $\mathbf{X}$, $E\{\}$ denotes expectation operation and $\mathbf{Q}_L$ is the inverse discrete Fourier transform matrix of size NL. $\mathbf{Q}_L$ is given by:

$$\mathbf{Q} = \frac{1}{\sqrt{N}} \begin{bmatrix} 1 & 1 & \cdots & 1 \\ 1 & e^{\frac{j2\pi}{NL}1.1} & & e^{\frac{j2\pi}{NL}1.(NL-1)} \\ & \vdots & \ddots & \vdots \\ 1 & e^{\frac{j2\pi}{NL}(NL-1).1} & \cdots & e^{\frac{j2\pi}{NL}(NL-1).(NL-1)} \end{bmatrix} \tag{4}$$

In this study, the PAPR performance is evaluated using the complementary cumulative distribution function (CCDF). It is defined by the probability that the PAPR value exceeds a given threshold γ. For L=1, it can be expressed as [45]:

$$CCDF_{PAPR} = Pr[PAPR(\mathbf{x}_L) > \gamma, L = 1] \approx 11(11e^{-\gamma})^N \quad (5)$$

It is also demonstrated in [45] that the real PAPR value can be approximated independently of L when $L \geq 4$ by:

$$CCDF_{PAPR\{x(t)\}} = Pr[PAPR(\boldsymbol{x}_L) > \gamma, L \geq 4] \approx 1 - (1 - e^{-\gamma})^{2.8\,N} \quad (6)$$

In this work, we consider L=4 and use this expression as a theoretical PAPR reference value of the original OFDM signal.

3.4.2.2 Existing TR-PAPR reduction methods

3.4.2.2.1 General principle

In an OFDM based system (like DVB standards), the main idea of the TR technique is to use reserved pilots in order to reduce the PAPR value at the input of the power amplifier of the time domain transmitted signal.

Let us consider M as the number of channel estimation pilots used for PAPR reduction issue and $\mathbf{P} = [P_0, \dots, P_{M-1}]$ as the M pilot positions dedicated for PAPR reduction, and $\mathbf{C} = [C_0, \dots, C_{M-1}]$ be the set of M pilots transmitted on these positions, as shown in Figure 82. Then, the N modulated symbols $\{X_k\}_{k=0\dots N-1}$ of the OFDM symbol in frequency domain are expressed as:

$$X_k = \begin{cases} C_k & if\ k \in \boldsymbol{P} \\ S_k & if\ not \end{cases} \quad (7)$$

where S_k is the data symbol transmitted on subcarrier k and C_k is a pilot symbol used for PAPR reduction.

The OFDM baseband signal in time domain, after pilot insertion, becomes:

$$\mathbf{x}_L = \mathbf{Q}_L\mathbf{X}_L = \mathbf{Q}_L(\mathbf{C} + \mathbf{S}_L) = \mathbf{Z}_L\mathbf{C} + \mathbf{s}_L \quad (8)$$

Where $\mathbf{S}_L$ is the data vector represented in frequency domain of size N (where the values at the pilots positions are set to 0) and $\mathbf{s}_L$ is its time domain representation. $\mathbf{Z}_L$ is given by:

$$\mathbf{Z}_L = \frac{1}{\sqrt{\mathrm{N}}}\begin{bmatrix} 1 & 1 & \cdots & 1 \\ e^{\frac{j2\pi}{NL}1.p_1} & e^{\frac{j2\pi}{NL}1.p_2} & & e^{\frac{j2\pi}{NL}1.p_M} \\ \vdots & & \ddots & \vdots \\ e^{\frac{j2\pi}{NL}(NL-1).p_1} & e^{\frac{j2\pi}{NL}(NL-1).p_2} & \cdots & e^{\frac{j2\pi}{NL}(NL-1).p_M} \end{bmatrix} \quad (9)$$

and L holds for oversampling factor.

The added signal $\mathbf{c}_L = \mathbf{Z}_L\mathbf{C}$ has to cope with PAPR values. In literature, different techniques have been proposed to optimize this signal. Among them, the SOCP and the Gradient solutions are two of the most promising keys which have been extensively studied for optimization purposes. In the next section, we will give a general overview about these techniques. Performance of these techniques will be used as reference in comparison with our proposed technique.

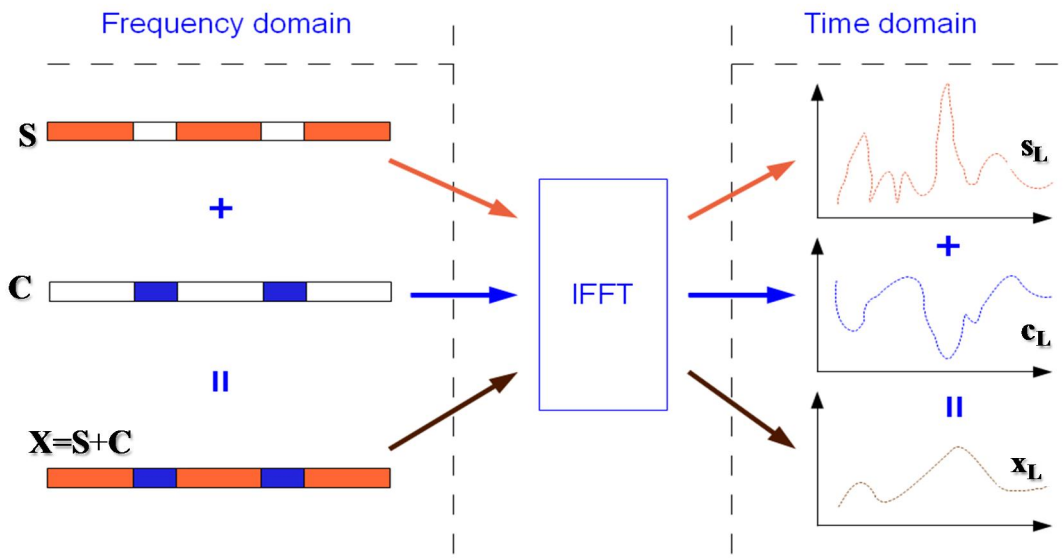

Figure 82- Pilots insertion scheme.

3.4.2.2.2 SOCP solution

The PAPR reduction problem can be formulated as follows: reducing PAPR value leads to the minimization of the maximum peak value of the combined signal ($\mathbf{s}_L + \mathbf{Z}_L\mathbf{C}$) while keeping the average power constant [12]. Mathematically speaking, this problem can be written as:

$$\min_{\mathbf{C}} \max_{n} \left|\mathbf{s}_L + \mathbf{Z}_{n,L}\mathbf{C}\right| \tag{10}$$

where $\mathbf{Z}_{n,L}^{row}$ denotes the n^{th} row of $\mathbf{Z}_L$.

Equation (10) can be also rewritten as:

$$\min_{\mathbf{C}} \left\|\mathbf{s}_L + \mathbf{Z}_{n,L}\mathbf{C}\right\|_{\infty} \tag{11}$$

where $\|.\|$ denotes the standard uniform norm.

Since the set $\mathbf{C}$ of pilots is used for PAPR reduction, the problem turns out now to find $\mathbf{C}$ which minimizes the PAPR of the current transmitted OFDM symbol. In the continuous domain, i.e. for $\mathbf{C} \subset \mathbb{C}^M$, this search is formulated as a convex optimization problem and solved using SOCP problem [40][41][43]. The optimization process can take the form of:

$$\begin{cases} \text{Minimize} & \beta \\ \text{subject to} & \left\|\mathbf{s}_L + \mathbf{Z}_{n,L}^{row}\mathbf{C}\right\| \le \beta \\ & \forall\, 0 \le n \le NL-1 \end{cases} \tag{12}$$

It has been shown that this technique provides the optimized value in terms of PAPR reduction but it presents a high calculation complexity [40][41][43]. In our study, we will use this technique as a comparison term with other techniques mainly with the proposed joint PAPR reduction and channel estimation scheme.

3.4.2.2.3 Gradient iterative based method

This method, adopted in DVB-T2 standard, is a suboptimal solution of the SOCP method. It is based on the gradient iterative method using the clipping process. In order to apply this technique, the technical specifications of DVB-T2 allowed 1% of active sub-carriers for PAPR reduction issues. The pilots signal used for PAPR, defined as a reference kernel signal, is given by:

$$p = \frac{N}{N_{TR}} \mathbf{Q}_L [1_{TR}] \quad (13)$$

where N_{TR} denotes the number of reserved subcarriers, $[1_{TR}]$ denotes the $(N,1)$ vector having N_{TR} elements of ones at the positions corresponding to the reserved carriers and $(N\text{-}N_{TR})$ elements of zeros at the others. This reference signal presents a peak at the position 0.

For each iteration, the peak position k of the initial signal is detected. Reference signal is shifted of k positions in order to allow the reduction of peak signal to a predefined clipping value V_{CLIP}. The reduction principle is described in Figure 83.

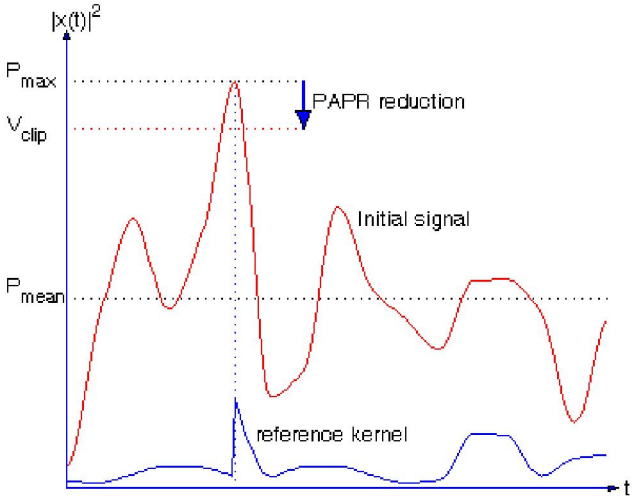

Figure 83- Principle of peak suppression by reference kernel signal.

The procedure of the PAPR reduction algorithm is given as follows:

Initialization:

1. *The initial values for peak reduction signal in time domain are set to zero:*
2. $\mathbf{c}^{(0)}=[0 \ldots 0]^T$ *where* $\mathbf{c}^{(i)}$ *denotes the vector of the peak reduction signal computed at* i^{th} *iteration.*

Iterations:

1. *i starts from 1.*
2. *Find the maximum magnitude of* $(x + \mathbf{c}^{(i-1)})$*, noted* y_i*, and the corresponding sample index* k_i*.*
3. *If* $y_i<V_{CLIP}$ *: go to the step 5.*
4. *If* $y_i > V_{CLIP}$ *: clip the signal peak to this value.*
5. *Update the vector of peak reduction signal* $\mathbf{c}^{(i)}$*.*
6. *If* $i< i_{max}$*, the maximum iteration number, increase* i *by one and return to step 2.*
7. *Terminate the iteration. The transmitted signal is obtained by:* $x'=x+\mathbf{c}^{(i)}$

The overall process of the gradient iterative based method is summarized in Figure 84.

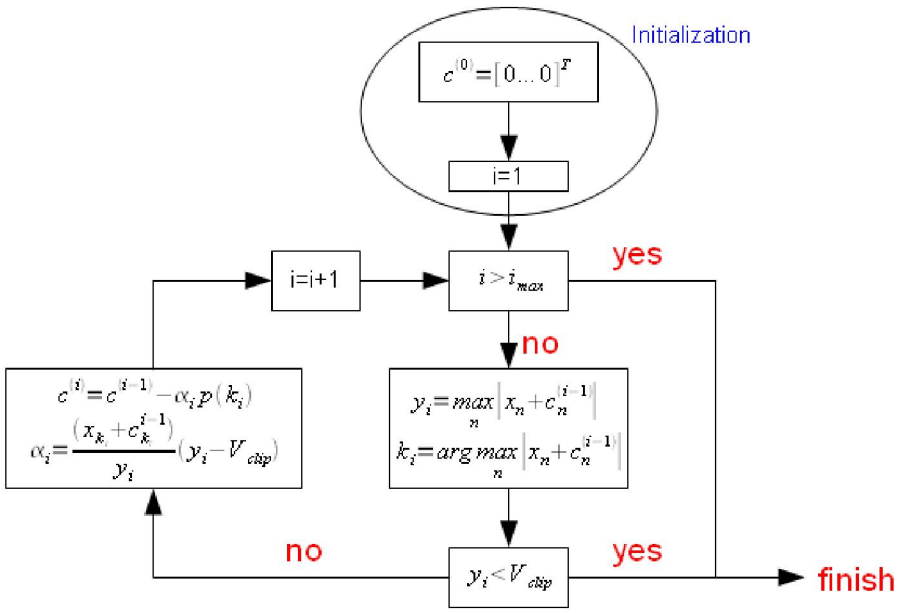

Figure 84- Principle of gradient iterative algorithm proposed in DVB-T2.

3.4.2.3 Proposed pilot-aided PAPR reduction method

The conventional TR method uses dedicated pilots for PAPR reduction issue leading to a spectral efficiency loss. In this proposition, we use some of the scattered pilots dedicated to channel estimation for both PAPR reduction and channel estimation purposes. The main problem turns out then to find the pilot symbols at the transmitter which minimizes the PAPR value but also to find these pilot symbols at the receiver in order to achieve channel estimation.

That is, in order to achieve both operations, i.e., PAPR reduction and channel estimation, the set $\boldsymbol{C}$ chosen for PAPR reduction has to undergo some particular laws known at the receiver. Figure 85 shows the general principle of the proposed method. In this scheme, the function *f*(.) reflects the particular law known at both the transmitter and receiver. In our proposition, we consider a simple multiplicative law given by:

$$C_{k+1} = C_k \times \Omega \qquad \forall\, k \in [0, \ldots, M-2] \quad \text{or equivalently} \quad C_k = \Omega^k C_0 \tag{14}$$

where $\boldsymbol{\Omega}$ denotes the step between two consecutive pilots and C_0 is the first pilot symbol.

The choice of C_k and $\boldsymbol{\Omega}$ could be either in continuous domain, i.e. the pilots could take any continuous value in $\mathbb{C}$, or they could take any discrete value from a discrete predefined set in discrete domain with a discrete value $\boldsymbol{\Omega}$. Since the estimation of the pilots and $\boldsymbol{\Omega}$ at the receiver in continuous domain could yield to a residual estimation error, and then to a slight system performance degradation, we propose to perform research in a discrete sub-set of $\mathbb{C}$. Equation (14) becomes:

$$\begin{aligned} C_0 &= \lambda e^{j\phi} \\ \Omega &= e^{j\Delta} \\ C_k &= \lambda e^{j(\phi+k\Delta)} \end{aligned} \tag{15}$$

where λ, ϕ and $\boldsymbol{\Delta}$ take values from a predefined set of discrete values. λ is the boost factor applied to the dedicated subcarriers, ϕ is the initial phase value of the first pilot symbol, and $\boldsymbol{\Delta}$ is the phase increment. The main reason to select a multiplicative law is due to simplicity issues and boost factor control, i.e. power

control of the transmitted sequences. Indeed, using (15), we can equivalently control the boost factor of all pilots (joint PAPR and channel estimation pilots). Again, we recall that the "discrete domain" means that instead of searching SOCP solution in $\mathbb{C}$, we search it in a predefined discrete set with a different discrete step for ϕ and Δ, called $\mu(\phi)$ and $\mu(\Delta)$ respectively. Figure 86 shows the multiplicative law scheme and the evolution of the pilots from one index to another. λ, ϕ and Δ have to be selected in such a way to optimize the PAPR reduction gain and to limit channel estimation errors. This compromise will be detailed in next sections.

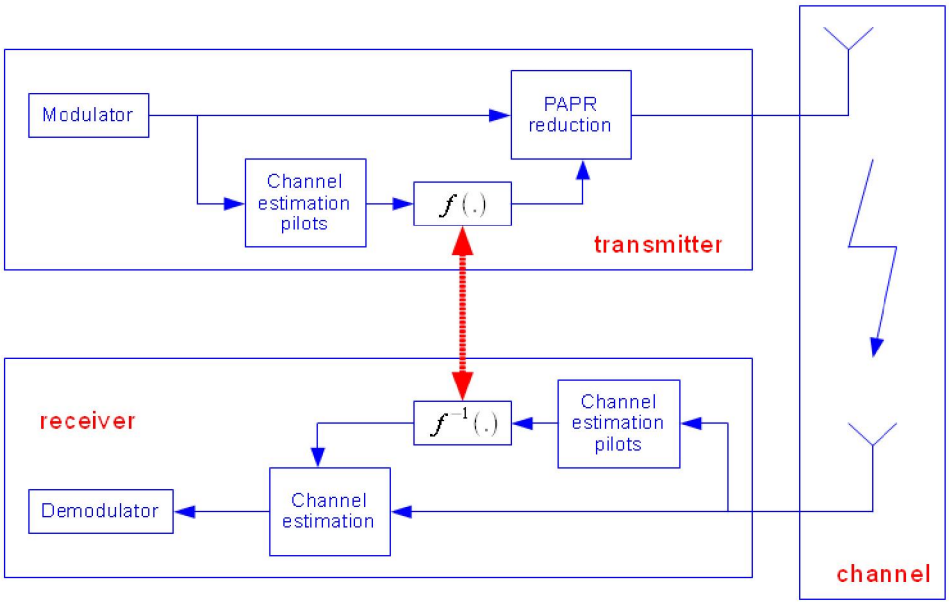

Figure 85- General principle of the proposed method.

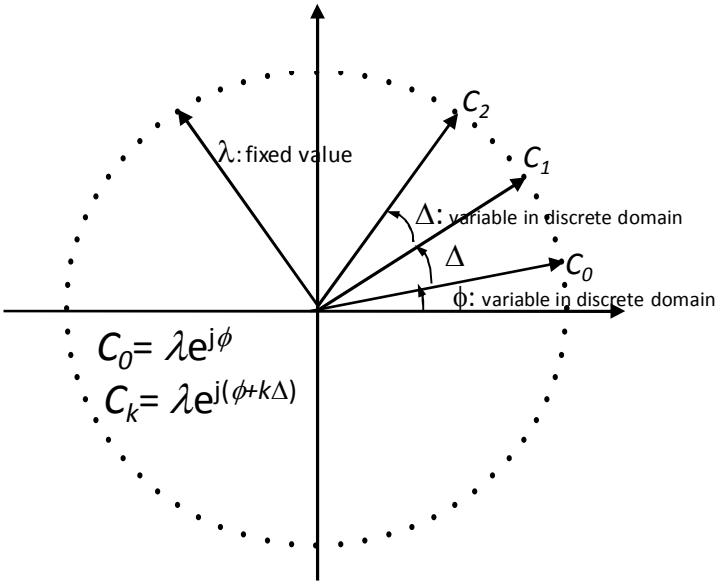

Figure 86- Multiplicative law scheme.

3.4.2.4 Pilots recovery and channel estimation

In order to describe the channel estimation scheme and pilots recovery, frequency non-selective fading per subcarrier and time invariance during one OFDM symbol are assumed. Furthermore, the absence of Inter-symbol Interference and Inter-carrier Interference is guaranteed by the use of a guard interval longer than the maximum excess delay of the impulse response of the channel. In conventional OFDM schemes and under these assumptions, the received signal at the output of the FFT operation could be written as:

$$\mathbf{R} = \mathbf{HS} + \mathbf{W} \tag{16}$$

where $\mathbf{H}$ denotes the $N \times N$ matrix which contains the complex channel coefficients and $\mathbf{W}$ is the additive white Gaussian noise vector.

In conventional OFDM systems, the channel estimation is done by estimating the pilot channel coefficients $\widehat{H}_p$ first and then by filtering the obtained coefficients using some conventional filters (the Wiener filter is widely used). The conventional OFDM channel estimation scheme is represented in Figure 87. Figure 88 shows the proposed channel estimation scheme when some pilots are dedicated for PAPR issues. It is clear that there is a slight difference with the conventional estimation scheme shown in Figure 87. In our scheme, the pilot symbols C_p used for PAPR reduction are not known a priori at the receiver. Therefore, the pilots' recovery and channel estimation procedure is performed in two steps. First, we determine the transmitted sequence $\hat{C}_p$ used for PAPR reduction. In the second step, we determine the actual channel coefficients $\widehat{H}_k$.

In order to accomplish the first step, we assume that the channel is almost constant between two successive OFDM symbols i.e. we assume that $\widehat{\mathbf{H}}^{(l)} \approx \widehat{\mathbf{H}}^{(l-1)}$ where l denotes the OFDM symbol index in time domain. Then, the pilot symbol used for PAPR reduction could be deduced by:

$$\bar{C}_p^l = \frac{R_p}{\widehat{H}_p^{(l-1)}} \quad \forall\, p \in P \tag{17}$$

By considering multiplicative law in discrete domain, received symbols at pilot positions are expressed as:

$$\bar{C}_p^l = \frac{H_p^l C_p^l + W_p^l}{\widehat{H}_k^{(l-1)}} \approx C_p^l + \frac{W_p^l}{H_p^l} \quad \forall\, p \in P \tag{18}$$

By combining (18) with (15), we have:

$$\bar{C}_p^l = \lambda e^{j(\phi + p\Delta)} + \frac{W_p^l}{H_p^l} \quad \forall\, p \in P \tag{19}$$

Since C is in discrete frequency domain, the estimate, $\hat{C}_p^l$, of C_p^l can be obtained from $\bar{C}_p^l$ by a simple quantization operation. As we consider that the boost factor λ is known at the receiver, the set C is characterized by two unknown variables of ϕ and Δ. Considering μ(ϕ) and μ(Δ) the elementary steps of ϕ and Δ in discrete domain, ϕ and Δ can be estimated as follows:

Estimation and decision of Δ:

$$\begin{aligned} \hat{\Delta} &= angle\left[\sum_{p=1}^{M-1} \bar{C}_p^l \left(\bar{C}_{p-1}^l\right)^*\right] \\ \bar{\Delta} &= D\left[\hat{\Delta}\big|_{\mu(\Delta)}\right] \end{aligned} \tag{20}$$

where $D[X|_\alpha]$ denotes decision function of X in discrete domain with a step α.

Estimation and decision of ϕ:

$$\hat{\phi} = angle\left[\sum_{p=0}^{M-1} \bar{C}_p^l e^{-jp\Delta}\right]$$
$$\bar{\phi} = D\left[\hat{\phi}\big|_{\mu(\phi)}\right] \quad (21)$$

In order to evaluate our detection algorithm, we define the error detection probability (EDP) of ϕ and Δ as:

$$\Pr(\Delta) = \Pr\left\{|\bar{\Delta} - \Delta| > \frac{\mu(\Delta)}{2}\right\} \quad (22)$$

$$\Pr(\phi) = \Pr\left\{|\bar{\phi} - \phi| > \frac{\mu(\phi)}{2}\right\} \quad (23)$$

where $\Pr\{|x| > \alpha\}$ denotes the probability that the absolute value of x is greater than α.

In Appendix A, these probabilities are calculated in the case of AWGN channel. We obtain:

$$\Pr(\Delta) = 1 - erf\left(\frac{\mu(\Delta)/2}{\sqrt{2\left(\frac{\sigma^2}{(M-1)^2\lambda^2} + \frac{2(M-1)\sigma^4}{(M-1)^2\lambda^4}\right)}}\right) \quad (24)$$

and

$$\Pr(\phi) = 1 - erf\left(\frac{\mu(\phi)/2}{\sqrt{\frac{\sigma^2}{M\lambda^2}}}\right) \quad (25)$$

The results of this computation are analyzed in next section.

The estimation and detection of ϕ and Δ allow us computing the transmitted pilot sequence. Once the transmitted pilot sequence is obtained, the second step consists of estimating the channel coefficients in the frequency domain. They could be obtained by the simple relationship:

$$\hat{H}_k^l = \frac{R_k}{\hat{C}_k^l} \quad \forall\, k \in P \quad (26)$$

Once the channel coefficients are computed on the pilot positions, the overall frequency channel response can be obtained by a simple Wiener filtering like in conventional channel estimation procedure. Both procedures are shown in Figure 87 and Figure 88 respectively.

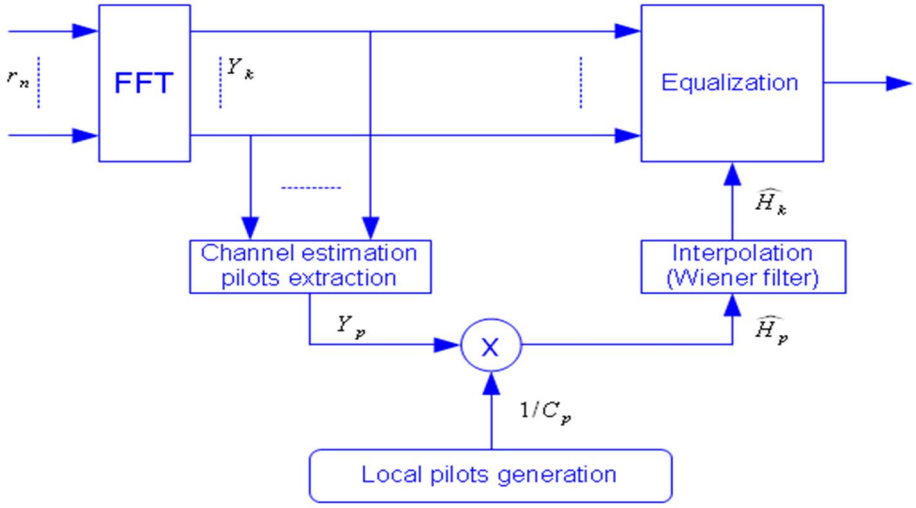

Figure 87- Conventional channel estimation scheme in OFDM systems.

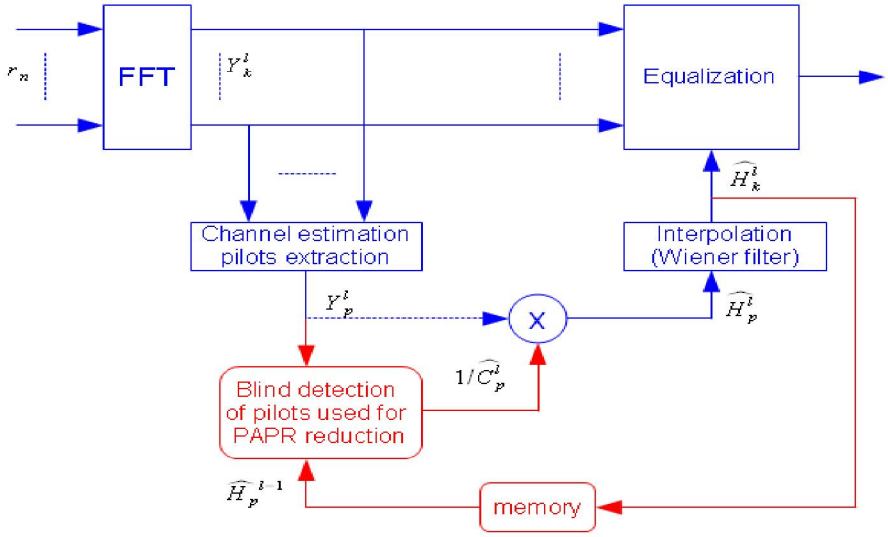

Figure 88- Modified channel estimation scheme.

3.4.2.5 Simulation results and discussion

Simulation results are performed using DVB-T2 parameters. Some of the main parameters are summarized in

Table 21. The PAPR parameters of the proposed method, i.e., λ, Δ and ϕ are variable parameters which allow an optimization of both PAPR reduction and channel estimation processes. They will be specified in each simulation scenario.

Let's consider SOCP solution with a number of pilot tones M equal to 8. In fact, the SOCP solution is not possible using multiplicative law in continuous domain since the problem is not convex. In order to solve the problem, we consider discrete values of ϕ and Δ while maintaining λ in continuous domain. More precisely, we consider λ in continuous domain and we change the values of ϕ from 0 to 2π with a step of $\pi/8$, while Δ varies from 0 to 2π with variable step μ, of $\pi/2$, $\pi/4$, $\pi/8$ and $\pi/16$. The results are presented in Figure 89 in terms of CCDF.

Mode (OFDM size)	2K
Number of subcarriers	NFFT=2048
Guard Interval length	GI=1/8
Modulation	16-QAM, 64-QAM
Coding rate	R=1/2
Over-sampling factor	L=4
Number of subcarriers used for PAPR reduction	M=8, 16, 32

Table 21- Simulation parameters, extracted from DVB-T2 standard.

Figure 89 shows the CCDF of the multiplicative law using SOCP solution with respect to the continuous λ value and different step values μ. The PAPR gain increases when the step value μ decreases since the solution is approaching the continuous domain. Moreover, the solution converges when the step value μ reaches a limit value $\mu_{lim} = \pi/8$. In other words, the PAPR gain increases when the pilots' values are optimized in continuous domain. The results obtained in Figure 89 show first that CCDF simulation results are close to theoretical value given in equation (6). Moreover, this figure shows that with a continuous λ value, a phase discretization using a step $\mu = \pi/8$ is enough to converge to the maximum PAPR reduction gain in the continuous domain.

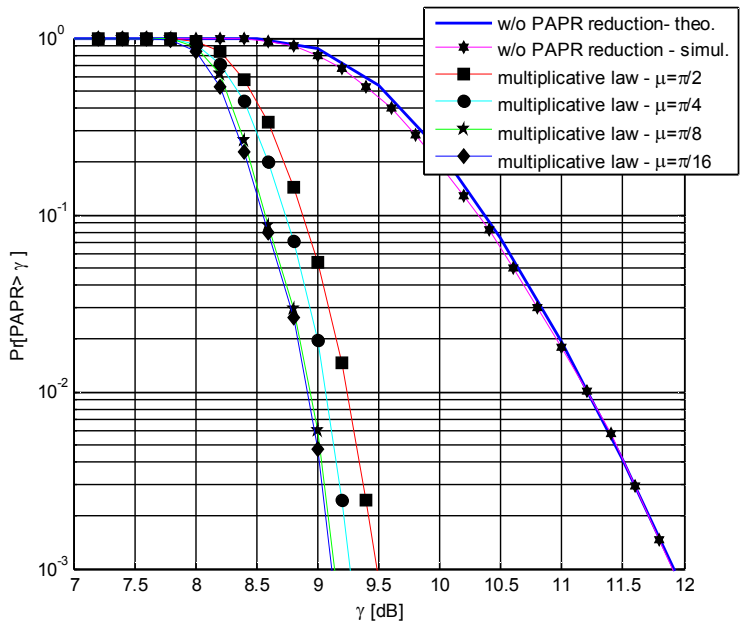

Figure 89- CCDF performance of multiplicative law using SOCP solution, continuous λ, 16-QAM, 2k mode.

3.4.2.5.1 Multiplicative law performance in discrete domain

We consider now the multiplicative law with ϕ and Δ in the discrete domain while λ takes a value from a predefined set. Firstly, we present CCDF performance for a fixed λ value and for ϕ and Δ varying from 0 to 2π with a step of $\pi/8$. The number of subcarriers used for PAPR reduction is always M=8. In this case, reducing PAPR is not a SOCP problem anymore but becomes a search of the optimum combination minimizing PAPR. At the receiver, pilots are recovered by a detection and estimation algorithm. Figure 90 gives a comparison between different PAPR reduction techniques namely, SOCP solution, Gradient technique and our proposed technique with a predefined power value $\lambda = 20\,dB$. This figure shows that using our solution and this λ value, we obtain slightly better results than in DVB-T2 gradient solution.

However, the Gradient solution requires an iterative complex implementation. Again, we recall that this method avoids the use of dedicated pilots for PAPR reduction issue, improving also spectral efficiency of the system (1% in case of DVB-T2 specification).

In Figure 91, we present the PAPR gain in terms of CCDF, in comparison with the curve obtained without PAPR reduction technique, as a function of λ. We assume that ϕ and Δ change from 0 to 2π with a step of $\pi/8$, $\pi/16$ and $\pi/32$. This gain is evaluated at a CCDF=10-3. It is also compared with the SOCP solution for multiplicative law (λ continuous). Figure 91 shows that the system performance is improved when the step of ϕ and Δ becomes smaller. This is because the number of pilot combinations increases when the step decreases. For each value of this step, there exists one optimum value of λ for which the PAPR gain in terms of CCDF reaches the maximum.

Now, considering a discrete λ value, we compare the performance of the proposed method, for a step of ϕ and Δ of $\pi/8$, when λ=20 dB which is the one maximizing the PAPR gain at CCDF=10-3 and when λ is discrete, varying from 5 dB to 25 dB with a step of 3 dB. The results are presented in Figure 92. For a CCDF=10-3, the performance in terms of PAPR when λ=20 dB is about 0.35 dB worse than the one of SOCP solution. It is about 0.17 dB worse than the case when λ is discrete. In other words, we lose only 0.17 dB when a predefined value of λ is selected instead of using a predefined set of discrete values.

In terms of complexity, the discrete solution is less complex than the SOCP solution (optimal solution). Indeed, our proposed PAPR reduction technique aims at searching the optimal solution in terms of λ, ϕ and Δ in a predefined discrete set of values while SOCP solution applies a search in continuous domain. Moreover, setting a predefined value of λ yields to a reduced complexity implementation in comparison with the discrete λ solution, however, with a 0.17 dB PAPR loss. On the other hand, in terms of channel estimation, setting a predefined value of λ implies an improved performance in comparison with the discrete case since we avoid quantization at the receiver. So, the proposed method with a predefined value of λ presents a good tradeoff between channel estimation performance and PAPR gain.

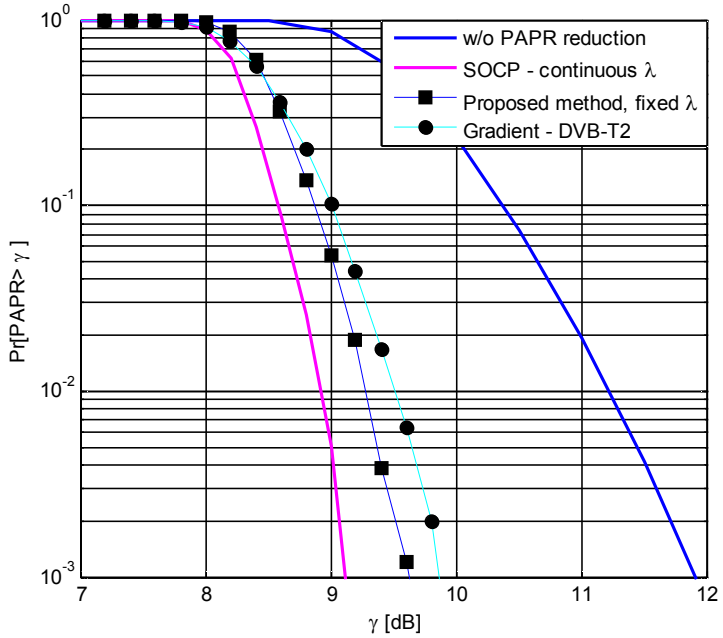

Figure 90- CCDF performance of multiplicative law in discrete domain, 16-QAM, λ = 20 dB

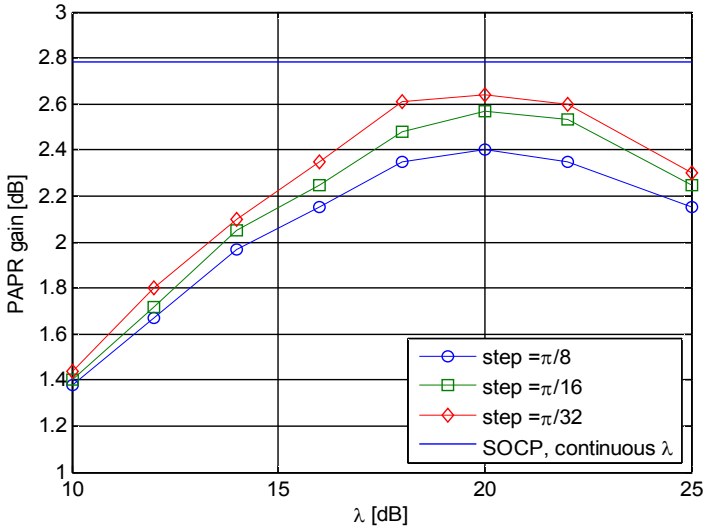

Figure 91- PAPR gain at a CCDF= 10-3 as a function of λ, M = 8, 16-QAM

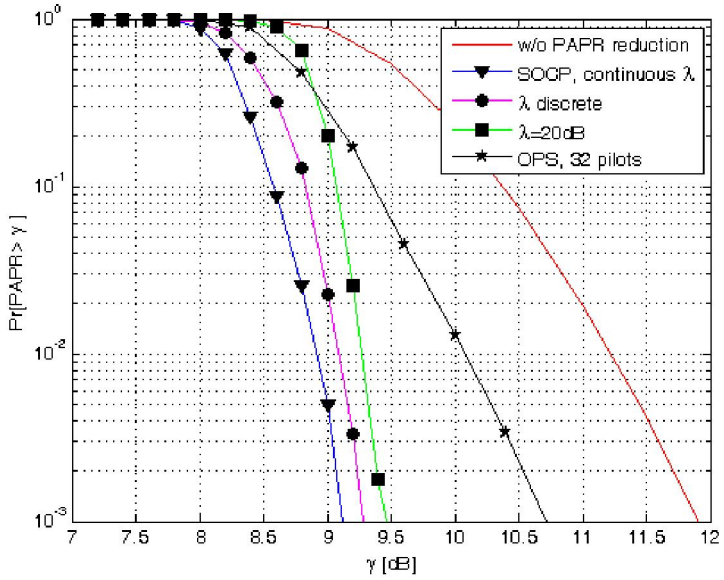

Figure 92- CCDF comparison in two cases: λ = 20 dB and discrete λ, with OPS technique [34], 16-QAM.

In [34], OPS technique using Walsh-Hadamard sequences is chosen in order to make a blind detection of the transmitted sequence at the receiver side. In Figure 92, performance of this technique is given for WH sequences with length Nc= 32 chips. We can easily see that the performance of our proposed method is much better than the one proposed in [34]. A gain from 1.2dB to 1.6dB in terms of PAPR reduction is obtained in this case.

Finally, the performance in terms of PAPR gain is presented in Figure 93 for M=8, 16 and 32 as a function of λ. Figure 93 shows that the PAPR gain performance slightly decreases when M increases, but we note that the optimum value of λ also decreases when M increases. This is important because it means that we can reduce the pilot's power when increasing the number of subcarriers used for PAPR reduction.

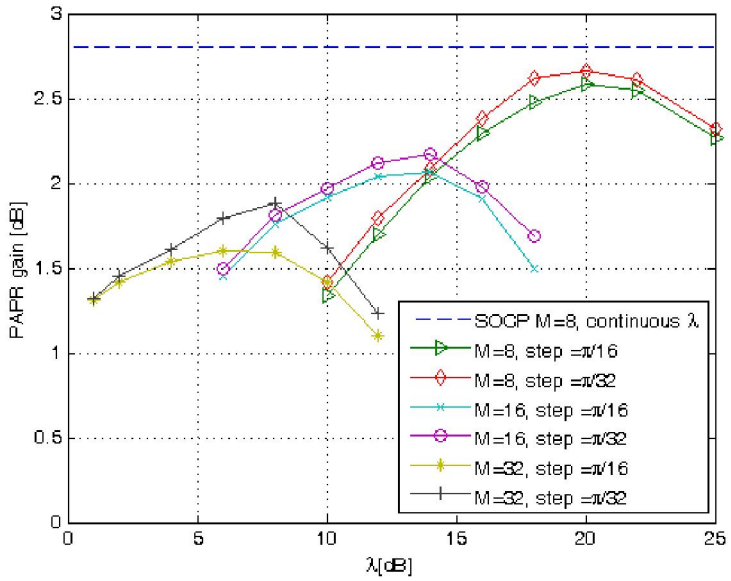

Figure 93- CCDF performance as a function of λ and M, 16-QAM

3.4.2.5.2 Comparison with DVB-T2 PAPR techniques

First of all, one of the main advantages of this technique is that it could be used with rotated constellation schemes of DVB-T2 standard. This is not the case for ACE technique adopted in DVB-T2 where there is a restriction on rotated constellations. On the other hand, when the pilots are boosted by a factor λ, the transmitted power increases also. So, in order to have a fair comparison, we define the PAPR effective gain as the difference in dB between the PAPR gain ΔG and the power increase ΔE due to the use of boosted pilots (in both techniques), i.e. $PAPR_{eff} = \Delta G - \Delta E$ (Figure 94).

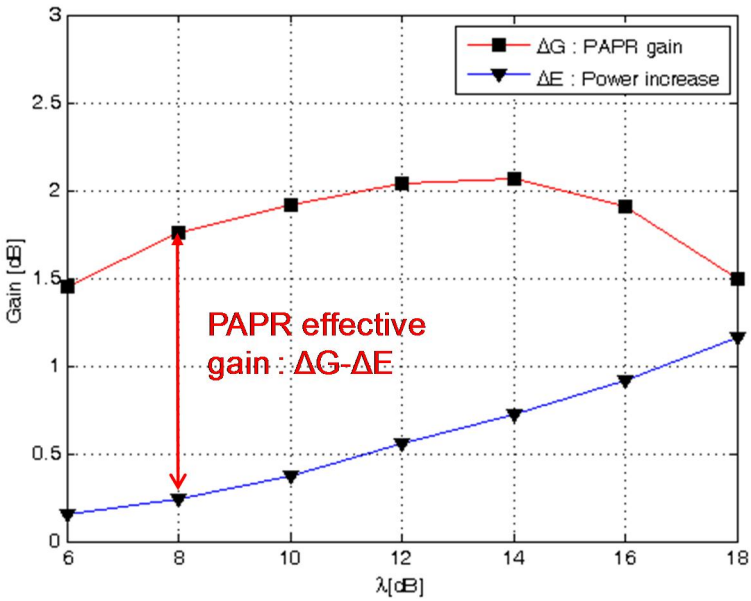

Figure 94- PAPR effective gain

We evaluate in Figure 95 the PAPR effective gain of the proposed method as a function of the pilot power λ, which represents as previously the boost factor of the used pilots for different values of M, and of the elementary step μ. We plot in the same figure the results obtained with the Gradient based method proposed in DVB-T2. We note that the Gradient solution proposed in DVB-T2 does not specify the boost factor of each dedicated pilot but specifies the maximum permitted power of these pilots. Hence, the boost factor of

these pilots in DVB-T2 could change from on symbol to another. In other words, the PAPR gain in Gradient-based solution of DVB-T2 depends on a variable λ value. The obtained results show that the performance of the proposed method is better than the one of the Gradient based method (TR technique) proposed in DVB-T2.

We also note that the optimal boost factor decreases when the number M of channel estimation pilots used for PAPR reduction increase. In DVB-T2 standard, it is specified that the boost factor of the channel estimation pilots could take values between 2 and 7 dB. Then, an optimal tradeoff should be found in terms of number of used pilots for PAPR reduction, PAPR effective gain and channel estimation specifications. The same kind of results and conclusions could be given from Figure 96 for a 64-QAM constellation. In Figure 95 and Figure 96, the performance of the DVB-T2 Gradient algorithm is given as a reference result with a clipping value VCLIP = 5 dB. We note however that the Gradient algorithm needs a smooth control of the transmitted powers of the PAPR pilots. Moreover, using the Gradient algorithm, the allocated powers are varying from one pilot to another.

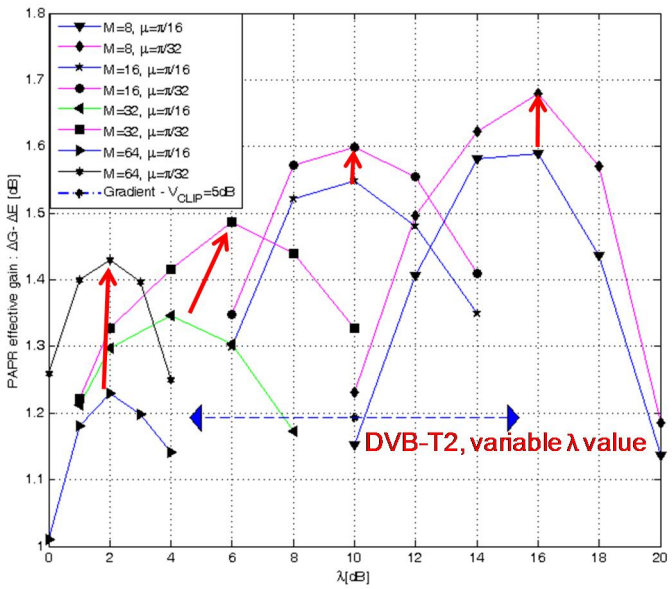

Figure 95- PAPR effective gain: comparison between proposed and DVB-T2 TR techniques, 16-QAM.

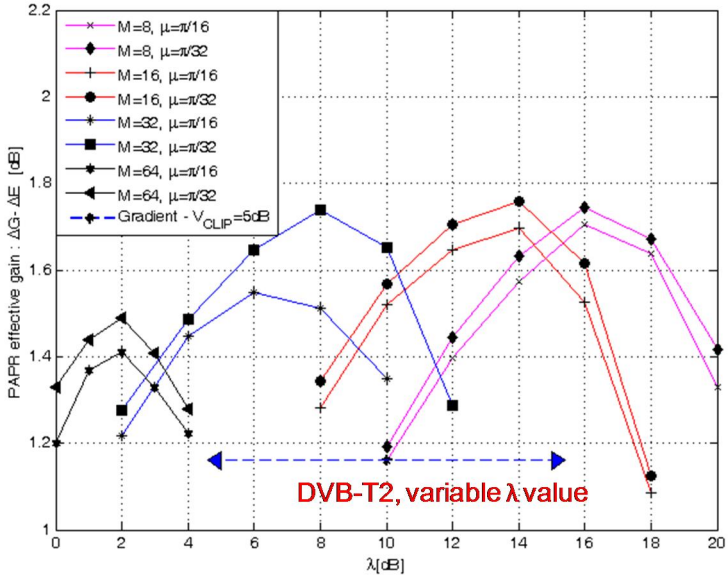

Figure 96- PAPR effective gain: comparison between proposed and DVB-T2 TR techniques, 64-QAM.

3.4.2.5.3 Channel estimation results

The goal of this section is to show how the system performance is affected by the use of dedicated channel estimation for both PAPR reduction and channel estimation issues.

In order to give more insights about the proposed technique, the error detection probability (EDP) of a sequence used for PAPR and channel estimation is first evaluated. Then, the mean square error (MSE) of channel estimation is performed with respect to the signal to noise ratio (SNR) of the system. The simulation results obtained hereafter are achieved at the output of the Wiener filter. The latter is a 1D filter applied in the frequency domain only. An improvement of the results could be obtained by filtering in 2D, i.e. frequency and time domain.

First, we verify the analytical performance evaluated in expressions (24) and (25). In order to evaluate the EDP values of Δ and ϕ, we consider appropriated elementary step such as for each evaluation, EDP of the other parameter is negligible. For instance, we choose $\mu(\Delta) = \pi/64$ and $\mu(\phi) = \pi/4$ in order to evaluate the EDP of Δ; $\mu(\Delta) = \pi/2$ and $\mu(\phi) = \pi/16$ in order to evaluate the EDP of ϕ. Figure 97 illustrates the comparison between analytical and simulated EDPs for different SNR values. It shows that our theoretical analysis matches perfectly with simulations.

Figure 98 shows the EDP obtained by simulations of the pilot sequence at the receiver as a function of SNR for different values of the elementary steps $\mu(\phi)$ and $\mu(\Delta)$. This figure shows that it is better to quantify the phase difference between two successive pilot symbols with small quantifications steps $\mu(\Delta)$ than quantifying with small steps the possible initial phase value of the first pilot, i.e. $\mu(\phi)$. In other words, it is more efficient to quantify more precisely Δ than the value of ϕ.

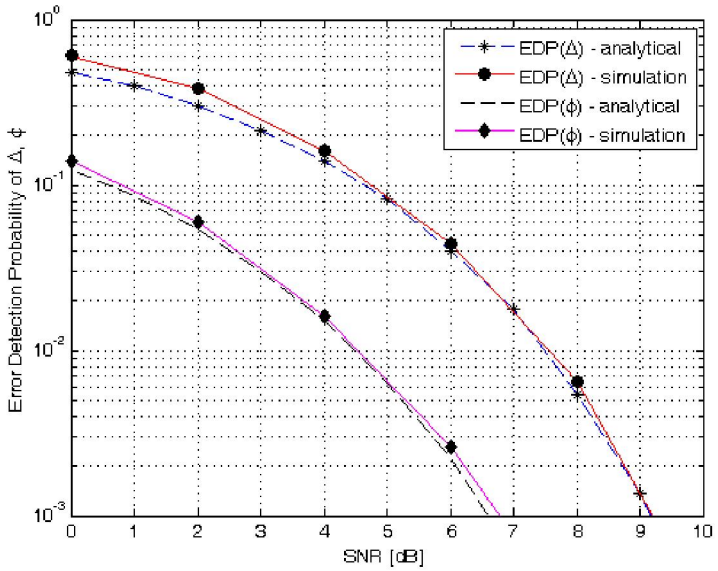

Figure 97- Analytical and simulated Error Detection probability.

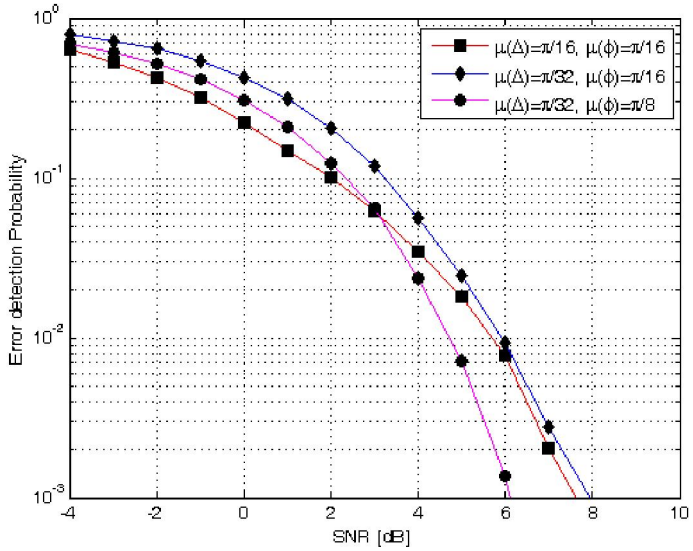

Figure 98- Error detection probability as a function of elementary steps.

Figure 99 presents the MSE of the channel coefficients estimation scheme using a F1 channel proposed in DVB-T2 [1] using the conventional channel estimation scheme presented in DVB-T2 and the proposed channel estimation scheme. The conventional channel estimation relies on a traditional Wiener interpolation based on received channel estimation on pilot positions at the receiver. For the proposed method, as explained in section V, channel response on pilot positions used for PAPR reduction issue is recovered first by using channel response of the previous OFDM symbol. Then channel estimation on all subcarriers is performed using traditional Wiener interpolation. This figure shows that the MSE of the channel coefficients estimated using our method is negligible for a SNR value greater than 6 dB. It is slightly higher than the conventional scheme for smaller SNR values. We recall that, for F1 channel and 16-QAM constellation, the required SNR value to obtain a BER=10^{-7} at the output of the channel decoder is equal to 6.2 dB at a coding rate R=1/2 [1]. The simulation results of this transmission scenario which is the most robust for a 16-QAM constellation are very important. Indeed, since the MSE is independent of the coding rate and, for higher coding rates the DVB-T2 requirements specify higher SNR values to make the system work properly, the proposed joint channel estimation scheme and PAPR reduction scheme will be always effective for these high SNR values.

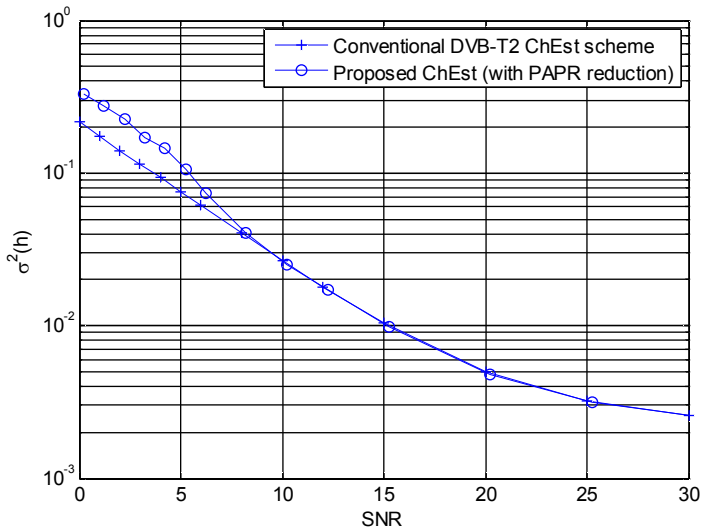

Figure 99- MSE of channel coefficients estimation, 2K mode, 16-QAM modulation, F1 [1].

We also evaluate the Bit Error Rate (BER) of the overall DVB-T2 system. The F1 channel coefficients are

estimated through dedicated pilots and then by applying a 2D Wiener filtering. Figure 100 shows the obtained BER performance using the conventional estimation scheme (Figure 87) and the proposed estimation scheme (Figure 88). As expected, the pilot sequence dedicated for channel estimation and used for PAPR reduction is well estimated at the receiver. Hence, the BER performance is not degraded.

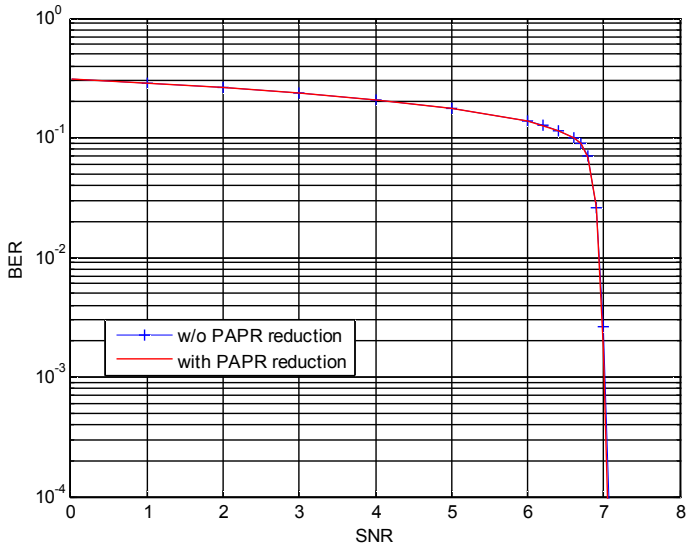

Figure 100- BER performance, 2K mode, 16-QAM modulation, F1 channel.

Now, we consider a time-varying TU6 channel model given in [46]. The Doppler frequency f_d is equal to 33Hz. Figure 101 gives the BER performance for a perfect channel estimation and a Wiener channel estimation without/with proposed PAPR reduction method. The obtained results show that the proposed scheme is efficient with high Doppler frequency scenario. We show in this figure that the overall degradation in comparison with perfect channel estimation is less than 1dB where only 0.1 dB of SNR loss is due to the joint application of PAPR reduction and channel estimation scheme.

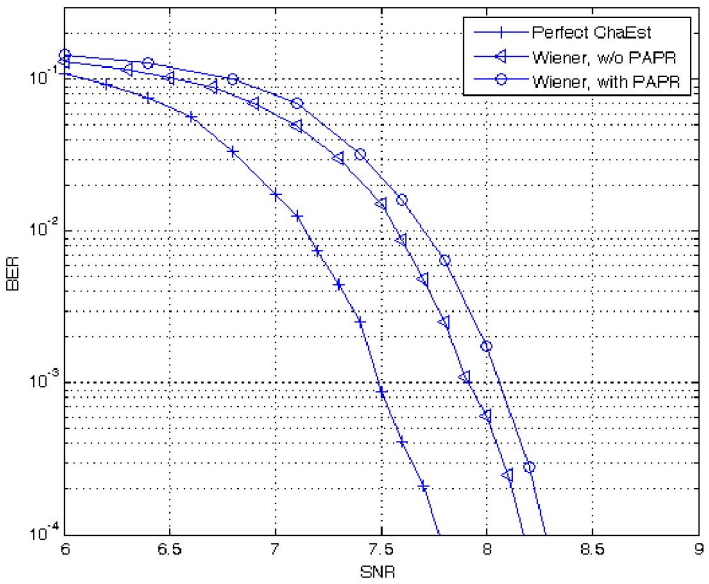

Figure 101- BER performance, 2K mode, 16-QAM modulation, TU6 channel.

3.4.2.5.4 Results summary

Based on the conclusions given in previous sections, this section summarizes optimal parameters and the corresponding PAPR effective gains using the proposed technique. The different results previously presented have been obtained in the 2k mode. The same analysis has been done in the 8k mode. Table 23 and Table 22 summarize the main parameters chosen as a good tradeoff between PAPR gain, channel estimation performance and optimal transmitted power in the 2k and 8k modes for 16-QAM and 64-QAM modulations. In all cases, the proposed technique presents better PAPR gain than the DVB-T2 TR technique, requires less transmitted power on pilot symbols (the maximum value of the boost factor λ of the PAPR pilots in DVB-T2 is equal to 10 dB) but also a spectral efficiency increase of 1% when it is compared with the actual DVB-T2 standard. It could be also applied using the rotated constellation adopted in DVB-T2. We should note that these parameters, i.e. M, λ, Δ and ϕ are applicable to the context of DVB-T2. However, they should be optimized to other contexts especially when the system parameters like the number of sub-carriers and the constellation size change. Nevertheless, the optimization process remains unchanged.

Modulation	Number of pilots : PP2	M	Elementary steps of ϕ and Δ	λ_{opt}	PAPR effective gain
16-QAM	143	32	$\mu(\Delta)=\pi/32$, $\mu(\phi)=\pi/8$	5dB	1.49 dB
	143	DVB-T2 (V_{CLIP}=5dB – 18 pilots)			1.19 dB
64-QAM	143	32	$\mu(\Delta)=\pi/64$, $\mu(\phi)=\pi/16$	7dB	1.80 dB
	143	DVB-T2 (V_{CLIP}=5dB – 18 pilots)			1.16 dB

Table 22- Optimal parameters using the proposed technique, 8K mode.

Modulation	Number of pilots: PP2	M	Elementary steps of ϕ and Δ	λ_{opt}	PAPR effective gain
16-QAM	569	128	$\mu(\Delta)=\pi/64$, $\mu(\phi)=\pi/16$	5dB	1.47 dB
	569	DVB-T2 (V_{CLIP}=5dB – 72 pilots)			1.39 dB
64-QAM	569	128	$\mu(\Delta)=\pi/128$, $\mu(\phi)=\pi/32$	5dB	1.48 dB
	569	DVB-T2 (V_{CLIP}=5dB – 72 pilots)			1.38 dB

Table 23- Optimal parameters using the proposed technique, 2K mode

3.4.2.6 Conclusion

A novel PAPR reduction method based on channel estimation pilots is addressed in this work. By using channel estimation pilots to reduce PAPR value, dedicated pilots for PAPR reduction purpose are avoided improving the spectral efficiency of the system. These pilots have to be related by a particular law in order to allow their detection at the receiver side. Multiplicative law in discrete frequency domain is then investigated. Simulations, using the new DVB-T2 standard chain, showed that with appropriate parameters, the proposed method can achieve up to 1.80 dB in terms of PAPR effective gain. In comparison with the Gradient based method initially proposed in DVB-T2, the proposed method presents better performance in terms of PAPR reduction while avoiding the use of dedicated pilots. As a consequence, it allows achieving 1% of spectral efficiency gain. At the receiver side, only a slight modification is required. Simulations have shown that no degradation is caused by this additional function. The obtained results demonstrate the relevance of this method for future broadcasting of OFDM based systems.

3.5 Time Frequency Slicing (TFS)

Time-Frequency Slicing (TFS) is a novel transmission technique that consists of transmitting a variable-bit-rate PLP (carrying one or more services) across several Radio Frequency (RF) channels (multiplexes) with frequency hopping and time-slicing (i.e., discontinuous transmission). TFS was originally proposed by Teracom in the standardization process of DVB-T2 (Terrestrial 2nd Generation) [47]. It was initially adopted for the baseline, but finally, it was not specified in the normative part of the T2 specification due to the need of implementing two tuners (front-ends) at the receivers. Instead, the details of TFS were specified in informative annex (Annex E) to the T2 specification [47] to be used for "future implementations". DVB-NGH (Next Generation Handheld) has adopted TFS because it can be operated with a single tuner without adding excessive complexity at the receivers. The reason is the reduced service data rates of mobile TV compared to HDTV DVB-T2 services as well as more realistic use cases for FEF and "guard periods", which makes possible to receive the signal with a single tuner.

This section reports the results of the feasibility analysis of TFS for DVB-NGH performed by **Teracom** and **Universidad Politécnica de Valencia/ iTEAM Research Institute (UPV-iTEAM).**

3.5.1 Introduction

In a traditional transmission, services are allocated in multiplexes that are distributed over the RF frequency band. The reception of a particular service is performed by tuning the RF channel where the service is transmitted. With TFS, services are allocated over a set of several RF channels, where each such RF channel contains a multiplex in case of non-TFS. Thereby, time slices of one service are transmitted sequentially in a different RF channel, implementing frequency hopping. This allows services to be potentially spread over the whole RF frequency band. The reception of a particular service is performed by implementing frequency hopping at the receiver side among the RF channels that transmit the time slices of the service. The way TFS works allows services to be spread in the time and frequency domains which supply a large time/frequency diversity that can be exploited in a number of different ways.

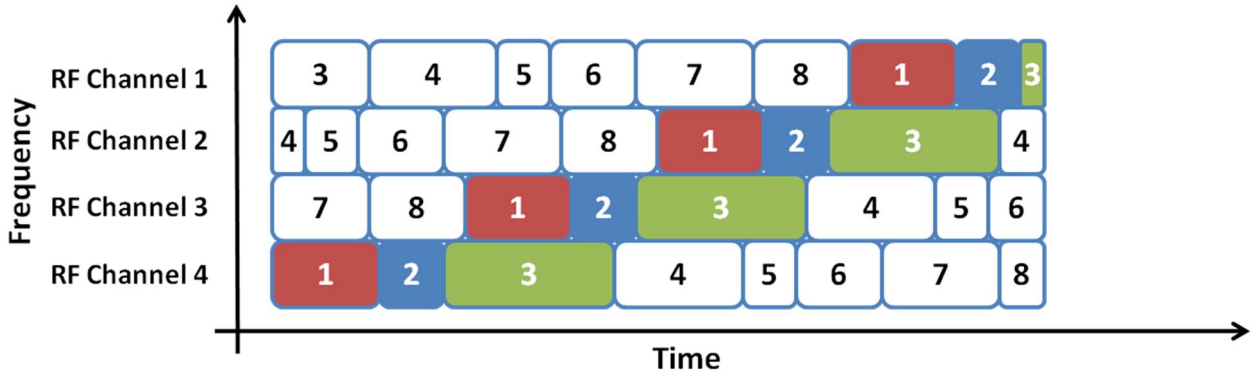

Figure 102: Example of TFS (intra-frame) with 4 RF channels. To receive service 1, receiver must perform frequency hopping between RF channels.

The major advantages of TFS are a gain in capacity and a gain in coverage [48].

The capacity gain of TFS is due to a more efficient Statistical Multiplexing (StatMux) for Variable Bit Rate (VBR) services. StatMux exploits the fact that video codecs generate video streams of a variable bit rate depending on the content encoded. Without StatMux, the capacity of a multiplex should be divided among services considering the maximum (peak) bit rate of each video stream in order to guarantee a correct transmission. This feature implies that, for lower instantaneous bit rates, there would exist an excess of bandwidth that is not being used by any service. Statistical multiplexing takes advantage of the fact that the overall peak bit rate of all video streams together would be significantly lower than the sum of peak bit

rates for the individual video streams. This feature makes possible to make a more efficient use of spectrum. Figure 103 shows the bundling of 4 video streams considering the peak bit rate of each service (left) and statistical multiplexing (right). The excess in capacity when using StatMux is defined as the StatMux gain.

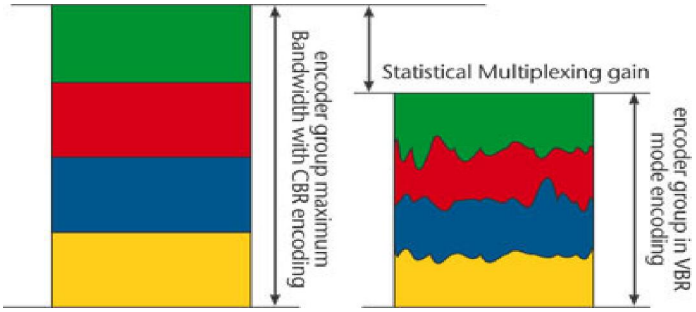

Figure 103: Efficient badwidth use provides StatMux gain when using VBR encoding instead of CBR encoding.

The StatMux gain depends on the number of services jointly multiplexed. Obviously, there is no gain for a single service, but the gain increases as a function of the number of services until saturation.

The coverage gain of TFS is due to increased frequency diversity. The signal of each RF channel is affected by different propagation conditions that not only depend on the characteristics of the scenario but also on the frequency of the RF channel. In a traditional transmission the coverage of a DTT network is determined by the channel with the worst signal level in each location. With TFS, it is possible to homogenize the coverage of all RF channels in such a way that the service area of the whole set of channels is increased (whereas the area where at least one RF channel is received decreases). Figure 104 shows an example of the coverage of 3 different multiplexes (left) and the effect in the coverage of implementing TFS within the same 3 RF channels.

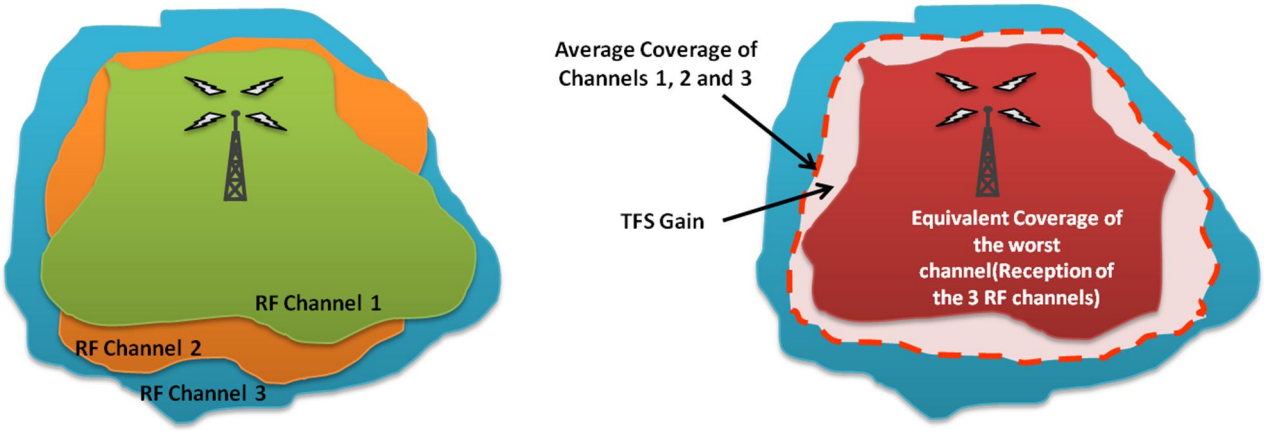

Figure 104. Example of coverage differences between 3 RF channels in a DTT network without TFS (left) and effect of TFS on the coverage of the channels.

The coverage advantage provided by TFS is known as TFS coverage gain and it is closely linked to the number of RF channels involved in transmission and the frequency spacing among them. In general, TFS gain increases with the number of RF channels as this would increase diversity and with frequency spacing as distant channels (in frequency) suffer from different propagation conditions.

3.5.1.1 TFS in DVB-T2

The main driving force for DVB-T2 was to increase spectral efficiency of the DTT networks for the transmission of high quality services such as HDTV and 3DTV [49]. One of the techniques that could afford this aim is TFS, which was proposed by Teracom, the Swedish DTT operator. However, the inclusion of this technique in the standard was conceived as informative as a result of the necessity of implementing two tuners in the receiver which makes design much more complex and also expensive.

It is a fact that DVB-T2 can provide greater capacity and spectral efficiency than DVB-T; however, the bandwidth requirements of HD services make capacity for this kind of services to be limited within a multiplex. The idea behind TFS was to offer the possibility of combining multiple (up to 6) RF channels to create a high-capacity system that could offer gain in capacity for almost ideal statistical multiplexing across several HD services using VBR encoding.

Figure 105 shows an example of the performance of StatMux gain for HDTV services with the number of services.

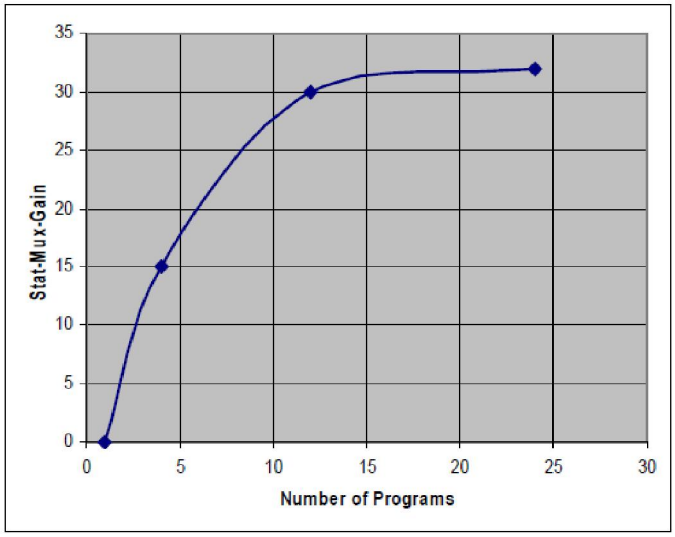

Figure 105: Example of StatMux gain with number of services for MPEG-4 AVC video streams in DVB-T2.

TFS is defined for input mode B, where multiple PLPs are used in transmission. . In this case, P1 symbols, L1 signalling and common PLPs must be repeated simultaneously on each RF channel as these should always be available while receiving any other data. Each type 1 PLP only occurs on one RF channel in one T2-frame but different type 1 data PLPs are transmitted on different RF channels. TFS can operate from frame by frame (inter-frame TFS) for type 1 data PLPs and within the same frame (intra-frame TFS) for type 2 data PLPs. The RF channel for a type 1 PLP may change from frame to frame (inter-frame TFS) or may be the same in every frame (Fixed Frequency) according to the L1 signalling configuration. The sub-slices of type 2 data PLPs are sent over multiple RF frequencies during the T2-frame reaching an interleaving applied both in time and frequency domains.

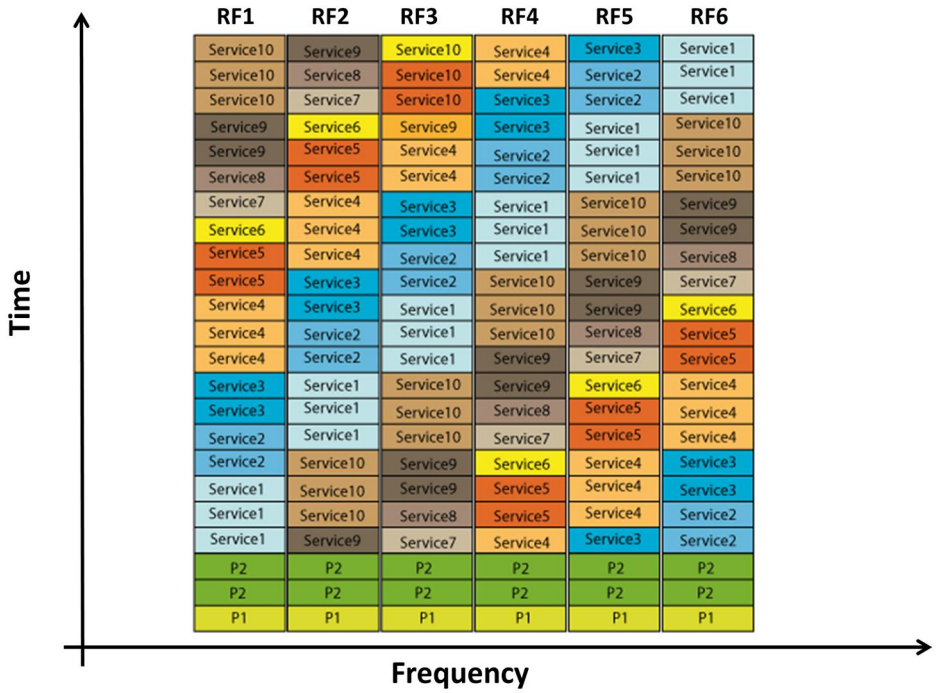

Figure 106: Example of Intra-frame TFS within 6 RF channels.

DVB-T2 Annex E introduces these features, which are not specified for the single profile defined by the standard, but allow future implementation of TFS. The main requirements for TFS implementation in DVB-T2 include both signalling and frame structure. The basic blocks, specified in the DVB-T2 transmission chain, apply when TFS is used; however, frame builder and OFDM generation modules are modified in order to add branches that corresponds to each of the N RF channels.

The major disadvantage that leads to reject implementation of TFS in DVB-T2 is the requirement of providing two tuners at the receiver. It is necessary to guarantee a time interval between slots to perform frequency hopping among RF channels correctly when using a single tuner. Implementation of inter-frame TFS is less strict as there is enough time to perform frequency hopping between slots of the same service; however, implementation of intra-frame TFS requires a complex scheduling in order to assure the necessary time interval. Moreover, it is not always possible to provide a time interval between slots when transmitting high bit rate services. Therefore, the standardization process of DVB-T2 leads to refuse the implementation of intra-frame TFS with a single tuner, which highlighted the need of two front-ends to receive TFS transmissions.

Regarding StatMux gain, previous studies for DVB-T2 have shown that StatMux gain increases with number of VBR statistical multiplexed services in a multiplex. StatMux gain reaches saturation at approximately 9-12 HD programs. High Statmux gain is also obtained for lower number of programs.

Studies are presented as a comparison between a non-TFS case (which almost reaches 15% StatMux gain of HDTV services) and TFS for 3 and 6 channels which reaches 30% and 32% of StatMux gain assuming HD services of 9.0 Mbps. StatMux gain here referes to the possible bit rate reduction, where (for clarity) a hypothetical 50% reduction would allow a 100% increase in number of services. A 30% bit rate reduction therefore allows about 43% (1/(1-0.30)-1) more services. The increase in capacity is also important as increasing the number of RF channels, capacity is larger. This factor added to additional StatMux gain allows the inclusion of almost 3 HD programs with TFS-6RF and 2 with TFS-3RF. However benefits of StatMux gain appear to be negligible for SD services as large number of programs per RF channel already leads to Statmux gain saturation for a single RF channel. Moreover, there exists a loss in terms of total bit-

rate due to the additional overhead of TFS.

Regarding TFS network gain, increased frequency diversity leads to consider two kinds of gain, one related to coverage and the other to interference. A choice of TFS architecture leads to a system where the error correction is applied to each individual service within a TFS multiplex rather than applying the error correction to the TFS multiplex as a whole. Thus, frequency hopping allows for an advantage as a service is affected by disturbance RF channel by RF channel making possible the recovery of each service as good received bursts can compensate bad ones.

Large-scale field measurements show a potential gain of 4-5 dB for TFS-4RF for fixed reception which offer the possibility of increasing the coverage of broadcasted services. These measurements also indicated a similar gain for portable and roof-top reception. This dB gain could also in principle be partly converted to an additional capacity increase, should that be preferred (there is always a trade-off between capacity and coverage/robustness).

Interference gain, although not quantified, was shown to exist in principle in networks based on the frequency allocation plan GE'06. The studies suggest that even higher interference gain could be obtained with changes in the frequency plan.

3.5.1.2 TFS in DVB-NGH

In a similar way as for DVB-T2, Time-Frequency Slicing could also be very beneficial for NGH, offering a gain in capacity due to efficient StatMux and a gain in coverage due to increased frequency diversity. The point of view from which TFS is addressed in DVB-NGH is slightly different from DVB-T2, as reception conditions and demands from users and operators are not the same in a mobile scenario than for fixed reception. The nature of mobile terminals, in general of reduced dimensions, is not intended to the reception of a service offering of HDTV which can make possible to lower data rates of services. Low data rates in NGH raises the possibility of receiving services with a single tuner that is hopping from RF channel to channel as time constraints turn out to be more relaxed than they were in T2. Moreover, the most important issues that prevail in a mobile communications scenario are related to improvements in coverage and low power consumption at the receiver for longer battery life. Therefore, whereas the main goal of TFS in T2 was increase capacity, NGH would be focused on coverage advantage.

TFS coverage gain in NGH can go beyond the considerations in DVB-T2, where fixed reception was the most important issue. The increased frequency diversity offered by TFS is likely to provide a significant reduction in required C/N. Link budget can be improved for static reception or pedestrian, where time diversity (interleaving) provides little or no gain and space diversity is difficult due to size and cost constraints. Moreover, increased frequency diversity can reduce requirements for time interleaving depth, offering a reduced zapping time for NGH.

From the interference point of view, TFS can also provide additional gains. TFS coverage gain is obtained exploiting the statistical variations of the signal on various frequencies whereas noise remains constant. However, interferences from other transmitters are statistically independent from the signal of the desired transmitter and will not be the same on all frequencies in the TFS. In general the better C/I performance could be exploited as an improved coverage (the C/I-limited coverage area will increase) and/or a tighter frequency reuse could be used, i.e. more NGH networks could fit within a given spectrum.

The use of TFS over NGH would also offer the potential possibility to find spectrum for NGH services more easily, without causing excessive interference into existing DVB-T/T2 services. The development of TFS technique in NGH is also done taking into account potential interferences caused by the deployment of LTE services in the upper part of the UHF band (channels 61-69) as the result of the digital dividend after DTT transition. There is then the risk that these transmissions will have an adverse effect on broadcast reception on RF channels close to LTE. However, using the TFS principle typically only a small part of the NGH

signal (the one close to LTE) would be affected and reception could still be successful thanks to the successful reception of the other parts.

Regarding capacity, TFS capacity gain in DVB-NGH should be analysed in depth as it is not clear to quantify the possible gain when using NGH services allocation in FEFs due to the expected limited capacity of them. Another important issue is that NGH is not intended for the transmission of HDTV services and, SDTV services already achieve very good StatMux gain.

The implementation of TFS in NGH was part of two Call for Technologies responses submitted by Teracom, oriented to a reuse of the T2 specification, and Sony and the Technical University of Braunschweig, oriented to an adaptation of DVB-C2 (2nd generation Cable) specification.

The Sony/TUBS proposal concerning TFS is based on Data Slicing concept (implemented in DVB-C2) that consists of dividing a wide transmission bandwidth of a RF channel (e.g. 8 MHz) in the frequency domain into narrower Data Slices (sub-bands) with a maximum bandwidth of 1.7 MHz. Hence, the receiver only needs to decode a single Data Slice out of the overall transmitted bandwidth which provides the system a very low power consumption on receiver side as segmentation in N bands of the overall channel bandwidth allows the receiver tuner to operate 1/N of the bandwidth and at N times slower rate.

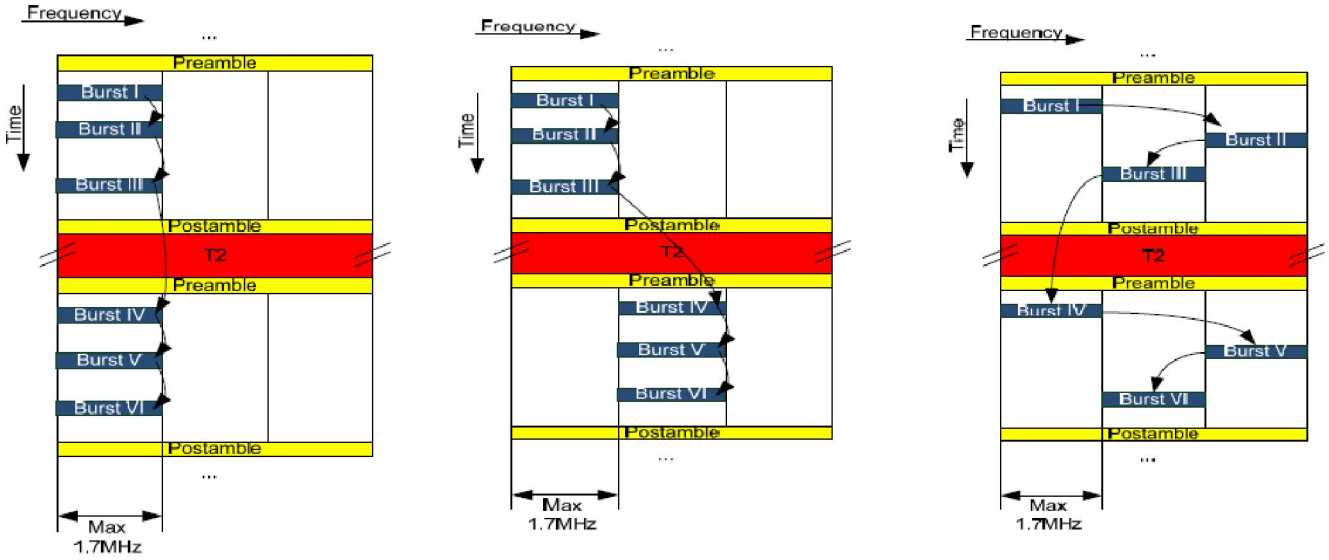

Figure 107: Operation modes of the Sony/TUBS Data-Slicing proposal

Data-Slicing was rejected as a T2-like frame structure achieves better performance in most of the possible NGH scenarios and Data Slice bandwidth (1.7 MHz) is not enough to achieve bit rates higher than 1Mbps at reasonable spectral efficiencies.

Teracom proposal for DVB-NGH consists of an adaptation of TFS mode described in DVB-T2 but with the requirement of using a single tuner to perform frequency hopping. TFS frequency hopping can be performed by using full bandwidth channels (8 MHz, 7 MHz, 6 MHz, 5 MHz and 1.7 MHz) bundled across RF band (inter-channel TFS) or internally within an RF channel (intra-channel TFS), similarly as Sony/TUBS Data Slicing, which allows almost the same performance as in full bandwidth case but with a notable reduction of power consumption.

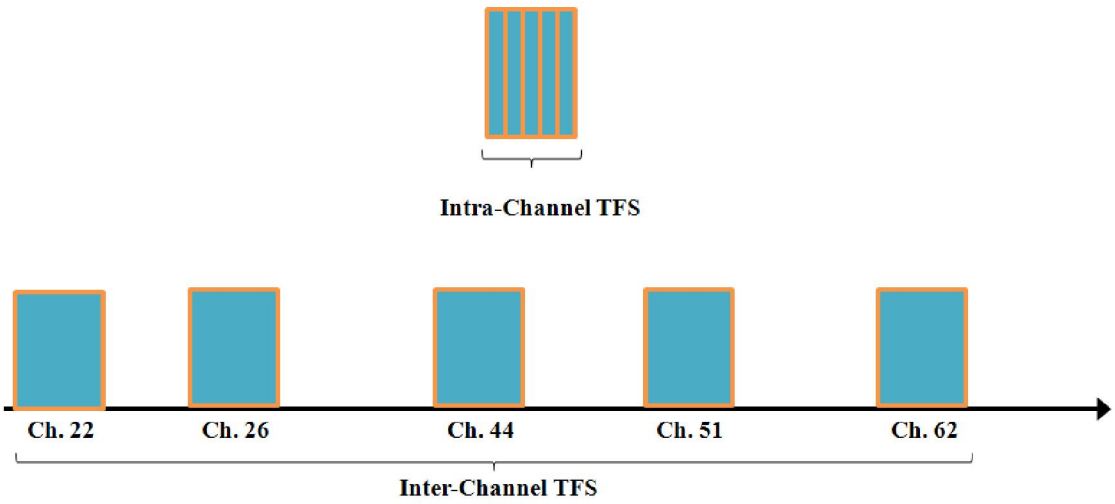

Figure 108: Intra-Channel0 (above) and Inter-Channel (below) modes proposed by Teracom.

TFS can be implemented within the same frame (intra-frame TFS) and frame-by-frame (inter-frame TFS). These two methods are oriented to a particular operation mode for NGH and directly depend on frame size as soon as frames should be large enough to be received with a single tuner.

Intra-frame TFS is thought to be implemented when there exist a whole 250 ms frame entirely dedicated to NGH services. However, NGH is more likely to be implemented in FEFs (Future Extension Frame) of a DVB-T2 frame (in a structure of e.g. 250 ms dedicated to a T2 frame and e.g. 50 ms for a NGH FEF) where inter-frame TFS should be used due to impossibility of using intra-frame due to tuning time constraints with such a reduced frame length.

3.5.2 TFS Concept

TFS concept is to be developed in two different ways in DVB-NGH. Although NGH services will probably be allocated in the FEFs of DVB-T2 frames, and consequently inter-frame TFS should be the most suitable mode of operation, there exists the possibility of implementing intra-frame TFS within large frames. Nevertheless, both modes of TFS operation should intrinsically involve the use of a single tuner (front-end) in the receiver.

Intra-frame TFS may be implemented as a reuse of the informative T2 Annex E, but assuming a single tuner in the receiver, which is one on the requirements in NGH standardization. The solution for intra-frame TFS works with type 2 PLPs, those which have 2 or more sub-slices in a frame. Time constraints for intra-frame TFS operation with a single tuner implies the necessity of providing enough time for tuning between slots. To achieve this aim frames should be long enough and service data rates lower compared to T2. Using a "guard period" of Type 1 PLPs in each frame, or a FEF between frames, makes it easier to perform the frequency hopping, since hopping at the border between two frames is the most critical case.

When the NGH frame time is short (such as 200 ms T2 frame + a 50 ms NGH in the T2 FEF), there is not enough time to perform frequency hopping inside the frame and it has, instead, to be done between frames. This case leads to consider implementing frequency hopping between frames (inter-frame TFS) where both type 1 and type 2 PLPs could be used. In this case, when type 2 PLPs are used there is, however, no frequency hopping within each frame only between frames. This use case can be seen as a special case of the FEF bundling, in which an NGH frame is not mapped to a single T2 FEF but could be extended over several FEFs. A T2 FEF could even include the end of one NGH frame and the beginning of the next one.

3.5.2.1 Intra-Frame TFS

Intra-frame TFS is performed inside the frame. The receiver implements frequency hopping between sub-slices. This mode of operation implies intra-frame time interleaving and it is only possible for type 2 PLPs. In this case, the sub-slices which belong to a service are transmitted in parallel over the set of RF channels. That means sub-slices of all services are spread over the set of RF channels. Critical parameters in intra-frame TFS operation as frame duration, MODCOD and number of subslices should be controlled to guarantee single tuner reception, although, as mentioned above, the use of FEFs and/or guard periods could simplify the frequency hopping.

Scheduling of services for intra-frame TFS shall consider variation in the bit rates of the services that makes sub-slices have a variable length. However it is possible to implement a deterministic scheduling of the amount of services which can lead to a regular distance between sub-slices or an almost constant hopping time between slots. These mechanisms are implemented in the scheduler which is part of the physical layer mechanisms of DVB-NGH.

In general, the service data is written into the frame during the frame duration TF. Each frame consists of different cells which contain data from one service (PLP) and their size depends on the instantaneous bit rate of the services. Moreover, the size of the TFS frame in bits is not constant because of the dynamic size of the subframes and physical channel specific MODCOD parameters. However, the size is constant in OFDM symbols (or useful carriers) per frame.

The starting point for scheduling is a set of PLP cells which are disposed one after the other as a matrix with $N_{subslices} \cdot N_{RF}$ columns.

The size of each cell is determined by the bit rates of the services mapped into the same physical channel. Therefore, cell size may change from frame to frame according to the bit rate variation of the services but the frame size is fixed. In the Figure 109, an example of a matrix with 6 PLPs is shown. In this case, there are 2 sub-slices per RF channel and 3 RF channels (6 columns).

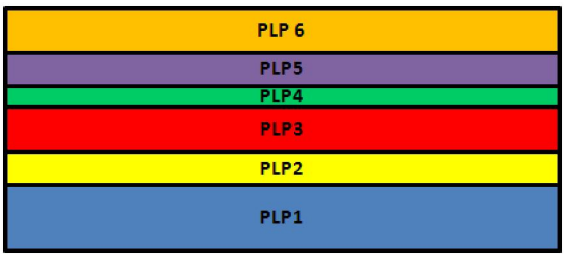

Figure 109: Example of a matrix with 6 PLPs, starting point for the scheduling.

The total number of PLP cells is divided into the number of sub-slices per RF channel ($N_{subslices}$) of equal size. Figure 110 shows the result of this operation.

Figure 110: First step of the scheduling.

All the resultant sub-slices are disposed in column. According to the total number of PLP cells (in this case 6), the parameter sub-slice interval is defined as the distance between two sub-slices of the same PLP cell.

$$Subslice_{Interval} = \frac{Total\ number\ of\ cells}{Total\ number\ of\ subslices}$$

The resultant structure is then divided (by columns) according to the number of RF channels involved in the TFS transmission. For this particular example there exist 3 columns (one for each RF channel) containing slots of the PLP cells.

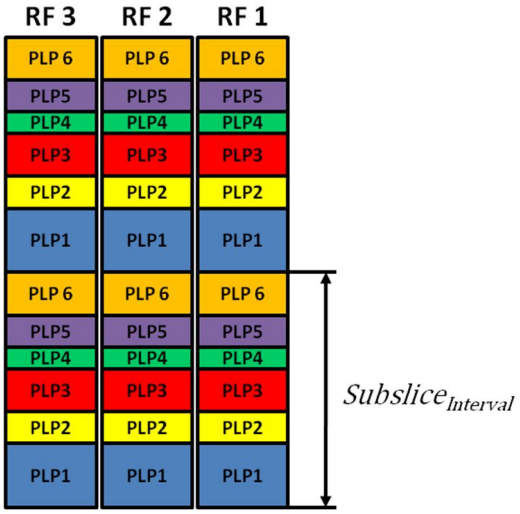

Figure 111: Second step of the scheduling.

Intra-Frame TFS transmission implies that services are transmitter in parallel in each RF channel. However, there should exist some mechanisms that guarantee that a single tuner can perform frequency hopping among channels and receive services regularly and one after the other.

To achieve this feature, a time shift is implemented in the set of slots corresponding to each RF channel.

$$RF_{Shift} = \frac{Subslice_{Interval}}{N_{RF}}$$

Figure 112 shows the effect of time shifting in each RF channel.

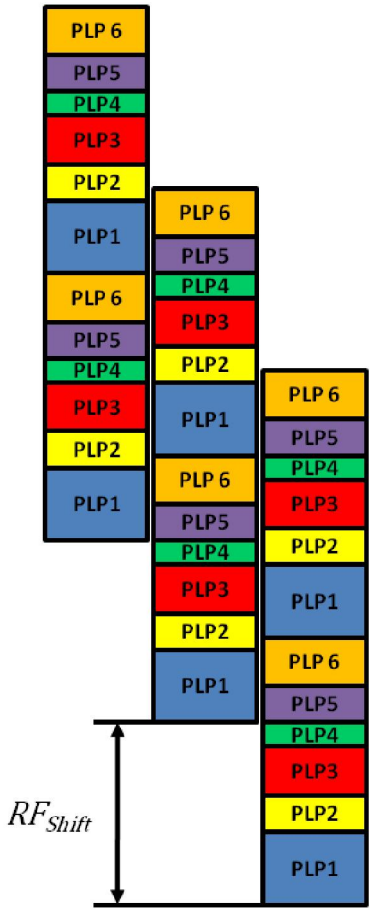

Figure 112: Effect of time shifting in each RF channel.

The slots that exceed the frame length must be folded back. As a result of the time shift and folding the TFS frame is ready to allocate services and to perform frequency hopping.

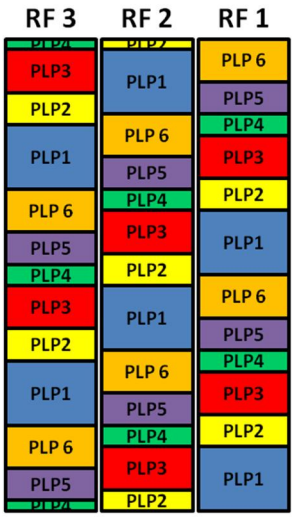

Figure 113: The slots exceeding the frame length are folded back.

It should be noted that the previous process has defined the scheduling for Intra-frame TFS implementation; however, scheduled cells has not yet been filled with data. Only positions in the frame have been defined.

Time interleaved PLP cells are introduced into sub-slices in the natural time sequence, independently of RF channel. The first time interleaved cell is therefore introduced in the first cell position of the first sub-slice of the PLP (independently of the RF channel in which it appears).

3.5.2.2 Inter-Frame TFS

Another technique to implement TFS for the transmission of NGH services is known as inter-frame TFS. Otherwise than as in intra-frame TFS, frequency hopping is performed between frames and not within the frame. Inter-frame TFS is thought to be implemented when allocating NGH services in the FEFs of DVB-T2 (Figure 114) as frame length makes impossible to implement intra-frame TFS. However, inter-frame TFS can also be used in a dedicated multiplex to NGH services.

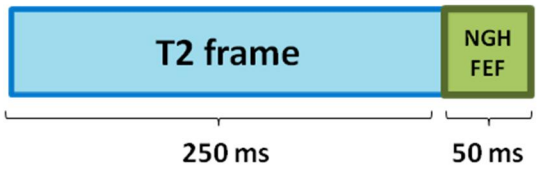

Figure 114: NGH services allocation in FEFs of the T2 frame.

With inter-frame TFS, the slots of the services are not transmitted in parallel over the set of RF channels but are allocated inside FEFs which are distributed in time and frequency along RF channels. Frequency hopping is performed at the receiver side with relaxed time restriction due to the duration of the frames and the large time intervals among them. This makes scheduling of inter-frame TFS transmission to be not as critical as inter-frame TFS.

An example of an inter-frame TFS transmission is shown in Figure 115. As in Figure 114, blue frames correspond to DVB-T2 services whereas green slots correspond to FEFs where NGH services are allocated. Frequency hopping is performed at the receiver within a concrete number of RF channels (in this example, 3 channels).

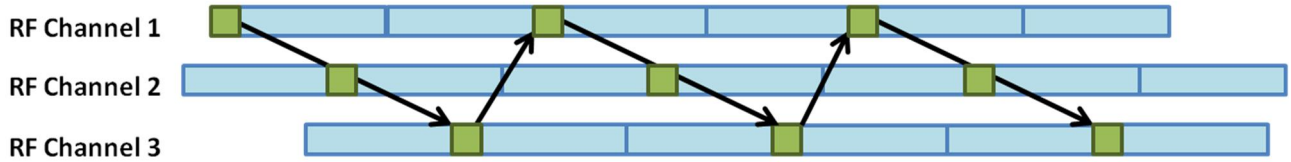

Figure 115: Example of inter-frame TFS transmission.

The main factors involved in this mode of transmission are time interleaving, zapping time and also power saving. The transmission of services among FEFs implies that there must exist some time interleaving among them to guarantee time diversity as the use of only one FEF deals to too little interleaving depth. Power saving control depends on the implementation of Inter-Frame TFS as frequency hopping is one of the most important factors with implication in power consumption. A large spacing in time between FEFs reduces power consumption as frequency hopping is produced less often. However, assuming there exist some time interleaving among FEFs, zapping time is increased with spacing among FEFs. To solve this problem, the solution proposed is the use of time-shifted superframes as shown in

Figure 116 (right).

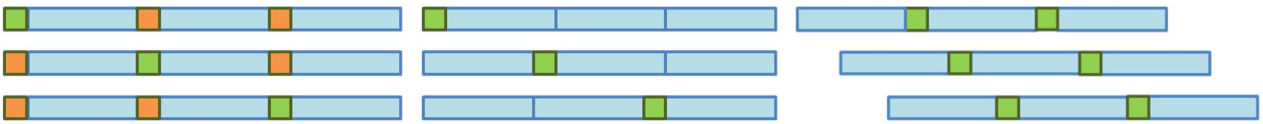

Figure 116: Interleaving over FEFs with frequency hopping between RF channels using co-timedT2 frames (left), time shifted FEFs but co-timed superframes (center), and time-shifted superframes (right).

3.5.2.3 Time constraints for TFS operation modes

3.5.2.3.1 Requirements for the tuning time

The transmitter must guarantee that the slots in which services are allocated are separated at least by a certain time interval such that receivers can perform frequency hopping with a single tuner and, therefore, successfully receive TFS transmission. The minimum frequency hopping time period between slots is measured from the end of one slot to the beginning of the next one that belongs to the same service.

Frequency hopping in the receiver implies to perform operations that involve PLL tuning, AGC tuning, fine frequency synchronization and channel estimation. The tuning operations between two slots in the middle of the frame need a time interval for the finalization of channel estimation for the current slot (T_{CHE}), the performance of frequency hopping (T_{tuning}) and finally the reception of the symbols needed for channel estimation and fine synchronization (T_{CHE}). Figure 117 illustrates this timing.

Therefore, the minimum frequency hopping time between data slots is calculated as $2* T_{CHE} + T_{tuning}$.

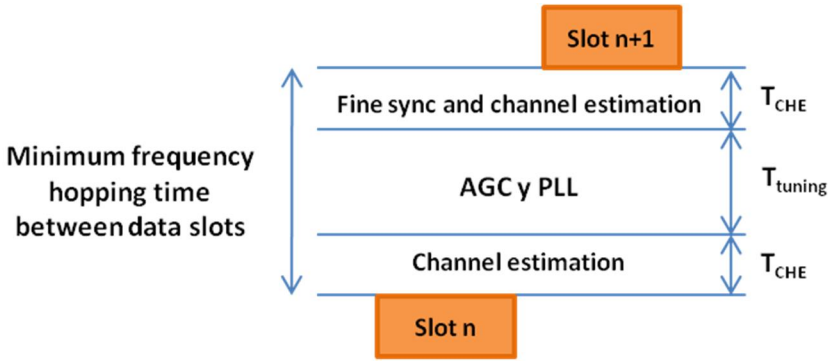

Figure 117: Illustration of the requirements for the tuning time.

It is assumed that the coarse frequency and symbol time synchronizations, which can be estimated from pilot symbols P1 and P2, need to be done before receiving the slot. It is reasonable to assume that PLL and AGC tuning takes about 5 ms. After that at least one OFDM symbol is needed for fine frequency error estimation. In addition to that, some more symbols may be needed in the channel estimation to make the time interpolation.

Table 24 shows the required frequency hopping time between data slots calculated during the T2 standardization process.

FFT size	T_U (ms)	Guard Interval						
		1/128	1/32	1/16	19/256	1/8	19/128	1/4
32K	3.584	2	2	2	2	2	2	NA
16K	1.792	3	3	3	3	3	3	3
8K	0.896	6	6	6	6	5	5	5
4K	0.448	NA	11	11	NA	10	NA	9
2K	0.224	NA	22	22	NA	20	NA	18
1K	0.112	NA	NA	10	NA	9	NA	8

Table 24. Values for S_{tuning} (number of symbols needed for tuning, rounded up, for 8 MHz bandwidth), when tuning time = 5 ms for DVB-T2

Therefore, the frequency hopping time depends on the used mode (FFT size and GI) and the number of symbols assumed to be used in the synchronization/channel estimation. A too tight period of time cannot be assumed, some margin must be left to take into account different implementations and possible effects of the channel.

Related to the minimum tuning time, another important time restriction is the time shift among slots in a frame (the distance in time between the two slots that belong to the same service). This time is required to be larger than the frequency hopping time in order to avoid overlapping and malfunction of the TFS transmission. The minimum shift is calculated as $RF_{shift} \geq Max\_Slot\_Length + 2^* T_{CHE} + T_{tuning}$.

Requirements for the guard period between frames

Deterministic scheduling for intra-frame TFS, which has been previously explained, guarantees frequency hopping internally in a frame with a single tuner. However, a guard period is needed at frame boundaries to allow enough tuning time (for e.g PLP 1 in

Figure 118).

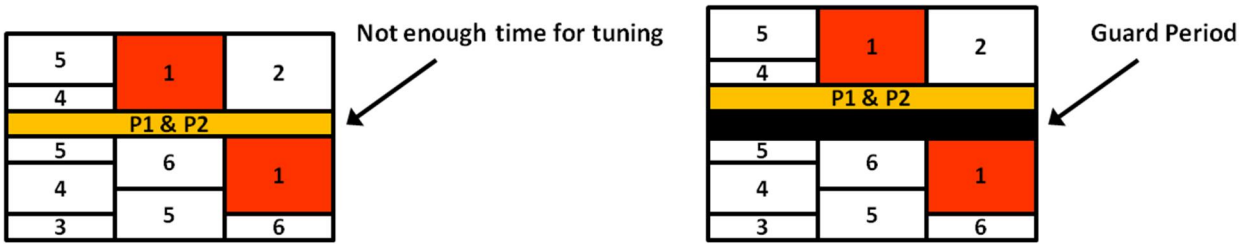

Figure 118: Illustration of the need for a guard period.

Critical jump, produced at the frame boundary between slots carrying the same service when there is not enough time for tuning and receiving preamble, should be avoided during transmission of frames. To enable simple slot allocation algorithms, that avoid complicating the scheduling, it is suggested that an additional time slot of the length of the tuning time is added on every frequency before the signalling symbols P1 and P2 (Figure 118).

The symbols transmitted during the guard period are not redundant, but could be filled with some low bit rate service, like radio or auxiliary (teletext –like) services. Furthermore, it is possible to implement guard periods by means of FEFs between frames or Type 1 PLPs that are located at the beginning of each frame.

Figure 119 shows two methods for implementing the guard period when using large frames entirely dedicated to the broadcasting of NGH services. As said before, to guarantee enough tuning time between

frames, FEF or Type 1 PLP durations could be used as guard intervals.

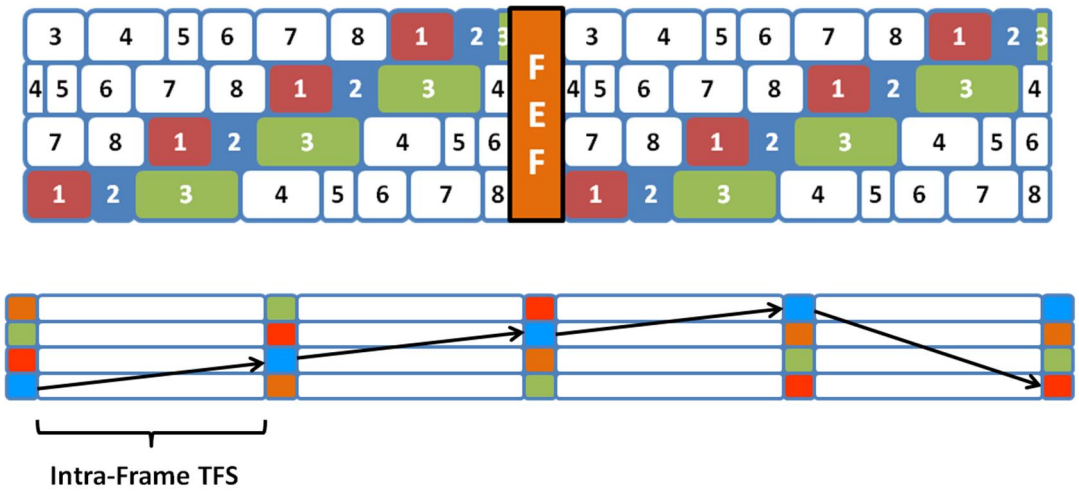

Figure 119: Two possible methods for the guard period implementation.

Inter-frame TFS time constraints are relaxed as there exist the possibility of transmitting more than one frame between two FEFs (slots), increasing the time interval for tuning.

4 REFERENCES

[1] Digital Video Broadcasting (DVB), Frame structure channel coding and modulation for a second generation digital terrestrial television broadcasting system (DVB-T2), ETSI EN 302 755, v1.3.1, 2011.

[2] C. Berrou, Y. Saouter, C. Douillard, S. Kerouédan and M. Jézéquel, "Designing good permutations for turbo codes: towards a single model," *Proc. of ICC'04*, Paris, France, June 2004.

[3] Y. Saouter, "Selection procedure of turbocode parameters by combinatorial optimization," Proc. *Int'l Symp. on Turbo Codes and Iterative Information Processing*, Brest, France, Sept. 2010.

[4] F. Kienle, N. When and H. Meyr, "On complexity, energy- and implementation-efficiency of channel decoders," submitted to *IEEE Trans. Commun.* in March 2010. Download at http://ems.eit.uni-kl.de/uploads/tx_uniklwehn/ARXIV_Efficiency_Channel_Decoders.pdf.

[5] TM-NGH 795, "Continuous_N_periodic_L1_sul", Jan Zöllner.

[6] TM-NGH 866, "L1-Pre performance with NGH signaling PLP", Jan Zöllner.

[7] TM-NGH 843, "Reduced overhead for L1-config and L1-dynamic" Erik Stare.

[8] TM-NGH 875, "L1 Signalling Optimization", Ismael Gutiérrez.

[9] J. Zöllner, "Further Considerations on n-periodic Transmission of L1-pre and L1-config", 17.05.2011

[10] D. Gómez-Barquero, P. F. Gómez, D. Gozálvez, B. Sayadi, and L. Roullet, "BB-iFEC for Next Generation Handheld DVB-NGH," *Proc. Of IEEE BMSB*, Erlangen, Germany, 2011.

[11] F. Pérez-Fontán, *et al*., "Statistical modelling of the LMS channel," *IEEE Trans. on Vehicular Technology*, vol.50, no. 6, pp. 1549-1567, 2001.

[12] D. Gómez-Barquero, D. Gozálvez and N. Cardona, "Application layer FEC for mobile TV delivery in IP datacast over DVB-H Systems," *IEEE Trans. on Broadcasting*, vol. 55, no. 2, pp. 396-406, 2009.

[13] D. Gómez-Barquero, P. Unger, T. Kurner, and N. Cardona, "Coverage estimation for multi-burst FEC mobile TV services in DVB-H systems," *IEEE Trans. on Vehicular Technology*, vol. 59, no. 7, pp. 3491-3500, 2010.

[14] M. A. Ismail, W. Dabbous, and A. Clerget, "A multi-burst sliding encoding for mobile satellite TV broadcasting," *Proc. IEEE INFOCOM*, Rio de Janeiro, Brasil, 2009

[15] B. Sayadi, Y. Leprovost, S. Kerboeuf, M. L. Alberi-Morel, and L. Roullet, "MPE-iFEC: an enhanced burst error protection for DVB-SH systems," *Bell Labs Technical Journal*, vol. 14, no. 1, pp. 25-40, 2009.

[16] ETSI TS 102 772 v1.1.1, "Multi-Protocol Encapsulation – inter-burst Forward Error Correction (MPE-iFEC)," 2010.

[17] ETSI TS 102 584 v1.2.1, "Guidelines for the Implementation for Satellite Services to Handheld devices (SH) below 3GHz," 2011.

[18] C. Abdel Nour and C. Douillard, "Rotated QAM Constellations to Improve BICM Performance for DVB-T2*," Proc. IEEE ISSSTA*, Bologna.

[19] ETSI EN 302 755 v1.2.1, "Frame Structure Channel Coding and Modulation for a Second Generation Digital Terrestrial Television Broadcasting System (DVB-T2)," 2011.

[20] ETSI draft TR 102 831 v0.10.4, "Implementation Guidelines for a Second Generation Digital Terrestrial Television Broadcasting System (DVB-T2)," 2010.

[21] DVB Document, "Commercial Requirements for DVB-NGH," 2009.

[22] M.-L. Alberi, S. Kerboeuf, B. Sayadi, Y. Leprovost, and F. Faucheux, "Performance Evaluation of Channel Change for DVB-SH Streaming Services," *Proc. IEEE ICC*, Cape Town, South Africa, 2010.

[23] ETSI TS 102 591-2 v1.1.1, "Digital Video Broadcasting (DVB); IP Datacast: Content Delivery Protocols (CDP) Implementation Guidelines; Part 2: IP Datacast over DVB-SH," 2010.

[24] J. Boutros and E. Viterbo, "Signal space diversity: A power- and bandwidth-efficient diversity technique for the Rayleigh fading channel," *IEEE Trans. Inform. Theory*, vol. 44, no. 4, pp. 1453–1467, July 1998.
[25] C. Abdel Nour and C. Douillard, "Improving BICM performance of QAM constellations for broadcasting applications," *5th International Symposium on Turbo Codes & Related Topics*, Lausanne, Switzerland, Sept. 2008, pp. 55-60.
[26] ENGINES Technical Report TR4.1 "Interim report on Hybrid Access Technologies", September 2011.
[27] B. Le Floch, M. Alard, and C. Berrou, "Coded Orthogonal Frequency Division Multiplex," *Proceedings of the IEEE*, vol. 83, pp. 982–996, June 1995.
[28] D. Pinchon, P. Siohan, and C. Siclet, "Design techniques for orthogonal modulated filter banks based on a compact representation," *IEEE Trans. Signal Processing,* vol. 52, no. 6, pp. 1682 – 1692, June 2004.
[29] N. Laurenti and L. Vangelista, "Filter design for the conjugate OFDM-OQAM system" *First International Workshop on Image and Signal Processing and Analysis*, July 14-15, 2000, pp: 267-272.
[30] H. S. Malvar "Modulated QMF Filter Banks with Perfect Reconstruction", *Electronics Letters*, June 1990, vol.26,nb.13,pp: 906-907
[31] A. Skrzypczak, P. Siohan and J.-P. Javaudin "Analysis of the Peak-to-Average Power Ratio for OFDM/OQAM", *7th IEEE Workshop on Signal Processing Advances in Wireless* Communications, *SPAWC'06*, July 2006, Cannes, France.
[32] M. Renfors, T. Ihalainen, T. H. Stitz, A block-Alamouti scheme for filter bank based multicarrier transmission, *European wireless Conference*, Lucca, Italy, April 2010.
[33] R. Van Nee and R. Prasad, "OFDM for Wireless Multimedia Communications", *Artech House Publisher*, March 2000.
[34] M. J. F.-G. Garcia, O. Edfors and J. M. Paez-Borrallo, "Peak Power Reduction for OFDM Systems with Orthogonal Pilot Sequences", *IEEE Transactions on. Wireless Commun*ications, vol. 5, no. 1, pp 47-51, Jan. 2006.
[35] S. H. Han and J. H. Lee, "An overview of Peak-to-Average Power Ratio reduction techniques of multicarrier transmission", *IEEE Wireless Commun*ications, vol. 12, no. 2, pp. 56-65, April 2005.
[36] X. Li and and J. L. Cimini, "Effect of Clipping and Filtering on the performance of OFDM", *47th IEEE Vehicular Technology Conference*, vol. 3, pp. 1634-1638, Phoenix, USA, May 1997.
[37] S. H. Muller and J. B. Huber, "OFDM with reduced Peak-to-Average Power Ratio by Optimum Combination of Partial Transmit Sequences", *Electronics Letters*, vol. 32, no. 5, pp. 368-369, Feb. 1997.
[38] R. W. Bauml, R. F. H. Fisher and J. B. Huber, "Reducing the Peak-to-Average Power Ratio of multicarrier Modulation by Selected Mapping", *Electronics Letters*, vol. 32, no. 22, pp. 2056-2057, Oct. 1996.
[39] D. S. Jayalath and C. Tellambura, "Reducing the Peak-to-Average Power Ratio of Orthogonal Frequency Division Multiplexing signal through bit of symbol interleaving", *Electronics Letters*, vol. 36, no. 13, pp. 1161-1162, June 2000.
[40] J. Tellado-Mourelo, "Peak-to-Average Power Ratio reduction for multicarrier Modulation", *PhD thesis, Stanford University*, Sept. 1999.
[41] M. Mahafeno, Y. Louet and J.-F. Helard, "PAPR reduction using SOCP-based Tone Reservation for Terestrial DVB Systems", *IET Communications Journal*, vol. 3, no. 7, pp. 1250-1261, July 2009.
[42] Aggarwal and T. H. Meng, "Minimising the Peak-to-Average Power Ratio of OFDM Signals Using Convex Optimization," *IEEE Transactions on Signal Processing*, vol. 54, no. 8, pp. 3099-3110, Aug. 2006.
[43] S. Zabre, J. Palicot, Y. Louet and C. Lereau, "SOCP Approach for OFDM Peak-to-Average Power Ratio Reduction in the Signal Adding Context", *IEEE Symposium on Signal Processing and Information Technology*, pp. 834-839, Vancouver, Canada, Aug. 2006.

[44] M. Sharif, M. Gharavi-Alkhansari and B. H. Khalaj, "On the peak-to-average power of OFDM signals based on oversampling", *IEEE Transactions on Communications*, vol. 51, no. 1, pp. 72-78, Jan. 2003.
[45] R. Van Nee and A. de Wild, "Reducing the peak-to-average power ratio of OFDM", *48th IEEE Vehicular Technology Conference*, vol. 3, pp. 2072-2076, Ottawa, Canada, May 1998.
[46] DVB "Implementation guidelines for a second generation digital terrestrial television broadcasting system (DVB-T2)", *ETSI TR 102 831 V0.9.17*, Nov. 2009.
[47] DVB BlueBook A122, "Digital Video Broadcasting (DVB); Frame structure channel coding and modulation for a second generation digital terrestrial television broadcasting system (DVB-T2)", July 2011.
[48] E. Stare, "Time-Frequency Slicing (TF-Slicing). A new concept for DVB-T2", TM-T20112.
[49] D. Gozálvez, D. Gómez-Barquero, D. Vargas and N. Cardona, "Time Diversity in DVB-T2 Systems"
[50] E. Stare and S. Bergsmark, "Time-Frequency Slicing gains", TM-T20280, 2007-09-24.
[51] M. Makni, J. Robert and E. Stare, "Performance Analysis of Time Frequency Slicing", 14th ITG Conference on Electronic Media Technology in Germany, March 2011.